

AN ANALYSIS OF DELTA PWM INVERTER

CENTRE FOR NEWFOUNDLAND STUDIES

**TOTAL OF 10 PAGES ONLY  
MAY BE XEROXED**

(Without Author's Permission)

MOHAMMAD ALI CHOUDHURY









AN ANALYSIS OF DELTA PWM INVERTER

BY

© Mohammad Ali Choudhury,  
B.Sc. Engg. (Elect.), M.Sc. Eng. (Elect.)

A thesis submitted in partial fulfilment  
of the requirements for the degree of  
Master of Engineering

Faculty of Engineering and Applied Sciences

Memorial University of Newfoundland

August 1984

St. John's

Newfoundland

Canada A1B 3X5

ABSTRACT

At present, various modulation techniques are in use for PWM inverters in ac motor drives. This thesis is devoted to the analysis and implementation of a newly proposed modulation technique for inverter operation. The technique known as delta modulation, has been used previously in voice transmission. In inverter applications, analog implementation of DM has several distinct advantages over other modulation techniques. These are easy implementation, inherent V/f ratio control, low order harmonic attenuation and easy harmonic and commutation controls.

In this thesis, the delta modulation technique as applied for inverter switching waveforms generation is analyzed. A Fourier analysis of the delta modulated inverter output has been carried out in order to study the harmonic behaviour of the inverter output. The analytical results confirm the advantageous features of the delta modulation technique. Practical implementation of the modulation process for inverter operations was realized and the results obtained in analytical studies were verified for a single phase bridge inverter.

Loading characteristics of a single phase delta modulated inverter were studied under different types of passive and dynamic loads. The passive loads were resistive and R-L loads. The dynamic loads were single phase induction.

motors. Theoretical results are verified experimentally for loading characteristics.

A modulation and a logic circuit were designed and implemented for a three phase inverter switching. The implementation involved the design and construction of a three phase sine reference wave generator, a three phase modulation circuit and the logic circuits for generation of proper switching waveforms of the three phase inverter switches.

A comparison has been made in the study between the proposed delta modulation technique and conventionally used sine PWM technique. Several suggestions have been put forward for the further study.

ACKNOWLEDGEMENT

I would like to express my sincerest gratitude to professors Dr. M.A. Rahman and Dr. J.E. Quaiocoe for their valuable help and constant guidance throughout the preparation of the thesis.

Thanks are due to my friends and to the technicians of the Faculty of Engineering and Applied Science at Memorial University of Newfoundland for their help in setting up the experiments. The help of others directly or indirectly involved with this study is gratefully acknowledged.



CONTENTS

	<u>Page</u>
ABSTRACT	ii
ACKNOWLEDGEMENT	iv
TABLE OF CONTENTS	v
LIST OF FIGURES	viii
LIST OF SYMBOLS	xiii
CHAPTER 1	
1.1 Introduction	1-1
1.2 Inverter Controlled Variable Speed AC Drives	1-4
1.3.1 The Pulse Width Modulated (PWM) Inverters	1-8
1.3.2 Survey of PWM Technique	1-12
1.3.3 Sine PWM Inverter Strategy for AC Motor Drives	1-17
1.3.4 Delta PWM Inverter	1-18
1.4 Objective of the Present Works	1-19
CHAPTER 2	
2.1 Delta Modulation Technique for PWM Inverter	2-2
2.1.1 Delta Modulation Technique	2-2
2.1.2 Delta Modulated Inverter	2-6
2.2 Implementation of Delta Modulation Control Circuit for PWM Inverters	2-9
2.3 Features of Delta Modulated Inverters	2-12
2.3.1 Fourier Analysis of Delta Modulated Inverter Output	2-14
2.4.1 Experimental Verification for Delta Modulation Technique	2-27
2.4.2 Fundamental Volts/hertz Characteristics of Delta Modulated Inverter Output	2-32
2.4.3 Harmonics in Delta Modulated Inverter	2-38
2.4.4 Number of Commutations	2-41
2.5 Comparison of Delta Modulation with Sine Modulation	2-43
CHAPTER 3	
3.1 Analysis of Delta PWM Inverter with Passive Loads	3-1
3.1.1 Basic Equations for Passive Loads fed with Inverters	3-2

	<u>Page</u>
3.2 Verification of Theoretical Results with Resistive Load	3-5
3.3 Verification of Theoretical Results with R-L Load	3-6
 CHAPTER 4	
4.1 Induction Motor as Variable Frequency Inverter Fed Drive	4-1
4.2 Single Phase Induction Motor Model and Equations for Inverter Drives	4-2
4.3.1 Steady State Analysis of Single Phase Induction Motor Fed from Delta Modulated Inverter	4-7
4.3.2 Theoretical Results of Steady State Performance of Single Phase Induction Motor Fed from Delta Modulated Inverter	4-8
4.3.3 Experimental Verification of the Results	4-15
 CHAPTER 5	
5.1 Three-Phase Delta Modulation Circuit Design and Implementation	5-1
5.2 Three Phase Sine Reference Wave Generator	5-2
5.3 Three Phase Modulator Circuit and the Logic Circuit	5-5
 CHAPTER 6 SUMMARY AND DISCUSSIONS	
REFERENCES	R-1
 APPENDICES	
Appendix A - Single Phase Induction Motor Model and Analysis for Inverter Drives	A-1
Appendix B - Delta Modulation, Circuit Implementation and Logic Circuit for Producing Gating Signals for Thyristors of the Inverter	A-5
Appendix C - Fourier Analysis of Delta Modulation with Sinusoidal Input	A-10
Appendix D - Fourier Analysis of Sine PWM Inverter Output	A-14

	<u>Page</u>
Appendix E - Three Phase Delta Modulation Circuit Implementation and Logic Circuit Development for the Inverter Switching Signals	A-18
Appendix F - Tables of Test Results	A-24
Appendix G - Motor Parameters	A-28
Appendix H - Computer Programs	A-29

LIST OF FIGURES

	<u>Page</u>
1.1 Voltage to frequency characteristics for constant torque and constant power mode operation of ac motors	1-6
1.2 Torque speed characteristics of variable speed ac motors	1-7
1.3 Various pulse width modulation technique	1-11
a) single pulse modulation	
b) multiple pulse modulation	
c) sinusoidal pulse modulation	
2.1 Graphical illustration of delta modulation (DM) technique	2-4
2.2 Graphical illustration of DM technique for the inverter	2-8
2.3 Basic single phase bridge inverter circuit	2-10
2.4 A practical circuit for producing switching waveform of delta modulated inverters	2-11
2.5 Basic switching signals for the main and commutation thyristors of a single phase full bridge inverter	2-13
2.6 Fundamental voltage to frequency characteristics of DM inverter output	2-19
2.7 Harmonics of DM inverter output at various operation frequency	2-20
2.8 Variation of dominant harmonics with frequency of operation at $V_R = 5.5 \text{ V}$	2-21
2.9 Variation of dominant harmonics with frequency of operation at $V_R = 7.5 \text{ V}$	2-22
2.10 Variation of number of commutation with changing modulating signal level	2-24
2.11 Timing diagram of switching signals of single phase DM inverter	2-28

	<u>Page</u>
2.12 Block diagram of logic circuit to produce the signals of the timing diagram for the switching signals of the single phase DM inverter	2-29
2.13 Illustration of practically obtained waveforms of delta modulation circuit of the inverter	2-30
2.14 Actual switching waveforms at the output of the logic circuits at various frequencies	2-31
2.15 Experimentally obtained fundamental voltage to frequency characteristics of DM inverter	2-33
2.16 Frequency Spectrum of delta modulated wave at various frequencies	2-34
2.17 Harmonic content of the delta modulated wave at various frequency operation ( $V_R = 6.75$ )	2-39
2.18 Dominant harmonic contents of the delta modulated inverter output at various frequency operation ( $V_R = 6.75$ V)	2-40
2.19 Variation of number of commutations with frequency in a practical delta modulated inverter as modulating signal level is changed	2-42
2.20 Variation of harmonics in a sine modulated wave as frequency of operation is changed (number of pulses per cycle is kept constant)	2-45
2.21 Variation of harmonics in a sine modulated wave with frequency. (Modulation index is kept constant)	2-48
3.1 Schematic diagram of an inverter with load	3-4
3.2 Theoretical performance characteristics of resistive (R) load fed from a single phase delta modulated inverter (for various levels of modulating signal level)	3-7
3.3 Experimental performance characteristics of R-load fed from a single phase delta modulated inverter (for various levels of modulating signal level)	3-10

	<u>Page</u>
3.4 Experimental load current waveforms of R-load fed from a single phase delta modulated inverter	3-13
3.5 Theoretical performance characteristics of R-L load fed from a single phase delta modulated inverter (for various levels of modulating signal)	3-16
3.6 Theoretical current waveshape of R-L load fed from a single phase delta modulated inverter (for various levels of modulating signal)	3-19
3.7 Experimental performance characteristics of R-L load fed from a single phase delta modulated inverter (for various levels of modulating signal)	3-21
3.8 Experimental current waveshapes of R-L load fed from a single phase delta modulated inverter (for various levels of modulating index)	3-24
4.1 Harmonic equivalent circuit of a single phase induction motor	4-5
4.2 Theoretical performance characteristics of a single phase 1/4 hp induction motor fed from a delta modulated inverter ( $V_R = 5.5$ V)	4-9
4.3 Theoretical performance characteristics of a 1/4 hp single phase induction motor fed from a delta modulated inverter ( $V_R = 6.75$ V)	4-10
4.4 Theoretical performance characteristics of 1/4 hp induction motor fed from delta modulated inverter ( $V_R = 7.5$ V)	4-11
4.5 Theoretical performance characteristics of 1/2 hp induction motor fed from a delta modulated inverter ( $V_R = 5.5$ V)	4-12
4.6 Theoretical performance characteristics of a 1/2 hp single phase induction motor fed from delta modulated inverter ( $V_R = 6.75$ V)	4-13



	<u>Page</u>
4.7 Theoretical performance characteristics of a 1/2 hp single phase induction motor fed from a delta modulated inverter ( $V_R = 7.5$ V)	4-14
4.8 Experimental performance characteristics of 1/4 hp single phase induction motor fed from delta modulated inverter ( $V_R = 5.5$ V)	4-16
4.9 Experimental performance characteristics of a 1/4 hp single phase induction motor fed from delta modulated inverter ( $V_R = 6.75$ V)	4-17
4.10 Experimental performance characteristics of a 1/3 hp single phase induction motor fed from delta modulated inverter ( $V_R = 7.5$ V)	4-18
4.11 Experimental performance characteristics of a 1/2 hp single phase induction motor fed from a delta modulated inverter ( $V_R = 5.5$ V)	4-19
4.12 Experimental performance characteristics of a 1/2 hp single phase induction motor fed from a delta modulated inverter ( $V_R = 6.75$ V)	4-20
4.13 Experimental performance characteristics of a 1/2 hp single phase induction motor fed from a delta modulated inverter ( $V_R = 7.5$ V)	4-21
5.1 Block diagram of a 3 phase sine wave generator	5-4
5.2 States of three phase square wave	5-6
5.3 Waveshapes of different sections of sine reference wave generator	5-7
5.4 Timing diagram of three phase delta modulated wave generation	5-8
5.5 Block diagram of logic circuit to implement the 3 phase delta modulation	5-9
5.6 Output waveshapes of a 3 phase delta modulation circuit	5-10

#### List of Figures for Appendices:

A.1 Harmonic equivalent circuit of 1-phase induction motor	A-2
------------------------------------------------------------	-----

	<u>Page</u>
A.2 Actual circuit connection for logic circuits producing gating signals of 1-phase bridge inverters	A-7
A.3 Actual circuit connection for delta modulator, 1-phase use	A-8
A.4 Illustration of pulse position determination of delta modulated wave	A-12
A.5 Illustration of theoretical pulse position determination of sine wave modulated wave	A-16
A.6 Schematic and actual circuit diagram of 3 phase square wave generator	A-19
A.7 a) V/f converter used for 3 phase reference wave generator b) Square wave to sine wave converter	A-20
A.8 Actual Circuit diagram of 1-Phase of the 3 Phase delta modulator	A-22
A.9 Actual circuit diagram of the logic circuits for producing gating signals of 3 phase inverter	A-23

LIST OF SYMBOLS

$E_{dc}, V_s$	Logic power supply dc voltage
$\omega_r, \Omega_r$	Frequencies in radians
$n$	order of harmonics
$\delta$	pulse position
$\Delta v$	Quantization level in delta modulation
$v_n$	nth harmonic voltage
$A_n$	nth harmonic voltage
$A_{1s}$	Fundamental voltage level due to square wave
$m$	modulation index
$z$	impedances
$L$	inductances
$r, R$	resistances
$P$	power
$T$	torque
$k$	harmonic order
$x$	reactances
$S$	slip
$S_1$	Fundamental slip
$S_k$	slip due to kth harmonic

(other symbols are defined where they are used)

## CHAPTER 1

This chapter is devoted to an introduction to inverters and their applications to ac motor drives. The advances in power electronics made it possible to introduce various types of inverters in motor drives. The two basic types are the voltage source inverter and the current source inverter. According to the need of the applications, various controls and modifications are incorporated in the basic circuits. One of the most versatile control techniques is the pulse width modulation (PWM) technique. Presently various PWM techniques are in use for inverters to drive motors. The aim of the present work is a detailed analysis and the implementation of a newly proposed delta modulation technique for inverters for ac motor drives. This chapter reviews the silicon control rectifier (SCR) inverters in particular.

### 1.1 Introduction

Inverters are used to transfer energy from dc to an ac of arbitrary frequency and phase. More specifically, these are used typically in drive systems to provide power for adjustable frequency ac motors, to regenerate energy back to ac line from decelerating dc motors, and to pump rotor power back to the ac line from wound rotor induction motors.

In non drive systems, these are used to supply uninterruptible ac power to computers and to convert energy between ac and dc at the terminal of high voltage dc power transmission line. In large motor drive systems, inverters employ thyristors as controlled switching gates to form the desired ac waveform. Inverters are also used for standby power supplies and for induction heating.

Various types of inverter circuits have been developed so far, the variations were introduced by the requirements of load and cost effectiveness of inverters. In most inverters, it is necessary to control output voltage and frequency. As the inverter output is usually nonsinusoidal, harmonic reduction schemes are also desired.

In solid state inverters, both transistorized and thyristor circuits are used. Thyristor (SCR) circuits take precedence where high power is involved. However, other things being equal, there is a general preference for the use of transistors. This is primarily because there is no commutations in the transistor circuits. SCR circuits perform well wherever commutation can be successfully implemented and maintained. At present SCRs have greater power handling capability and find wide applications in inverters of high power ratings. However, this may change eventually with the evolution of high power transistors in the future. Because of the present SCR capability of higher

power handling, most inverters and converters for drive systems use the thyristors as the main controlling element,

Inverter applications are wide and increasing in all types of applications. In fact, semiconductor devices have their greatest impact in the electric power industry, especially on the technology of electric motor drives. These led to the widespread use of adjustable speed drives, a radical change in the control and conversion of electric power for commercial and industrial use, and the development of new motor drive systems. Motor drives probably represent the largest market for power semiconductors. Thyristors as the means for controlled rectification was the instrument for the rapid development of motor drives of all types, sizes and applications. Like other power semiconductor circuits, inverters find their widest applications in adjustable ac motor drives. Variations of ac motors' speed can be achieved most effectively by variation of voltage and frequency of the supply. Presently static controllers for such variation are voltage controllers, cycloconverters and inverters. AC voltage controller control the speed to a very limited range by voltage variation only. The cycloconverter circuit is limited to the use of speed variation for low frequency operation because of its restrictions of the output frequency. As a result, static inverters take precedence over other types of converters in ac motor drives.



## 1.2 Inverter Controlled Variable Speed AC Drives

Traditionally ac machines were considered for constant speed applications and dc machines were used in most variable speed applications. But employment of elegant commutation techniques in SCR inverters resulted in practical and efficient static variable voltage, variable frequency power supplies required for speed control of ac motors. Ac machines, especially the cage type induction motors, possess several distinct virtues in comparison with dc machines. These relate to lower cost and weight, lower inertia, higher efficiency, improved reliability, ruggedness, low maintenance and capability to operate in a dirty and explosive environment. Some of these properties are of great importance which make ac drives a must in some practical applications. However, when precise speed control or close speed tracking in multimotor drives are required, synchronous machines are the obvious choice. Thus variable speed ac drives may be classified into two distinct categories:

1. Variable speed Induction Motors,
2. Variable speed Synchronous Motors.

AC motors for variable speed drives may be made to have the essential features and the characteristics of dc drives over a wide speed range without the use of a mechanical commutator. Conventional synchronous machine slip

rings may be eliminated by the use of permanent magnet rotors or self synchronous drives. Hence the need for slip rings is removed too. Before the semiconductor inverter was introduced, speed control of ac machines required either a pole changing technique or a dynamic frequency changer. The cost of such techniques in ac machines gave way to the use of dc motors in variable speed applications. DC machines also had superior performance characteristics over constant speed ac motors. But their main disadvantages are commutation hazards at high speeds, relatively higher cost and higher weight than ac motors of the same frame size.

AC machine variable speed drive characteristics can be made similar of dc machines with precision variable speed drive at variable voltage and variable frequency. Speed variation by stator voltage and frequency is possible in three modes of operation in ac machines.

- Constant torque mode
- Constant power mode
- Constant voltage mode

In the constant torque mode, flux is maintained constant which requires voltage to frequency ( $V/f$ ) constant ratio of voltage control (Fig. 1.1). In the constant power mode the voltage must be raised as the power factor drops. Typical torque speed characteristics of such three modes of operation is shown in Fig. 1.2. This confers that speed

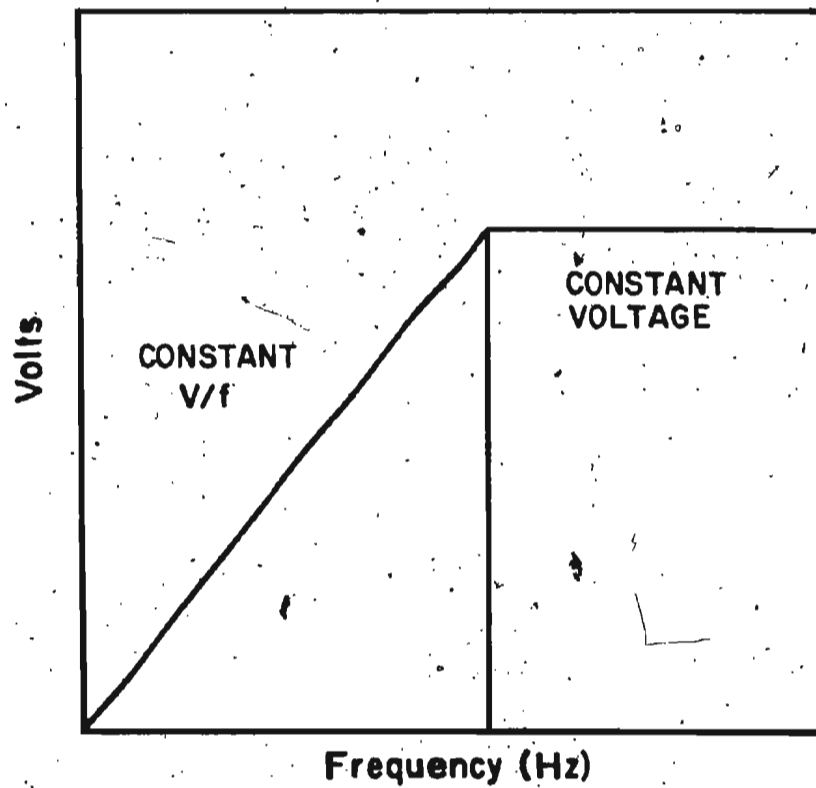


Fig. 1.1 Voltage to frequency characteristics for constant torque and constant power mode of ac motor operation

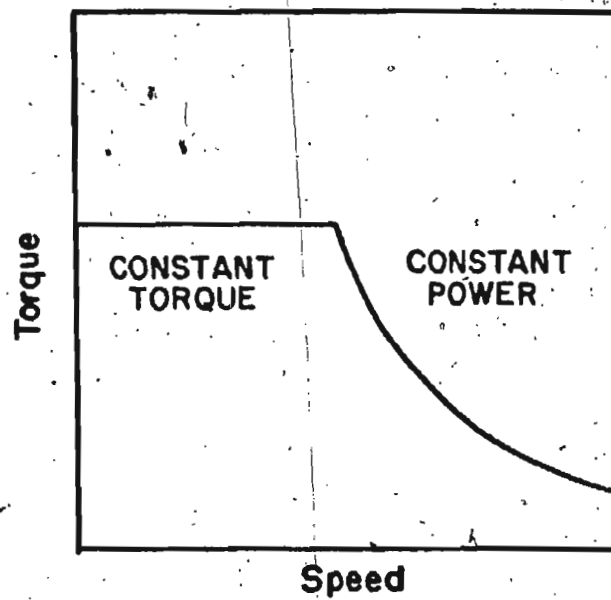


Fig. 1.2 Torque speed characteristics of variable speed ac motors

control via frequency provides the essential dc motor characteristics in AC motors.

Methods of induction motor speed control by static drives are a variation of stator voltage, rotor current and supply frequency. On the other hand methods of speed control in synchronous machines are supply frequency control and self synchronous control (multipole). Usual static devices for such speed control are ac voltage controllers and static frequency changer like inverters and cycloconverters. The type of static controller used in ac motor speed control depends largely on the type of application, effectiveness of the static devices and their economic constraints.

#### 1.3.1 The Pulse Width Modulated Inverters

It was mentioned earlier that static inverters are finding wide uses in ac motor drives. Two main inverter types using a dc link at one end are,

1. Voltage Source Inverters (VSI),
2. Current Source Inverters (CSI).

Classification is done by whether current or voltage at the dc link is the control parameter. Depending upon the control variability and commutation methods employed in SCR inverters, the inverters may be subgrouped in a variety of ways. Besides the main types, pulse width modulated inverters are very prominent in ac drive systems.

Normal voltage source inverters and current source inverters have the inconvenience of generating a square wave at the output of the inverter containing high low order harmonics. They also need double power conversion processes for simultaneous voltage and frequency control. Usually in ordinary inverters, voltage control is achieved with a controlled rectifier on the input side of the inverter. For simultaneous voltage control with frequency change, additional control circuit is necessary. However these problems can be overcome by using PWM operation of VSIs and CSIs. The objections to typical VSIs and CSIs disappear if the inverter is supplied by a fixed voltage dc link and switches are operated at higher frequencies so as to chop the output waves for the double purpose of voltage control and low order harmonic elimination. Basically PWM makes use of elaboration of the inverter control circuitry to permit variation of the ratio between dc input voltage and ac output voltage of the inverter itself.

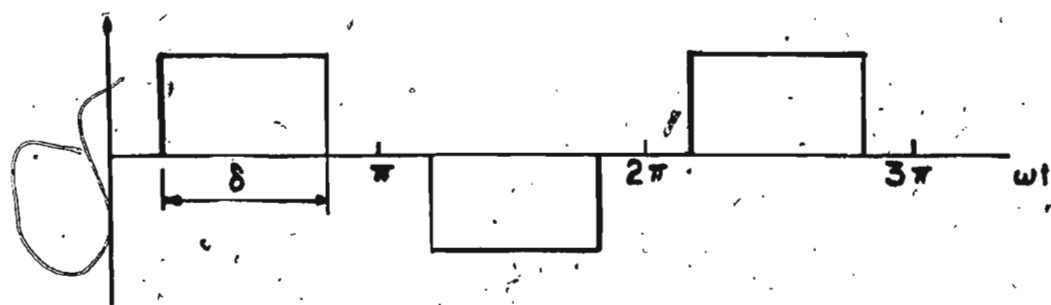
Pulse width modulation technique accomplishes both the voltage and frequency regulation in the output of the inverter. the input ac supply is rectified and filtered at fixed full voltage. The inverter section is arranged to switch the dc in such a manner that the line to line voltage consists of a series of pulses. Pulses are arranged to be of varying width so that its average leads to a sine wave. This



technique is the most sophisticated and complex in static variable frequency drives. It has advantages when full torque capability is required at low speeds. Three most commonly used modulation techniques in PWM inverters are:

1. Single Pulse Modulation
2. Multiple Pulse Modulation
3. Sinusoidal Pulse Modulation

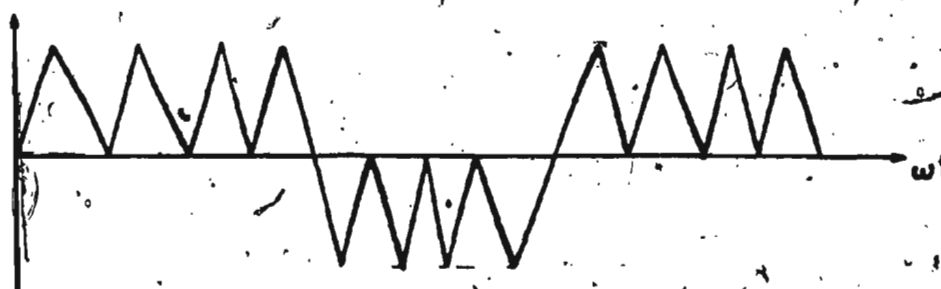
In single pulse modulation, the usual positive and negative half cycle of a square wave at the output of the inverter are width modulated to vary the output voltage. Frequency change is also achieved in the same circuit (Fig. 1.3(a)). In single pulse modulation, the harmonics at the output of the inverter increases as the pulse width of square waves are reduced. The harmonic contents at lower output voltages can be significantly reduced by using several pulses in each half cycle (Fig. 1.3(b)), the method is known as multiple pulse modulation. The most versatile modulation technique in use so far is the sinusoidal pulse modulation technique. In this method, the switching waveform's pulse widths are a sinusoidal function of the angular position in one cycle of each pulse. Good performance depends principally on the capability of the electronic control circuitry to define precisely the switching instants of the power stage in order to cause the output of the controller to be a train of pulses with a time average that approximates a sinusoid. Complex logic is needed to perform this task and



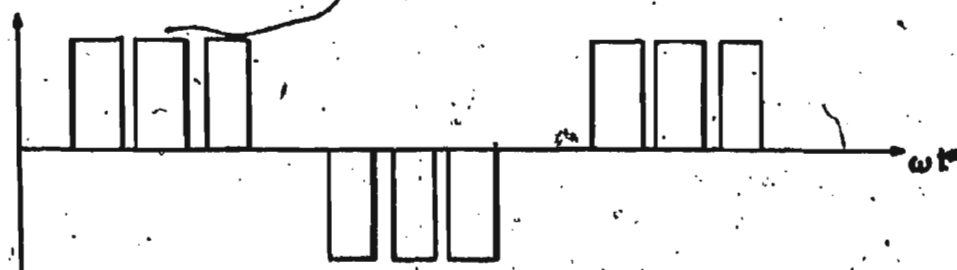
(a)



(b)



(c)



(d)

Fig. 1.3

Various pulse width modulation technique

was introduced [11]. In the asynchronous mode the sine wave is compared with a constant frequency carrier wave. The disadvantage of such operation is, with the constant frequency carrier the ratio of sine and triangular wave frequencies cannot be maintained to an integer value. This gives rise to subharmonics at the inverter output when the ratio is not the desired integer value. The problem is overcome in synchronized sine PWM mode where the carrier wave frequency is varied with the modulating wave frequency to keep the ratio to the desired integer value. This, however, complicates the implementation of such a technique. The principal disadvantage of synchronous PWM method is that, since the modulating and carrier waves are synchronized, the carrier frequency must vary over a wide range as the output frequency changes. It is not usually practical, especially in inverters for ac motor drives, to allow the carrier frequency to vary widely. Because, if the carrier frequency is too high, the commutation hazard increases as the number of commutations per second increases. Also an increased number of commutations causes larger commutation losses in the power circuit of the inverter. For drives, a very low carrier frequency also creates problems since the motor constants are insufficient for adequate smoothing of current drawn by the motor. To overcome this problem with the fixed ratio method [6], pulse width modulation with ratio changing

the conventional means for implementing the switching algorithm is the subharmonic or triangulation approach involving an electronic comparison between a reference sinusoid and a triangular carrier waveform as illustrated in Fig. 1.3(c).

### 1.3.2 Survey of PWM Techniques

PWM techniques of switching the inverters was introduced with a view to accomplish voltage and frequency control in one power stage and also to reduce harmonics at the output of the inverter. It is possible by surveying the literature over the last decade to trace the historical developments of PWM inverter control techniques and relate them to the changes in technology.

The foremost modulation technique in inverters were single pulse and multiple pulse modulation [1,2,3,4,22]. These modulation technique are capable of controlling inverter voltage and frequency in one power stage and capable of eliminating only selected harmonics at the output of the inverter. These modulation procedures were superseded by the introduction of the more complicated and versatile sine modulation [4,5]. Sine modulation is a variation of multiple pulse modulation where the pulse duration and numbers are determined by comparison of a modulating sine wave and carrier triangular wave. At first sine modulation used the asynchronous PWM mode and later the synchronous mode of PWM

at various operating frequencies is suggested [6,11,14]. In the variable ratio scheme, the carrier steps through a sequence of ratios as the operating frequency is increased. The later section maintains a high carrier frequency throughout the operating range thereby producing only high frequency harmonics at the output of the inverters which are easily filterable. The variability of types of sine PWM schemes put forward are due to implementation involvements, types of applications and technical and economic feasibilities. Currently three distinct approaches are in vogue to formulate the PWM switching strategy [7,10,12]. The first, and the one which has been most widely used because of its ease of implementation using analog techniques, is based on natural sampling technique [4,7] described already. The recent trend is, however, to generate the switching functions using microcomputers. The general tendency in microprocessor control is to use a new switching strategy known as 'regular sampling' [7,10,12,16,18]. In the regular sampling technique, the sine modulating wave is replaced by a sampled [stepped] sine wave and the switching points are determined from the crossover points of the carrier triangular wave with the stepped sine wave. In this mode of control, the amplitude of the modulating signal at the sample instant is stored by a sample hold circuit operated at the carrier frequency and is maintained at a constant level during the intersample period

until the next sample is taken. This produces a sample hold or amplitude modulated version of the modulated signal. As a result of this process, the modulating wave has a constant amplitude while each sample is being taken, and consequently the widths of the pulses are proportional to the amplitude of the modulating wave at uniformly spaced sampling time from where the terminology of uniform sampling or regular sampling came. It is an important characteristic of regular sampling that the sampling positions and sampling values can be defined unambiguously, such that the pulses produced are predictable both in width and position which is not the case with a natural sampling process. In a natural sampling process no direct way of finding the pulse width and pulse positions is available other than solving transcendental equations or bessel function approximations. Since it is possible to calculate the pulse widths using simple trigonometric equations, the potential for real time PWM generation using the computing ability of the microcomputer is greater more with the regular sampling technique rather than with the natural sampling technique.

The third approach uses 'Optimal' PWM switching strategies which are based on the minimization of certain performance criteria [19,20,21]; for example, elimination or minimization of particular harmonics, or the minimization of harmonic current distortion, peak current, torque ripple etc. These optimized PWM control strategies are currently



receiving considerable attention. As a result of the developments in microprocessor technology, the feasibility of implementing these strategies has now become a real possibility [10,19,20,21,13,14,17,16]. In contrast to natural and regular sampling, it has been usual to generate optimised PWM by defining a general PWM waveform in terms of a set of switching angles and then to determine these switching angles using numerical methods and the mainframe computer.

Besides the types of modulation techniques mentioned already, there are several other modulation processes put forward from time to time, such as trapezoidal and square wave modulation [27]. However, those modulation processes have not found their way toward inverter voltage and frequency control for drives.

Along with implementation of various modulation techniques in inverters, the analysis of such inverter have also been carried out by different authors at different times. Attention has been given to output voltage analysis and the input current harmonics. First attempts were aimed at the inverter output voltage analysis by the Fourier analysis method [25,26,27]. An approach to output voltage harmonic analysis based on double Fourier series expansion in two variables was introduced. This was necessary for the general case since there is no rational relationship between the modulating frequency and the carrier frequency.

Presently, more emphasis is given to optimization techniques [24,27]. Availability of some packages [PWLIB] for general analysis of PWM inverter outputs are also reported [48]. Also, some new analytical methods for input current harmonic analysis of the inverter are reported [28]. The analytical approach is drawing more attention due to the fact that the implementation of different modulation techniques, especially the optimum PWMs require a mathematical formulation for software development in their implementation. However, due to the complexity of the modulation process, no general approach has so far been standardized.

#### 1.3.3 Sine PWM Inverter Strategy for AC Motor Drives

The merits of sine PWM in solving one set of problems bring back others. The first is the increasing commutation problems, and secondly the low utilization of dc power available. Since commutation is not a problem at higher voltages associated with higher speed, drive stability is more easily ensured. It is advantageous to combine the merits of the two systems by using the PWM mode at lower speeds and the pure square wave at higher speeds [30,36] with transitional stage from one system to another at medium speeds. The frequently encountered load characteristics, which transforms from a constant torque requirement at higher speeds makes such a hybrid system even more attractive. However such drive calls for a very complex control strategy

for sine PWM inverters and increase the cost of the total drive system.

#### 1.3.4 Delta PWM Inverters

Recently a new modulation technique for inverters was put forward for drive applications [30]. The new scheme is simple to implement and it does not require additional circuit elements necessary for the sine modulation technique in order to give some of the characteristics required for an ac drive system. This new modulation technique, known as delta modulation, uses similar triangular and sine wave comparison to produce switching waveforms of the inverters. However the carrier triangular wave in delta modulation is generated by the modulating sine wave and has a variation which makes delta modulation capable of operating in both PWM and square wave modes without additional circuit elements. The technique also produces a modulation pattern with low harmonic content and a fundamental voltage variation which maintains an inherent constant voltage to frequency ratio. These features of delta modulation may make it very attractive for ac motor drives.

An induction motor's steady state performance is dependent on the harmonic voltages of the inverter output as well as on the fundamental voltage. The inherent characteristics of the delta modulation process, the linear fundamental voltage variation with frequency up to base

frequency and constant voltage beyond the base frequency, provides constant torque and constant power characteristics up to and beyond base frequency respectively. The harmonic contents in delta modulation are low and the dominant harmonics are at or near high carrier frequency. The harmonic contents, commutation timing and mode of operation can be changed easily by changing the amplitude of the modulating wave only. All these features seems to be so attractive in ac motor drives that it may find its way to drives soon.

#### 1.4 Objective of the Present Work

Though the delta modulation technique has been proposed [30] for induction motor drives, no significant detailed analysis of delta modulation has been undertaken for application in ac drive systems. The present work is aimed at a comprehensive study and analysis of the delta modulation technique in inverters. At first a detailed analysis was done on delta modulation. Secondly, the analysis is extended to find the performance of inverters for various load conditions.

Chapter two includes the theoretical analysis and details of implementation of delta modulation. It also includes the experimental verification of the principles of delta modulation.

In chapter three, theoretical and experimental study of the delta modulated inverter is presented with passive loads.

Chapter four contains the analysis and verification of results of steady state performance of single phase induction motors fed from full bridge delta modulated inverters. The features of delta modulation for which it seems attractive for ac motor drives are verified analytically and experimentally. Results are compared for two single phase induction motors of 1/4 and 1/2 hp ratings.

Chapter five describes a three phase delta modulation circuit which has been developed and implemented during this work and it is hoped that the significance of the new modulation technique will be further elaborated when analysis and experiments are carried out on 3-phase ac motors, both induction and synchronous types with conventional wire wound and permanent magnet excitation.

Chapter six concludes on the objective and experiments done in the study of delta modulated inverters. It gives an outline of further planned work.

## CHAPTER 2

This chapter deals with the development and analysis of the delta modulation technique as used in PWM inverters. The development of circuit implementation for the logic signals required for SCRs of the inverter is being discussed. The analysis includes the unique features of delta modulation technique with special emphasis on determination of harmonics at delta modulated inverter output, the constant volts/hertz characteristics up to base frequency and a constant power operation beyond the base frequency. A brief comparison has been made with the commonly used sine modulation technique to bring out the advantages of delta modulation. In few words, delta modulation is found to be more easily implementable than the SPWM technique and further improved operation characteristics are realised.

### 2.1 Delta Modulation Technique in PWM Inverter

Initially delta modulation was evolved as an efficient method of digitizing voice for secure, reliable communication and for voice input/output devices in data processing [31]. Recently, its possible use in inverters for variable speed ac motor drives was reported [30].

For induction motors the general requirement is to operate the motors at desired slip and keep the volts/Hz

constant to maintain the flux density at a particular value. For permanent magnet synchronous motors, the starting characteristics calls for the same volts/Hz characteristics up to the base speed. These various requirements have been met with different voltage and current control techniques in sine PWM inverters. The main objection to sine PWM was its certain percent utilization of dc voltage available at the bus, which was solved by its gradual transition from PWM mode to single pulse mode. To attain this, sine PWM control circuits require additional attachments to its normal control circuits:

The arguments put forward in using DM technique in PWM inverters for ac motor drives are its simple circuit implementation, smooth transition between PWM and single pulse mode of operation and constant volts/hertz operation without the need of additional circuit complexity.

#### 2.1.1 Delta Modulation Technique

In the past years, various modulation techniques were introduced for digital transmission of speech or image signals. Numerous methods of converting analog signal to digital form have been proposed for various applications with the hope of reducing cost, improving performance and reduction of bandwidth requirements. Delta modulation (DM) and differential encoding methods are the offsprings of classical pulse code modulation [PCM] used so far for

communication applications. DM technique has the advantage of greatly simplifying hardware. It is the simplest known method for converting an analog signal to digital form. In converting analog signal to digital form, there is a great deal of redundancy in the information to be transmitted. Past information should thus allow current information to be predicted fairly well, so that signals need only be transmitted if a significant change in the signal occurs.

As applied in signal processing, the delta modulation technique [32-34] can be illustrated with the aid of Fig. 2.1.

The signal  $x(t)$  is compared with a stepwise approximation  $\bar{x}(t)$  by subtraction, the difference being passed through a hardlimiter quantizer whose output equals  $\pm\Delta$  depending on the sign of  $[x(t) - \bar{x}(t)]$ . This in turn modulates the ideal sampling wave  $S_\delta(t)$  to produce  $x_p(t)$  where the modulated wave  $x_p(t)$  is given by

$$x_p(t) = \sum_k \Delta \operatorname{sgn} [x(kT_s) - \bar{x}(kT_s)] \delta(t - kT_s) \quad 2.1.1$$

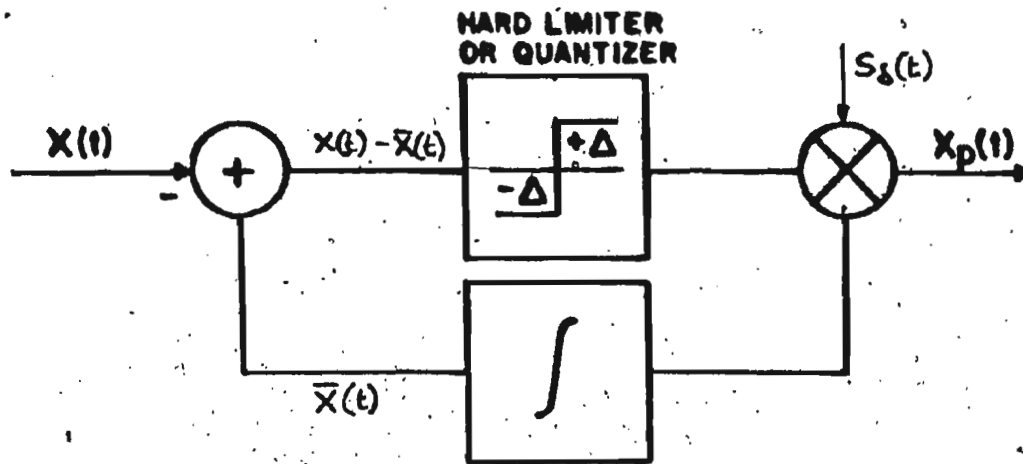
This is an impulse waveform from which  $X(t)$  is generated by integration.

Where

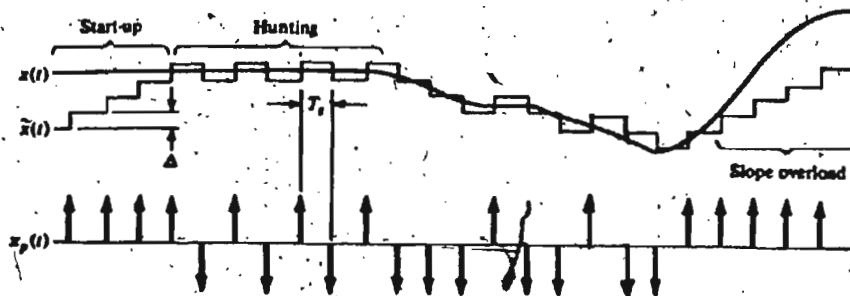
$\Delta$  = level of quantization.

$\operatorname{sgn}$  = indicates the sign of  $[x(t) - \bar{x}(t)]$





(a)



(b)

Fig. 2.1 Graphical illustration of delta modulation technique

$x(kT)_s$  = value of predicted signal at kth sampling time

$T_s$  = sampling time

$\delta(t-kT)$  = impulse function

In signal transmissions, DM has two distinct restrictions, resulting in wider bandwidth requirements. When  $\bar{X}(t)$ , the estimated or predicted signal is smaller than the actual signal  $X(t)$  at start, the first impulse has the weight  $+\Delta$ , when feedback and integrated, that impulse produces a stepwise change in  $\bar{X}(t)$  of height  $+\Delta$ . This produces a stepwise change in  $X(t)$  and causes a negative impulse. If  $X(t)$  remains constant,  $\bar{X}(t)$  follows it in stepwise function unless the rate of change is too great when the slope overload takes place. This occurs if the quantization levels  $\pm\Delta$  are too small to track a rapidly changing signal. This is due to the inability of the modulator to track large changes of the input signal  $X(t)$  in a small interval of time. This phenomenon is a basic limitation of DM in communications.

In DM,  $X(t)$  is not the transmitted signal, rather the transmitted signal is a binary representation of  $X_p(t)$ . The binary digits merely indicate the polarity of the difference between  $X(t)$  and  $\bar{X}(t)$  at  $t = kT_s$ . A variation of DM is differential pulse code modulation (DPCM) with multilevel quantiser instead of two level quantisation. Functionally differential PCM signal is a PCM representation of the difference signal  $[X(t) - \bar{X}(t)]$ , generated, where  $\bar{X}(t)$

has a variable step size ranging from  $\Delta$  to  $\pm Q \frac{\Delta}{2}$ ,  $Q$  being the number of quantum levels. It follows  $X(t)$  more accurately when this compounding is used in digitizing a signal, there will be much lower idle noise, faster start up and less chance of slope overload. Clearly, DPCM with  $Q > 2$  requires equipments just as complex as PCM. In return it offers potential transmission bandwidth reduction.

#### 2.1.2 Delta Modulated Inverters

In inverters, the modulation process to produce the switching signals for the thyristors determines the frequency and voltage at the output of the inverter. The delta modulation technique for generating such switching logic utilizes a sine reference waveform and a delta shaped carrier waveform to determine the switching frequency of the inverter switches (the SCRs).

The delta shaped carrier waveform is allowed to oscillate within the defined window extending equally above and below the reference wave. The minimum window width and the maximum carrier slope determine the maximum switching frequency. For inverter switching the modulation is prime object and no attempt of sampling the modulated wave to produce a binary signal is taken. The signal to be modulated is sine wave. The carrier wave acts as quantising the reference wave in two levels. It also determines the widths of the switching pulses. The key waveforms associated with

this technique are shown in Figs. 2.2(a) and 2.2(b). The switching waveform oscillates between  $\pm V_s$  and can be expressed as

$$V_I(t) = V_s \pm \Delta V \operatorname{sgn} [x(kT_s) - \bar{x}(kT_s)] \quad 2.1.2$$

where

$\Delta V$  = quantization level

$V_s$  = level of switching pulses

$x(kT_s) = \sin \omega(kT_s)$  = modulating signal in this case at  $kT_s$

$\bar{x}(kT_s)$  = Predicted signal at  $kT_s$

$T_s$  = Sampling time

In implementing the DM technique to produce the necessary switching function for inverters, the switching pulses are generated by the interaction of reference sine wave and delta shaped carrier wave. Whenever the carrier reaches the upper or lower window boundary, it reverses its slope and changes the switching waveform  $V_I$  from  $+V_s$  to  $-V_s$ . This process continues to generate a train of switching pulses. The switching frequency can be altered in three different ways, by changing the amplitude of reference wave  $V_R$  or by changing the slope of the triangular carrier wave or by changing the window width (quantization level)  $\Delta V$ . Thus it is important to set these values such that sufficient time is provided for proper turn on and turn off of SCRs. If a single phase full bridge inverter is to be switched by the

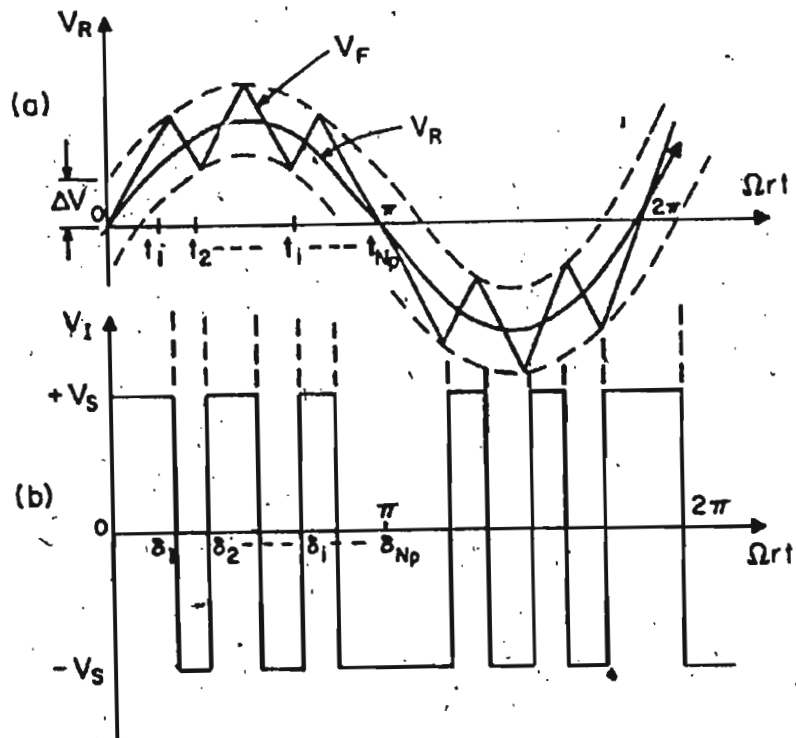


Fig. 2.2 Graphical illustration of DM technique for inverters

modulated wave, the sequence of the thyristors to be fired is shown in Figs. 2.2(b) and 2.3. Fig. 2.3 illustrates the basic single phase full bridge inverter circuit.

In practice, the slope of the carrier frequency and sampling rate are kept constant in implementation by circuit parameters. So it is obvious that overload error described earlier takes place, as the frequency is changed to higher value. This phenomenon is however useful for inverter operation. ~~As~~ the sampling rate is kept constant, sampling per cycle is kept constant as frequency of operation (sine modulating wave frequency) is increased. As the result of overload error in modulation, a transition from PWM to single pulse mode operation takes place when the modulating wave and carrier wave frequencies are equal. The modulated output continues to be single pulse square wave beyond that frequency.

## 2.2 Implementation of Delta Modulation Control Circuit for PWM Inverters

The delta modulation technique requires relatively simple circuitry to obtain the switching waveform for thyristor switching. Fig. 2.4 is an analog circuit that is capable of producing the waveforms shown in Fig. 2.2.

The operation of the circuit can be described as follows: Sine reference or modulating wave  $V_R$  is supplied to the input of the comparator  $A_1$  and the carrier  $V_F$  is

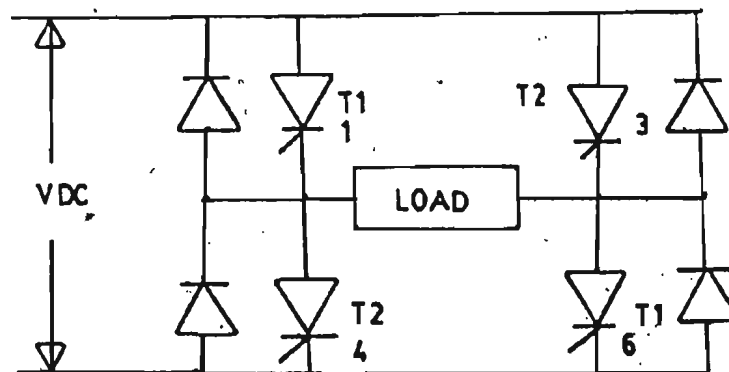


Fig. 2.3 Basic single phase bridge inverter circuit

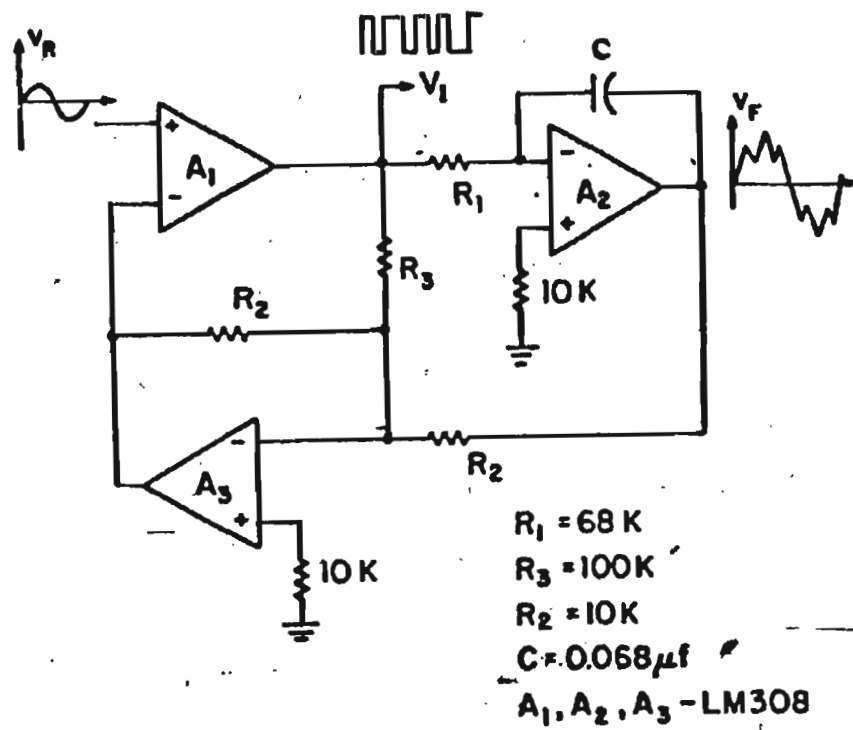


Fig. 2.4

A practical circuit for producing switching waveform of delta modulated inverters



generated in the following manner; Whenever the output voltage of  $A_2$  exceeds the upper or lower window boundary (preset by  $R_2/R_3$  ratio), the comparator  $A_1$  reverses the polarity of  $V_I$  at the input of  $A_2$ . This reverses the slope of  $V_F$  at the output of  $A_2$ . It forces carrier wave  $V_F$  to oscillate around the reference waveform,  $V_R$  at ripple frequency  $\omega_r$ . Once the switching waveform is obtained, the signals for the main and commutation thyristors can be obtained through the logic circuit implementation for such inverters. The basic signals for such inverter thyristor operation are shown in Fig. 2.5.

The timing diagrams for various logics and their block representations are shown in Figs. 2.11 and 2.12. Details of the implementation to get the desired signals with proper commutation delay time and commutation signals are elaborated in appendix B.

### 2.3 Features of the Delta Modulated Inverter

The intrinsic features of delta modulation schemes are:

1. Up to base frequency the fundamental voltage to hertz ratio remains constant.
2. Lower order harmonics in carrier and modulating waves are negligible.

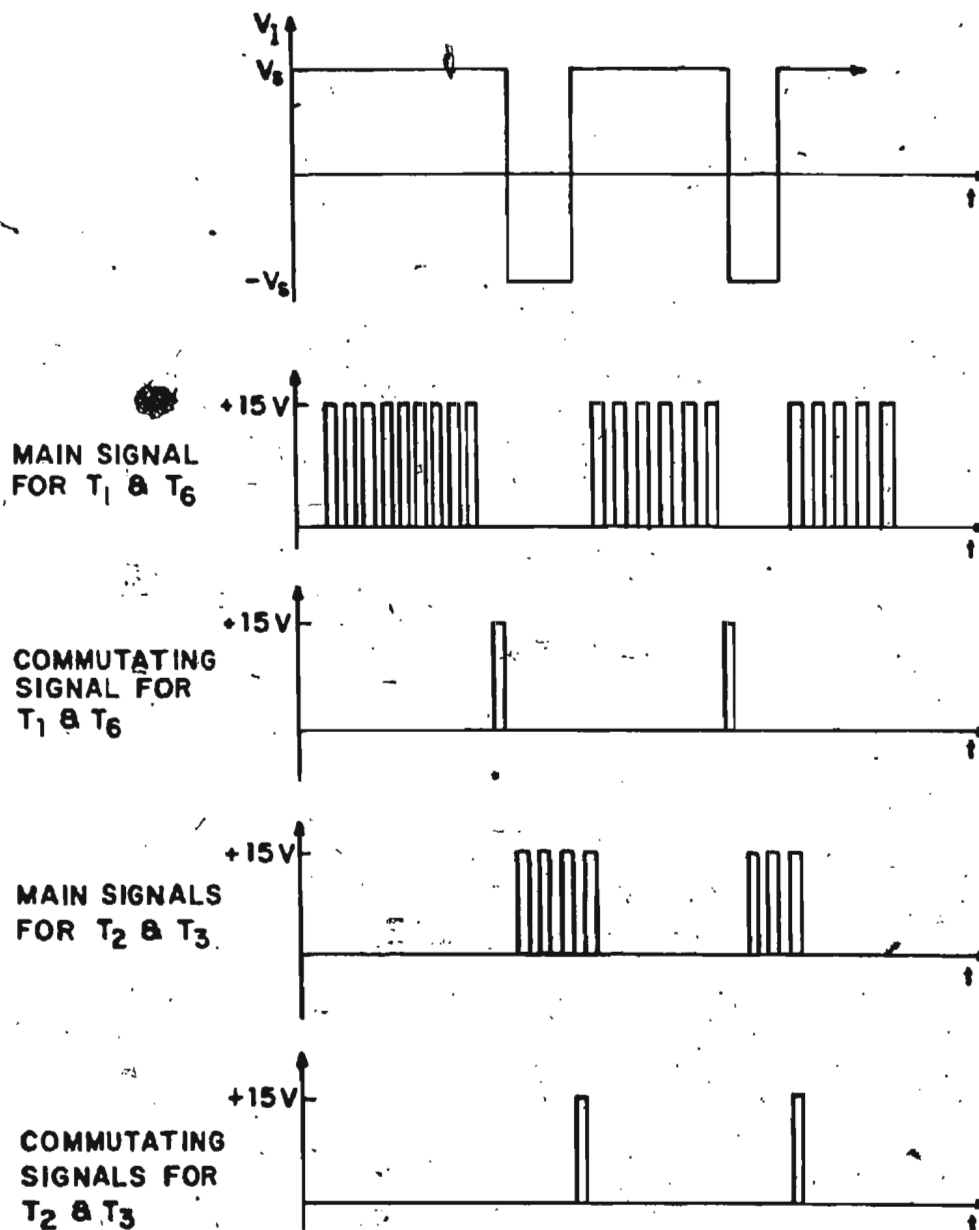


Fig. 2.5

Basic switching signals for the main and commutation thyristors of a single phase full bridge inverter

3. For fixed window width ( $\Delta V$ ), the ripple frequency increases as the amplitude of the modulating wave  $V_R$  decreases.

These features of delta modulation technique were observed both analytically and experimentally. The analytical method required the approach of Fourier analysis of the switching signal produced by the modulating and carrier waves. The expressions for fourier analysis of such waves are given in the following subsections.

#### 2.3.1 Fourier Analysis of Delta PWM Inverter Output

The fourier analysis of the PWM wave requires the determination of number of pulses per half cycle and their positions at different frequencies of operation. Once the pulse positions and the number of pulses are known accurately for such waves, the Fourier coefficients can be easily determined.

For DM technique, the pulse positions of the modulated wave is given by the following expression (detail derivation is given in appendix D)

$$t_i = \frac{2\Delta V + A t_{i-1}}{A} + \frac{V_R \sin \Omega_r t_{i-1} - V_R \sin \Omega_r t_i}{A * (-1)^i}$$

2.3.1

where

$A$  = slope of the carrier wave  $V_F$

$\Delta V$  = Window width

$V_R$  = Maximum voltage of the modulating signal

$t_i$  =  $i$ th pulse termination time

$\omega_r$  = ripple frequency of triangular wave  $V_F$

$\Omega_r$  = frequency of modulating sine wave  $V_R$

The window width  $\Delta V$  is determined by the circuit constants and logic power supplies. For the implementation circuit of Fig. 2.4

$$\Delta V = \frac{R_2}{R_3} V_S \quad 2.3.2$$

The slope  $A$  of carrier wave is dependent on modulating signal amplitude, but it may be considered constant up to base frequency with a constant amplitude of  $V_R$  for certain mode of operation. Once the pulse positions are known, the number of pulses/cycle or half cycle as required by Fourier analysis can be obtained easily. Since the modulated wave has  $f(\theta \pm n\pi) = -f(\theta)$  symmetry, it only contains the odd harmonics. The Fourier coefficients are given by the following equations (Detail derivation is given in appendix D).

$$A_n = \frac{2V_S}{n\pi} \sum_{i=1,2,\dots}^{N_P} (-1)^{i+1} (\sin n\delta_i - \sin n\delta_{i-1}) \quad 2.3.3$$

$$B_n = \frac{2V_S}{n\pi} \sum_{i=1,2,\dots}^{N_P} (-1)^{i+1} (\cos n\delta_{i-1} - \cos n\delta_i) \quad 2.3.4$$

and  $V_n = \sqrt{(A_n^2 + B_n^2)} \quad 2.3.5$

where

$V_g$  = Logic power supply voltage

$n$  = order of the harmonics

$N_p$  = number of pulses/half cycle

$\delta_i$  =  $i$ th pulse termination position in radians

These expressions are used in the theoretical verification of inherent features of the delta modulated inverter.

Volts per Hertz Characteristics:-

The output of the inverter has a fundamental voltage to frequency constant characteristics up to base frequency. Beyond the base frequency the fundamental voltage remains constant, because beyond the base frequency, the output wave becomes constant amplitude square wave. From circuit analysis point of view this is expected. The circuit implementation of delta modulation is shown in Fig. 2.4. In the circuit of Fig. 2.4, A2 acts as a low pass filter besides acting as an integrator. Hence

$$V_{Fn} = \frac{V_{In}}{n (R_1 C) \Omega_r} \quad 2.3.6$$

where

$V_{Fn}$  =  $n$ th order harmonic of the carrier wave

$V_{In}$  =  $n$ th harmonic of the modulated wave

$\Omega_r$  = frequency of sine reference wave

Also

$$V_{F1} = V_R \quad 2.3.7$$

From equations 2.3.6 and equation 2.3.7 one obtains

$$V_R = V_{F1} = \frac{V_{I1}}{(R_1 C) \Omega_r} \quad 2.3.8$$

or 
$$\frac{V_{I1}}{\Omega_r} = (R_1 C) V_R$$

Since the amplitude  $V_R$  of modulating wave is constant and independent of  $\Omega_r$ , the ratio of  $V_{I1}/\Omega_r$  is also constant and independent of  $\Omega_r$ . This is true until  $\Omega_r = \Omega_{rb}$  (i.e. the base frequency), at which point modulated wave becomes a square wave of the frequency  $\Omega_r$ . After this point, fundamental voltage component  $V_{I1}$  of the modulated wave remains constant. This was analysed with the help of Fourier analysis of delta modulated wave.

The fundamental component of inverter output voltage at any frequency is given by

$$A_1 = \frac{2V_s}{\pi} \sum_{i=1,2,\dots}^{N_p} (-1)^{i+1} (\sin \delta_i - \sin \delta_{i-1}) \quad 2.3.9$$

$$B_1 = \frac{2V_s}{\pi} \sum_{i=1,2,\dots}^{N_p} (-1)^{i+1} (\cos \delta_{i-1} - \cos \delta_i) \quad 2.3.10$$

and 
$$V_1 = \sqrt{A_1^2 + B_1^2} \quad 2.3.11$$

where

$N_p$  = number of pulses

$\delta_i$  =  $i$ th pulse termination position in radians.

$V_{I1}/f$  gives the fundamental voltage to modulating wave frequency ratio. The plots of theoretical  $V_{I1}/f$  ratio is given in plot 2.6. It confirms the validity of the results.

#### Harmonics in Delta Modulation:

The dominant harmonic frequency in the carrier ( $V_F$ ) and modulated ( $V_I$ ) waveforms are close to the ripple frequency of the carrier wave ( $V_F$ ). As a result, lower order harmonics in  $V_F$  and  $V_I$  are negligible, particularly in the low frequency operations. At high frequency operations, the fundamental itself is dominant the effects of higher harmonics are reduced even more. Especially, with passive R-L load and dynamic motor load, the effects of the dominant high frequency components at the output of delta modulated waves are quite negligible, since the impedance of such loads at high frequencies are higher as compared to that of the fundamental.

The theoretical harmonic analysis was carried out using the expressions for pulse termination and number of pulses as mentioned in the equations (2.3.1) to (2.3.5). The theoretical results show harmonic content to be significant at lower frequency operation. The harmonic content decreases with the increase of the operating frequency of the inverter. Fig. 2.7 shows the fact that, though the harmonics are high at lower frequency, they are so at or near the ripple frequency or at the multiple of ripple frequency of

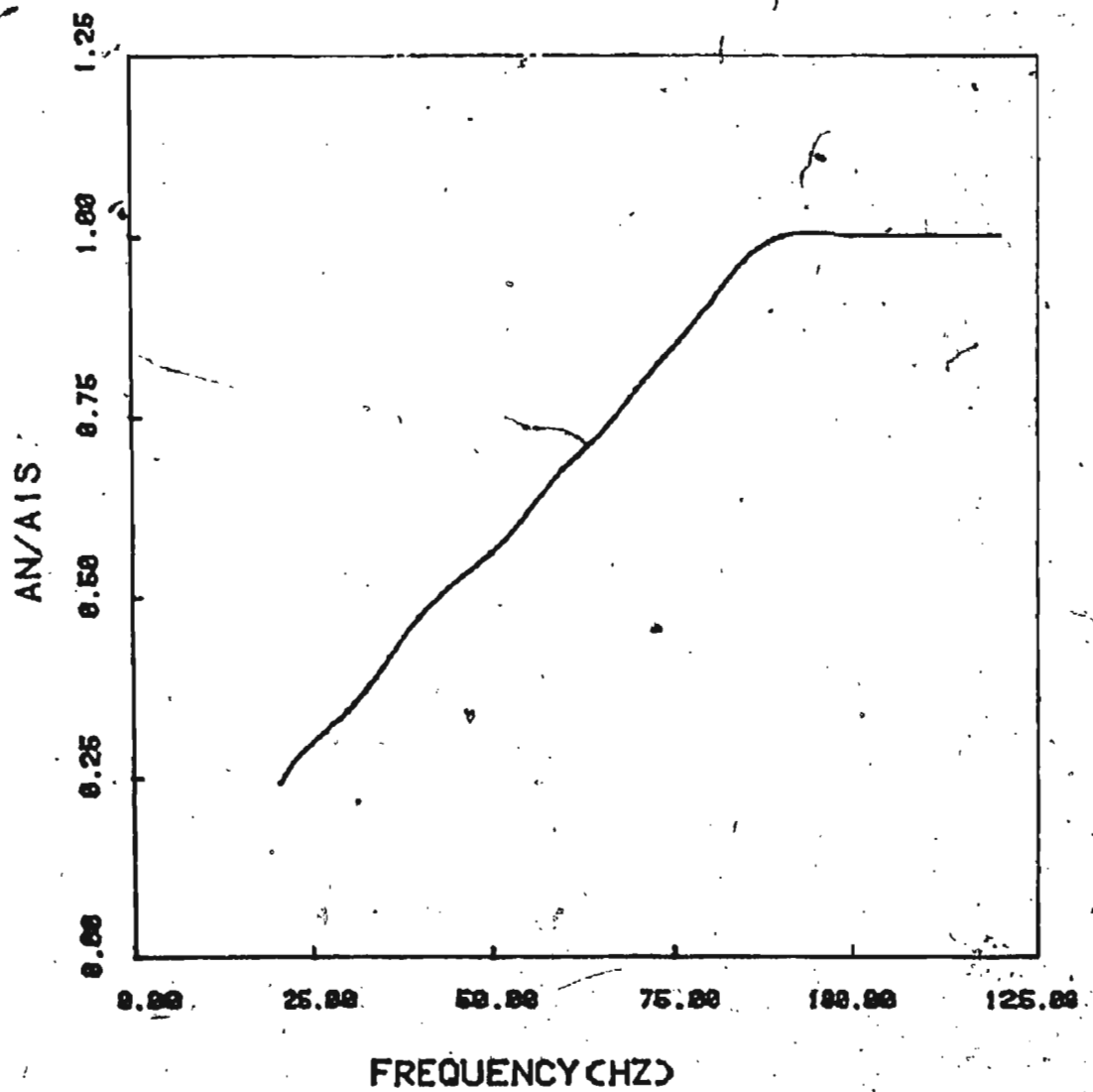


Fig. 2.6

Fundamental voltage to frequency characteristics  
of DM inverter output.



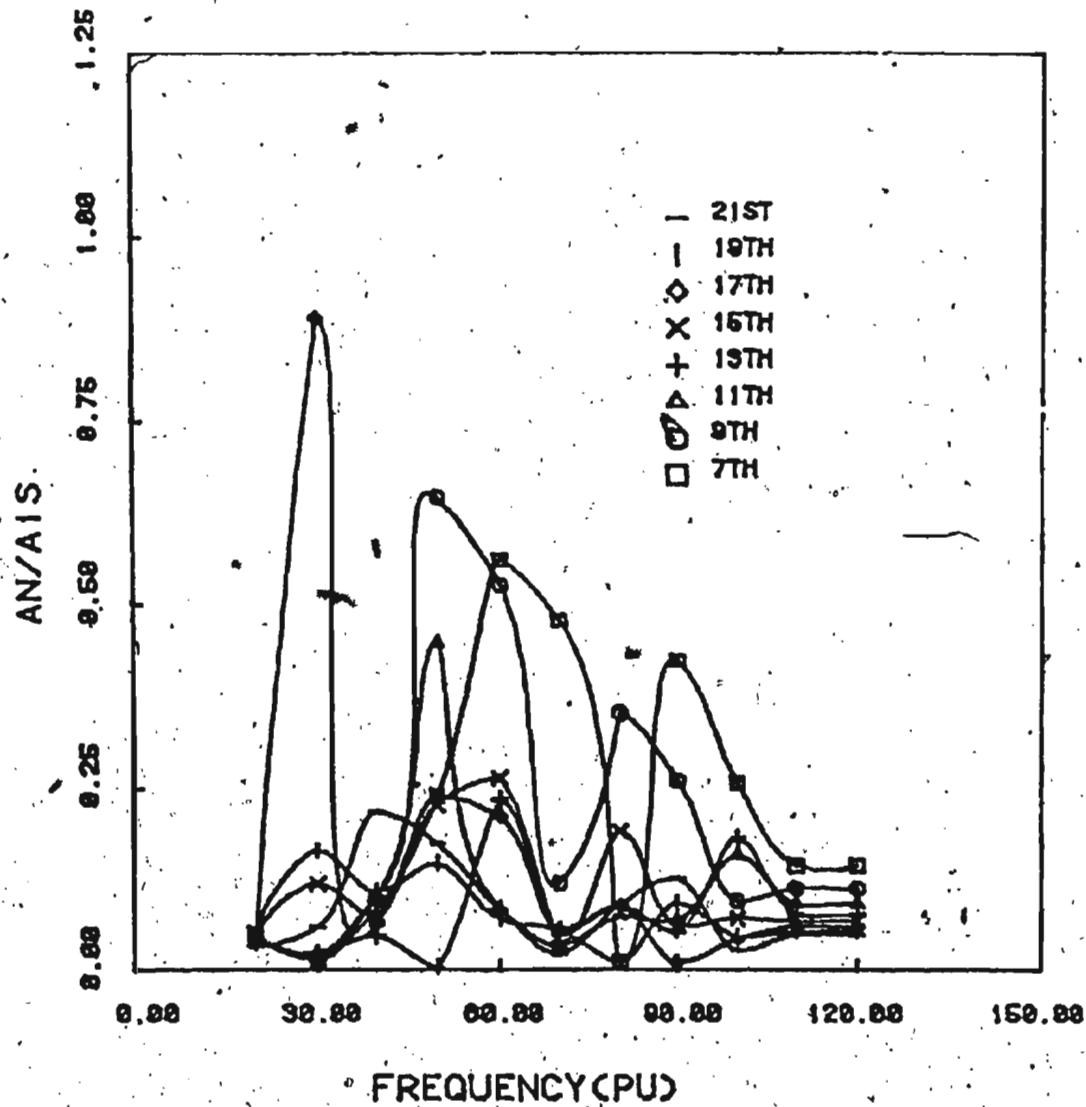


Fig. 2.8 Variation of dominant harmonics at  $V_R = 5.5V$

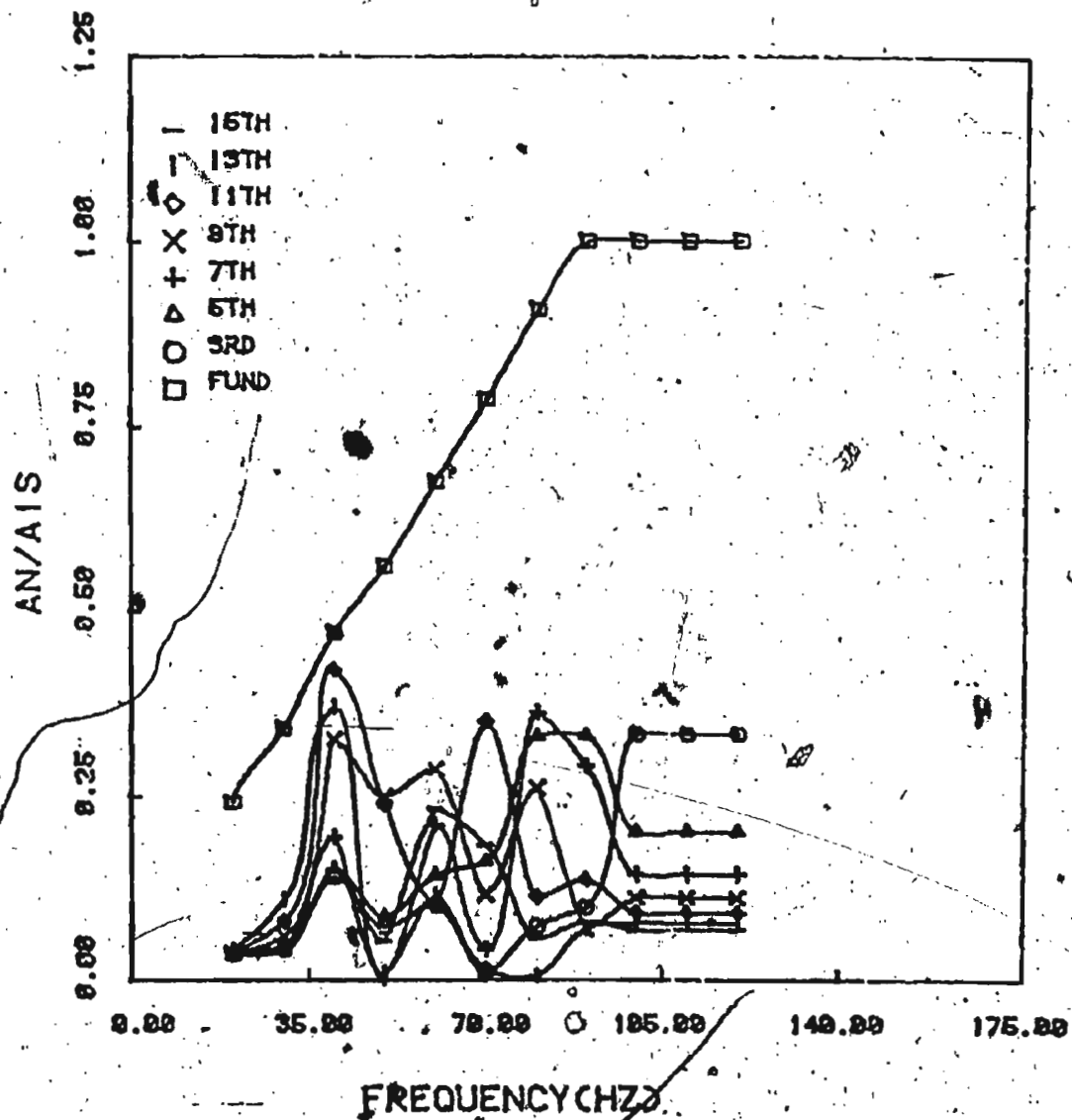


Fig. 2.7

Harmonics of DM inverter output at various operation frequencies

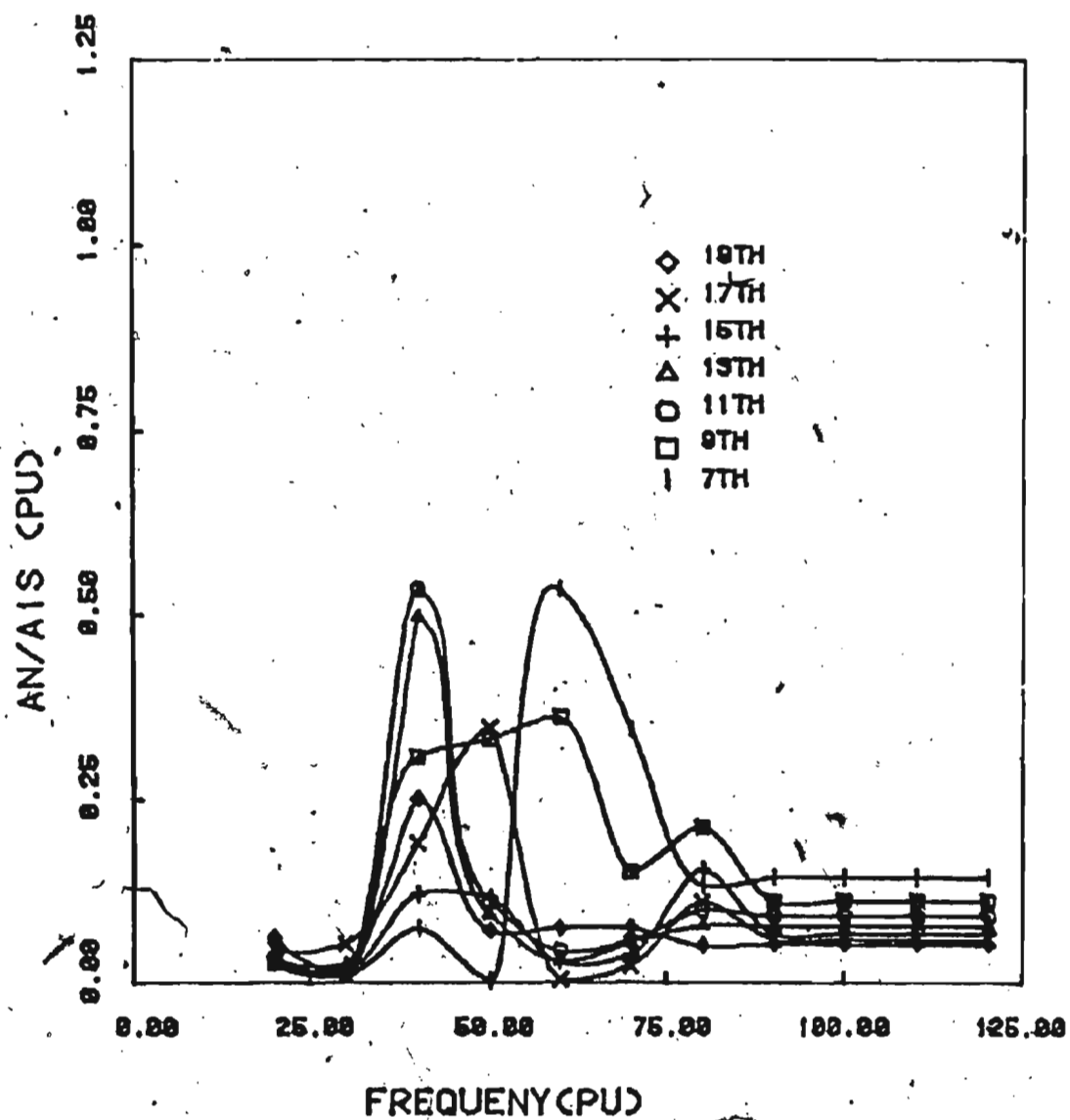


Fig. 2.9 Variation of dominant harmonics at  $V_R = 7.5V$

the carrier wave. At 50 Hz operation the dominant harmonics are 9th and 11th operating at 450 Hz and 550 Hz, respectively. Ripple frequency in this case is about 650 Hz as shown in Fig. 2.10. This shows that the effect of harmonics can be neglected with passive R-L Load or dynamic motor loads.

The dominant harmonics vs frequency plots of Fig. 2.8 and 2.9 show that the harmonic contents at the inverter output can be reduced by changing the modulating index  $m = \frac{V_R}{\Delta V}$  at any frequency of operation. This change can be readily attained by changing the amplitude  $V_R$  of the modulating sine wave. This can be done without any further modification of the circuits. This is advantageous for low frequency operation of inverters. At low frequency operation, the ripple frequency of carrier wave is low. The dominant harmonics at low frequency can be brought down by changing the modulating index  $m$  simply by changing the amplitude of modulating sine wave.

### 2.3.1 Ripple Frequency of Carrier Wave and Number of Commutation in Delta Modulation

Number of commutation in any inverter is an important feature of the inverter. The increase in commutations results in increased commutation losses of the inverters. Some applications such as the uninterruptible power supply system, requires the commutation in the inverters to be limited for the lowest commutation losses as

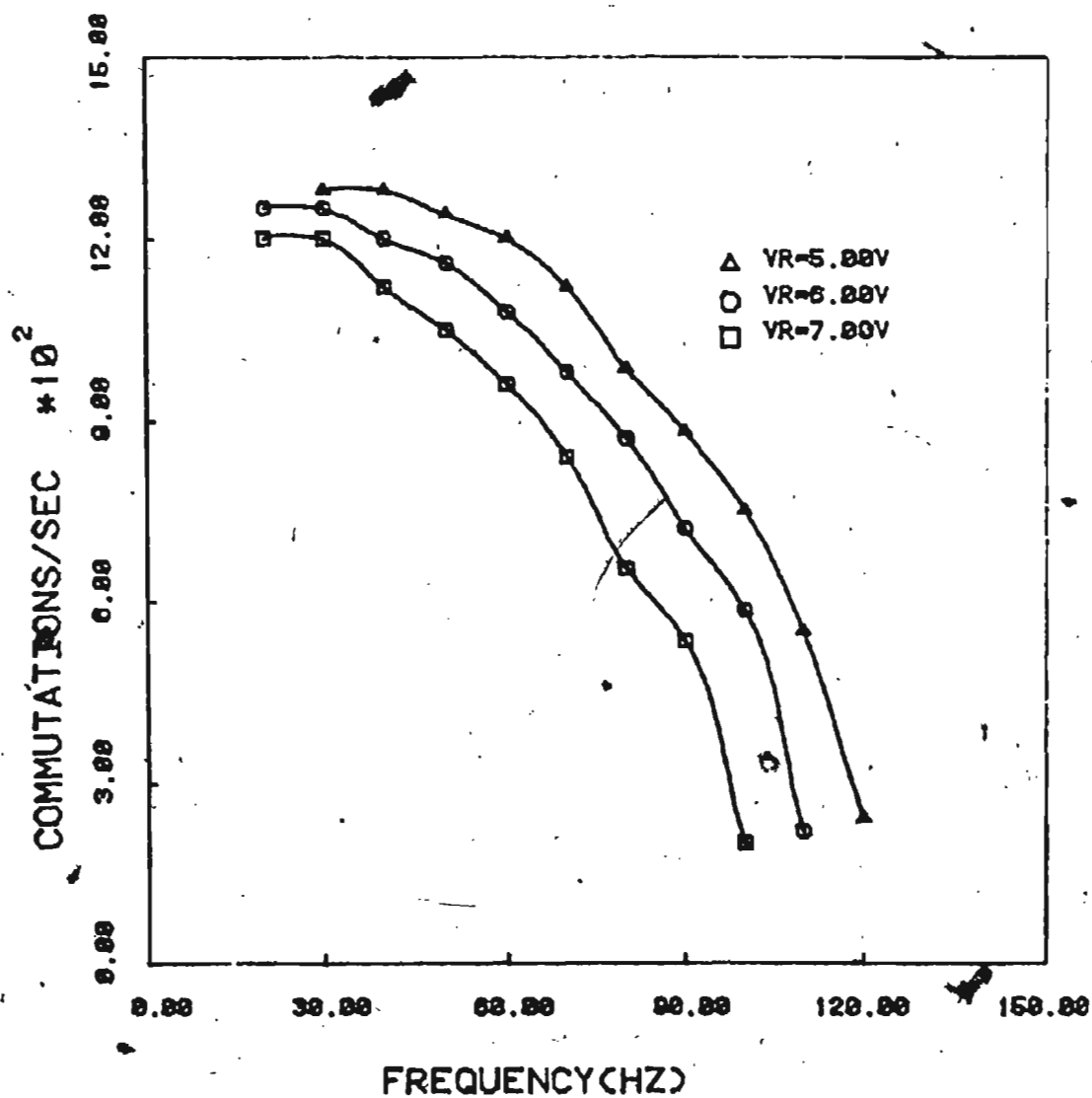


Fig. 2.10 Variation of number of commutation with changing modulating signal level

well as for perfect commutation process. In delta modulation the commutation number depends on the ripple frequency of the carrier wave. Because each ripple cycle corresponds to two transition points in the modulated waveform  $V_I$ , each of these transition points corresponds to a commutation in the inverter. In the delta modulation, if the window width  $\Delta V$  of Fig. 2.1 is kept constant, the ripple frequency  $\omega_r$  varies as the amplitude of the modulating wave varies. The decrease in  $V_R$  increases the ripple frequency, while the increase in  $V_R$  decreases the ripple frequency. In the delta modulation implementation circuit of Fig. 2.4, the window width  $\Delta V$  is determined by the circuit constants and the logic supply voltage as

$$\frac{\Delta V}{V_s} = \frac{R_2}{R_3} \quad 2.3.12$$

For particular  $V_R$ , the maximum number of commutation is given by [30]

$$N_{CM} = \frac{1}{2R_1C} \cdot \frac{R_3}{R_2} \quad 2.3.13$$

The design of logic circuit for delta modulation can be done for a certain maximum allowable number of commutation per second by choosing the appropriate capacitors and resistance in the circuit. The number of commutation at any operating frequency can be changed by changing  $V_R$ .

Since number of commutation is related to the number of modulated pulses per cycle, another easy way of finding the number of commutation is to determine the number pulses/cycle. The details are given in appendix B.

The pulse termination position is given by

$$\delta_1 = \Omega_r t_1 \quad 2.3.14$$

where  $t_1$  is given by equation 2.3.1. Solution of the equation (2.3.14) for  $\delta_1$  at  $\delta_1 = \pi$ , gives the number of pulses/half cycle of the modulating wave  $V_R$ .

$$i = N_p \quad [\text{f\"or } \delta_1 = \pi] \quad 2.3.15$$

where

$N_p$  = number of pulses for half cycle

The number of commutation per second is given by

$$N_c = 2 * N_p * f_r \quad 2.3.16$$

The ripple frequency of the carrier wave is given by

$$f_r = \frac{N_c}{2} \text{ cycles/second} \quad 2.3.17$$

Equations (2.3.14) and (2.3.17) are solved for varying frequency. The results are plotted in Fig. 2.10 with various values of modulating signal level  $V_R$ . The results show that without changing any circuit parameters, the number of commutation can be changed by varying  $V_R$  only. This gives a choice of changing number of commutation in delta modulation as desired.

## 2.4 Experimental Verification for Delta Modulation Technique

This section deals with the verification of the analysis of delta modulation carried out so far. The implementation of the logic circuits and verification of the main features of delta modulation are described in the following subsections in detail,

### 2.4.1 Implementation of the Logic Circuits

The basic circuit used for the delta modulation is shown in Fig. 2.4. Before the output of the modulator circuit can be used for the inverter SCR operation, the signals are to be processed through the logic circuits to produce appropriate gating signals for the main and commutation thyristors. Such a logic circuit was developed. The timing diagram of the signals and logic diagram are shown in Fig. (2.11) and (2.12) respectively. Details of the logic implementation are given in Appendix II. The circuit parameters for circuit in Fig. (2.4) are chosen as

$$R2 = 10 \text{ k ohm}$$

$$R3 = 100 \text{ k ohm}$$

$$C = .068 \text{ micro farad}$$

The design was based on maximum commutation number of 1500-1600 at 30 Hz operation for  $m = 1$ , the output waveforms of this circuit are shown in Fig. 2.13 for 30 Hz, 50 Hz and 90 Hz operation respectively. The oscillographs clearly indicate gradual transition from PWM mode to pure square wave



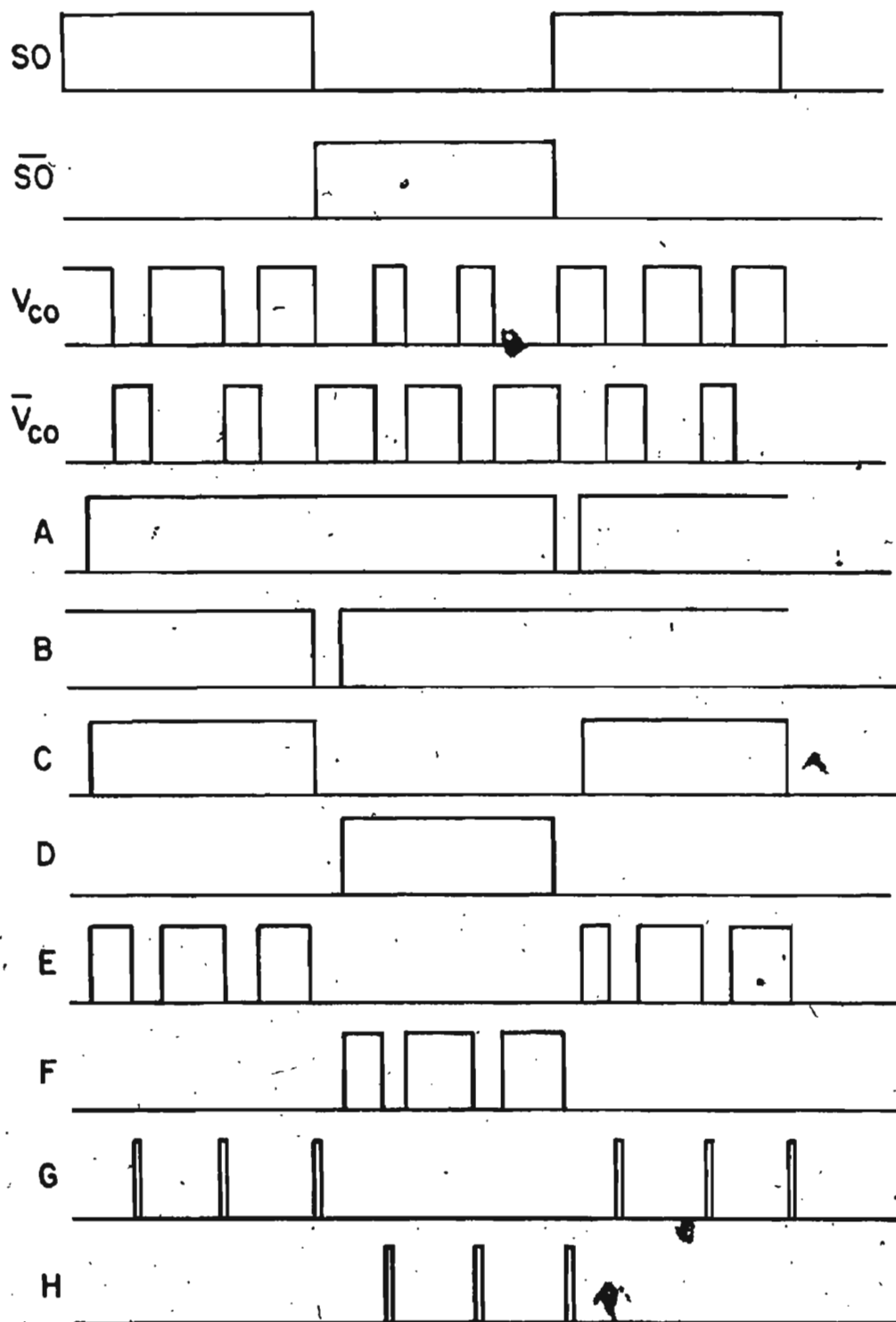


Fig. 2.11 Timing diagram of switching signals of single phase DM inverter



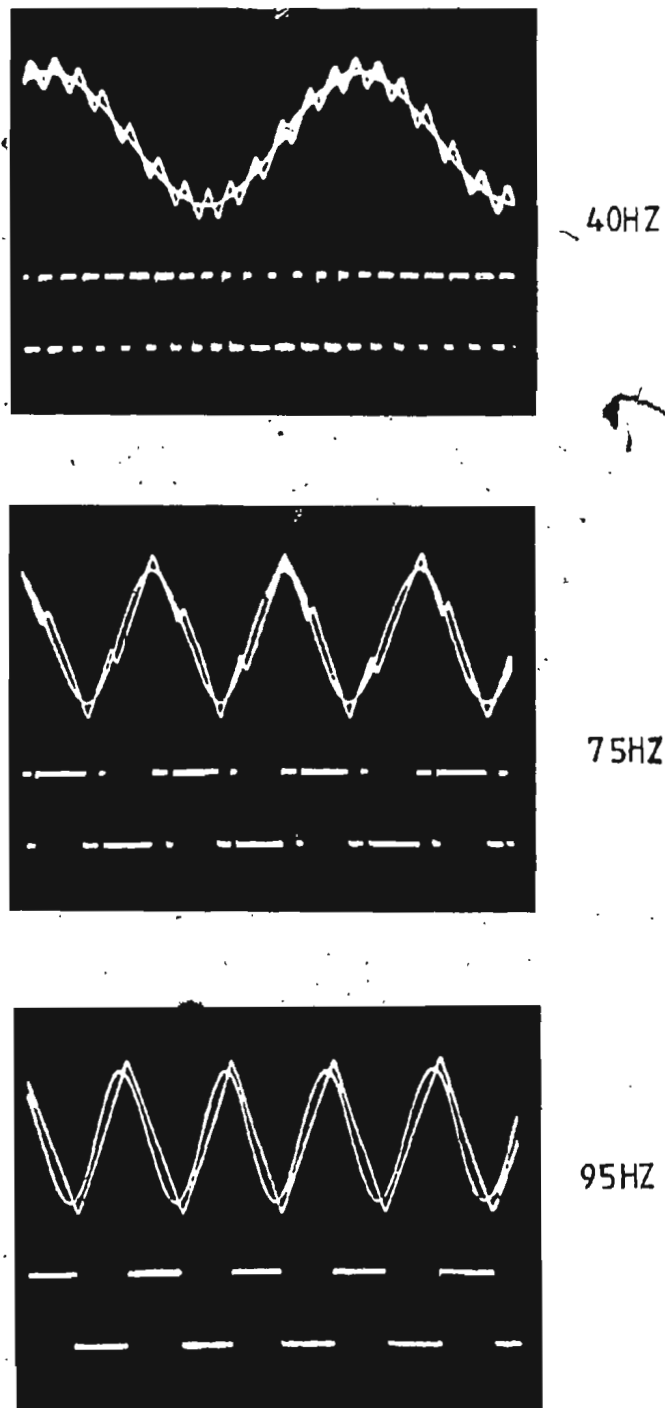
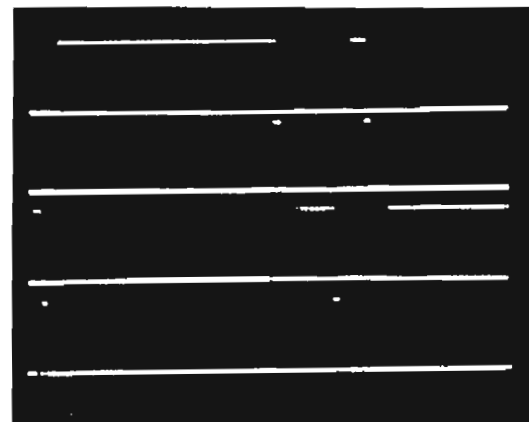
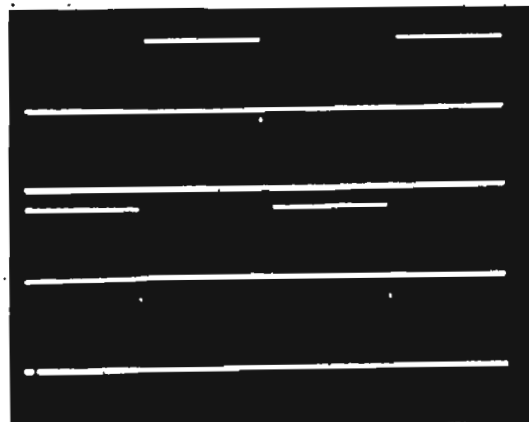


Fig. 2.13

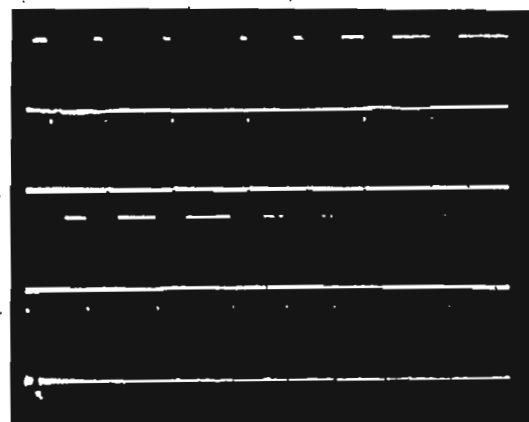
Illustration of practically obtained waveforms  
of delta modulation circuit of the inverter



75HZ



90HZ



40HZ

Fig. 2.14 Actual switching waveform at the output of the logic circuits at various frequencies

mode. Fig. 2.14 shows the actual signals generated by the modulated wave for the main and commutation thyristors of an inverter at 30 Hz and 70 Hz operation. The main thyristor signal is modulated with high frequency pulses of 1/3 rd duty cycle to avoid pulse transformer saturation in the inverter.

#### 2.4.2 Volts/Hz Characteristics of Delta Modulated Inverter Output

It has been shown in section 2.3.1 in the analysis of the delta modulation that the ratio of the fundamental output voltage to frequency remain constant from low frequency operation to base frequency. Beyond base frequency the fundamental voltage becomes constant as the transition from pulse mode to square wave takes place. This fact was verified experimentally with spectrum analysis of the output signal of the delta modulator using a spectrum analyzer. Figs. 2.16(a) to 2.16(d) show spectra for 20 to 120 hertz of operation of the modulator in the steps of 10 hertz. The spectrums clearly show that as the frequency of operation increases, the fundamental component also increases linearly.

A plot of fundamental for frequencies varying from 20-120 Hz is drawn in Fig. 2.15. These were obtained from experimental spectrums. Fig. 2.15 shows that the volts/hertz constant characteristics for fundamental voltage is realizable in practice without additional complexity in the control circuitry. The practically obtained V/f characteristics of Fig. 2.15 is comparable to theoretical V/f characteristics

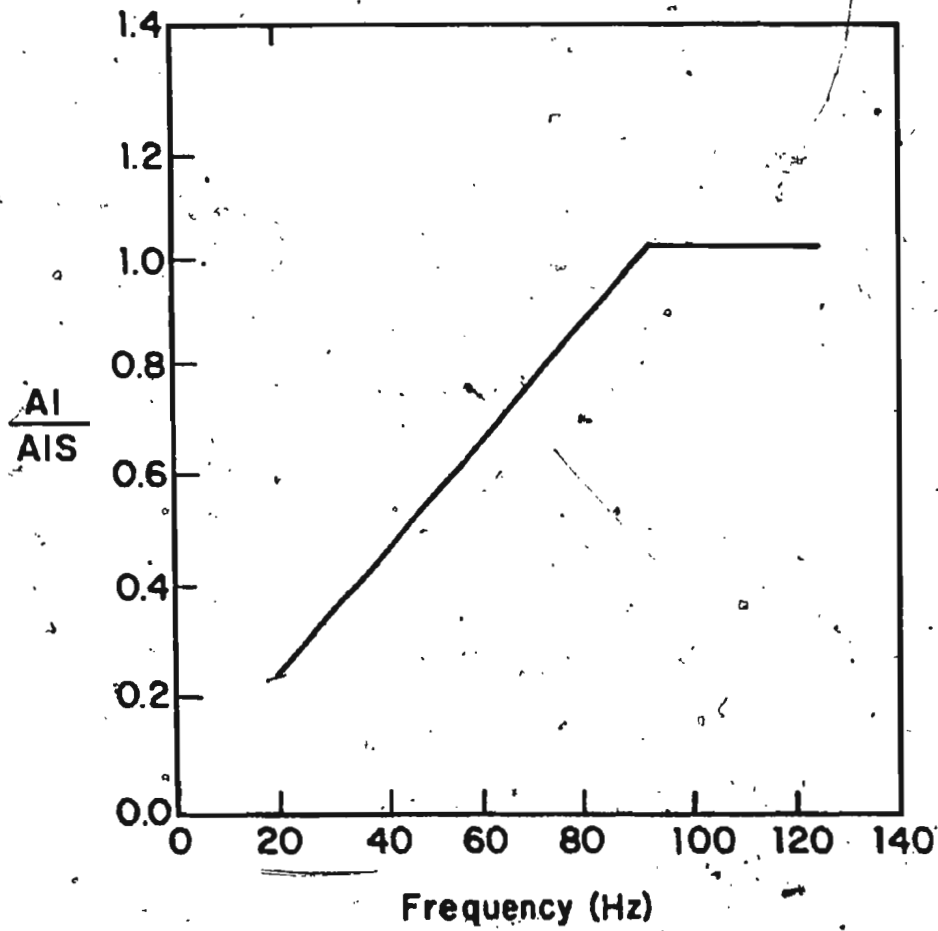


Fig. 2.15 Experimentally obtained fundamental voltage to frequency characteristics of DM inverter

Fig. 2.16(a) Frequency spectrum of delta modulated wave at various frequencies

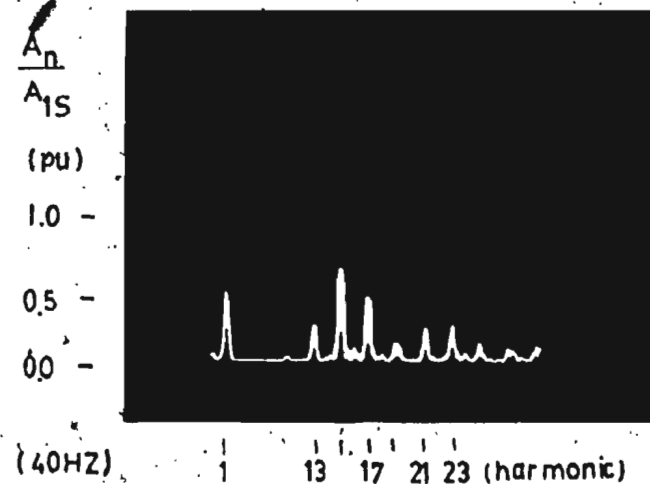
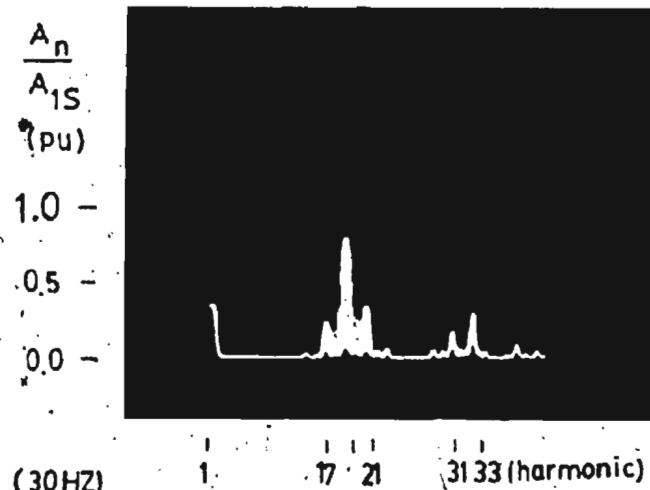
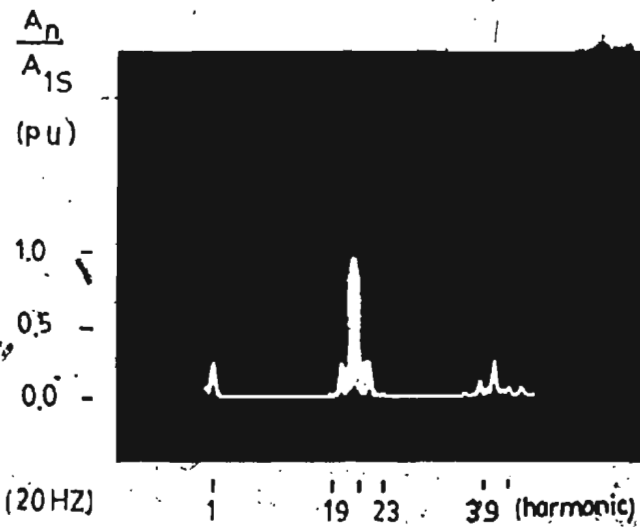


Fig. 2.16(b) Frequency spectrum of delta modulated wave at various frequencies

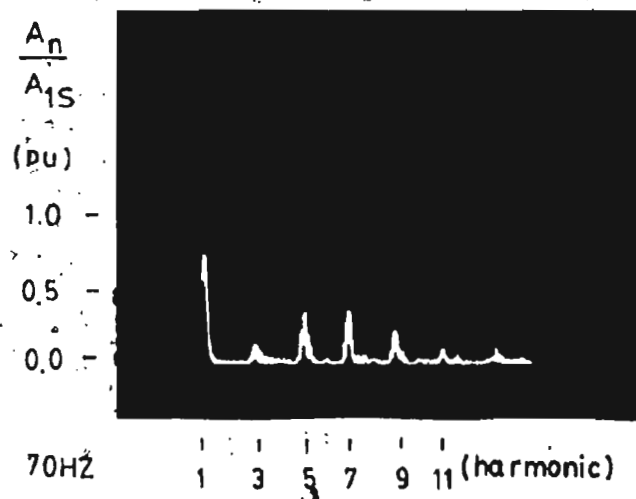
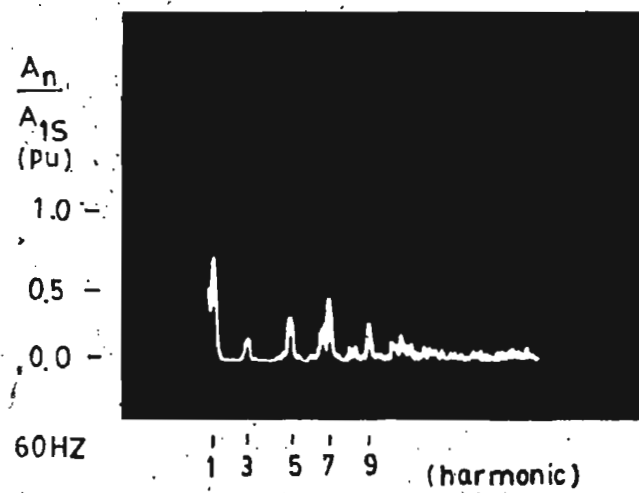
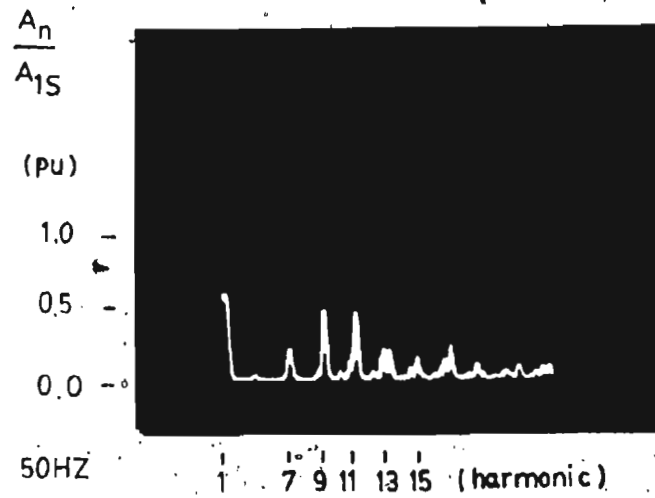
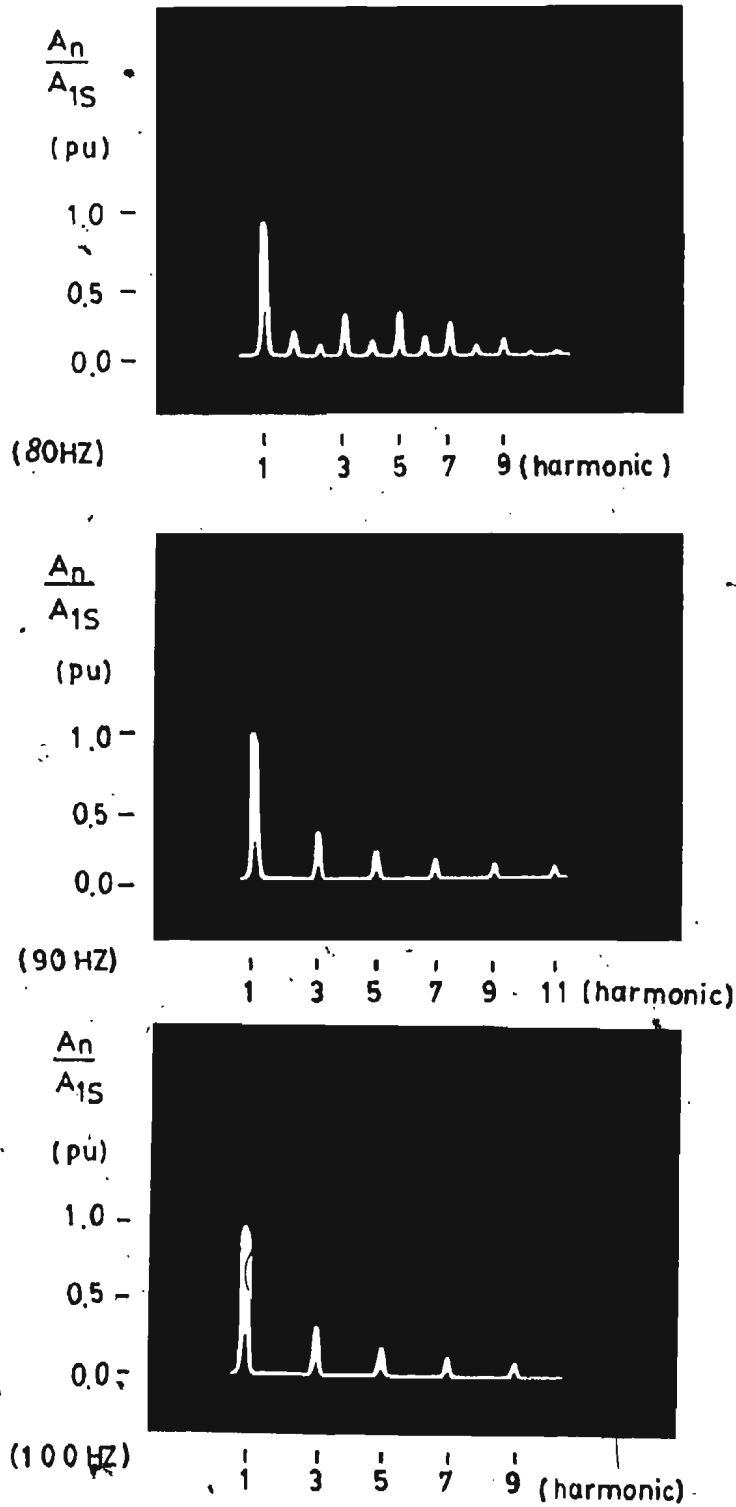




Fig. 2.16(c) Frequency spectrum of delta modulated wave at various frequencies



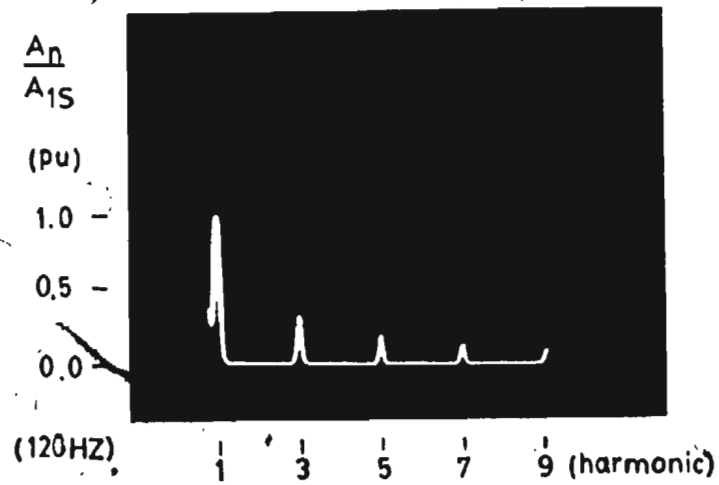
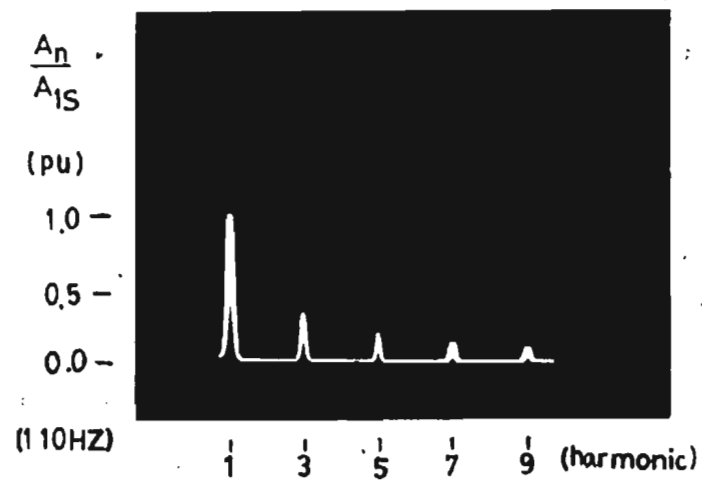


Fig. 2.16(d) Frequency spectrum of delta modulated wave at various frequencies

obtained previously in Fig. 2.6. Figs. 2.15 and 2.16 verify the fact that beyond base frequency the fundamental voltage to frequency ratio increases as the fundamental voltage remains constant due to the fact that the modulated wave is converted to constant amplitude square wave beyond base frequency.

#### 2.4.3 Harmonics in Delta Modulated Inverter

It was mentioned in section 2.3.1 that at low frequency operation, the dominant harmonics occur at low frequencies; and at high frequency operation, the dominant harmonics take place at higher frequencies. This is because dominant harmonics occur at or near the ripple frequency of the triangular carrier wave. At high frequency operation the fundamental becomes prominent and the harmonic components are small in magnitude. These results were obtained from the Fourier analysis of delta modulated wave theoretically. Practically, the output of the delta modulated wave was analyzed with the help of Hewlett Packard spectrum analyser, (Model 85520).

Fig. 2.17 shows that the fundamental voltage increases linearly with frequency upto base frequency and maintains a constant level after base frequency. At lower frequency of operation, the magnitude of the lower harmonics (3rd, 5th and 7th) are low, whereas the magnitude of the higher harmonics are greater. At high frequency operation,

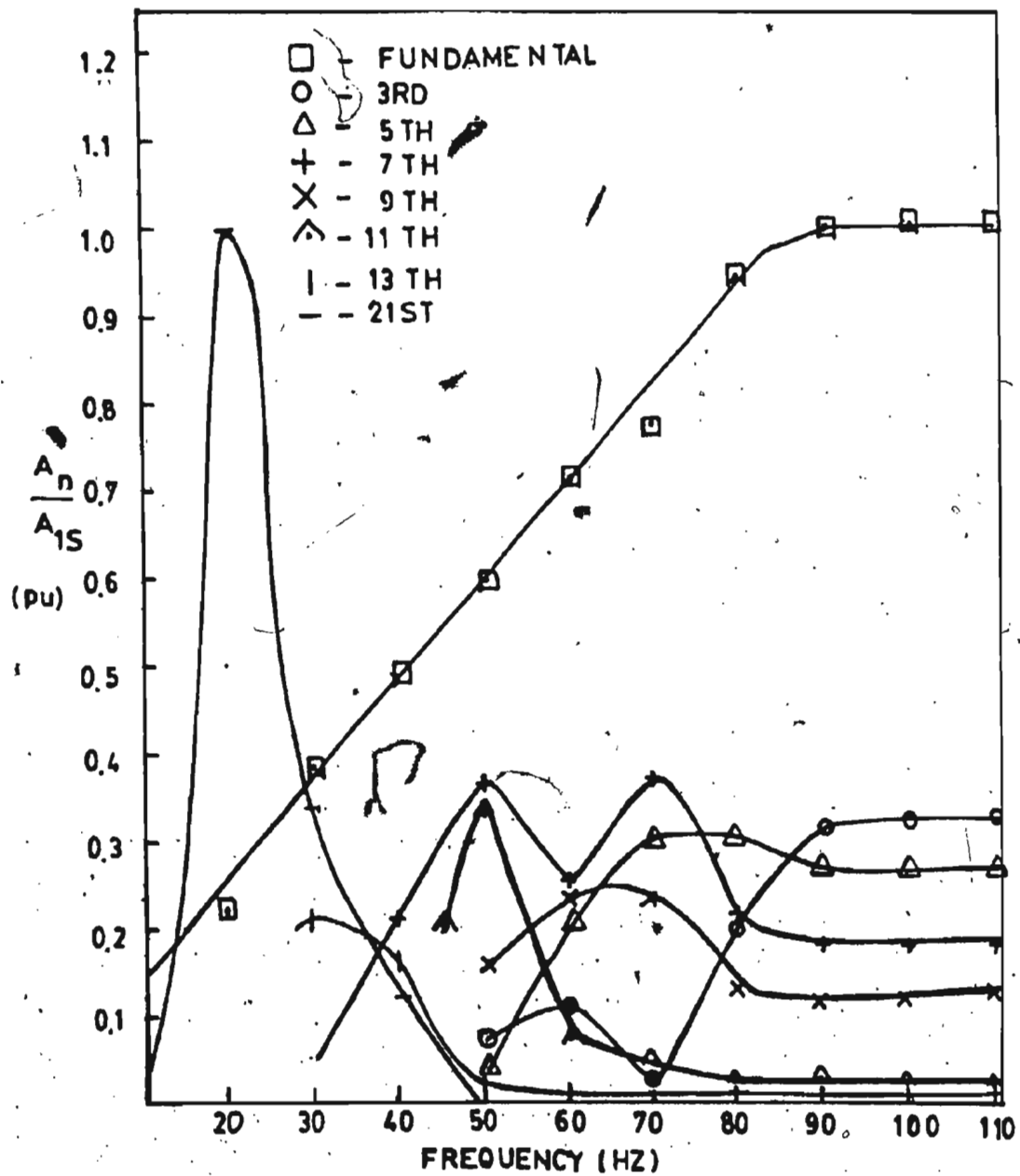


Fig. 2.17

Harmonic contents of the delta modulated wave  
at  $V_R = 6.75V$

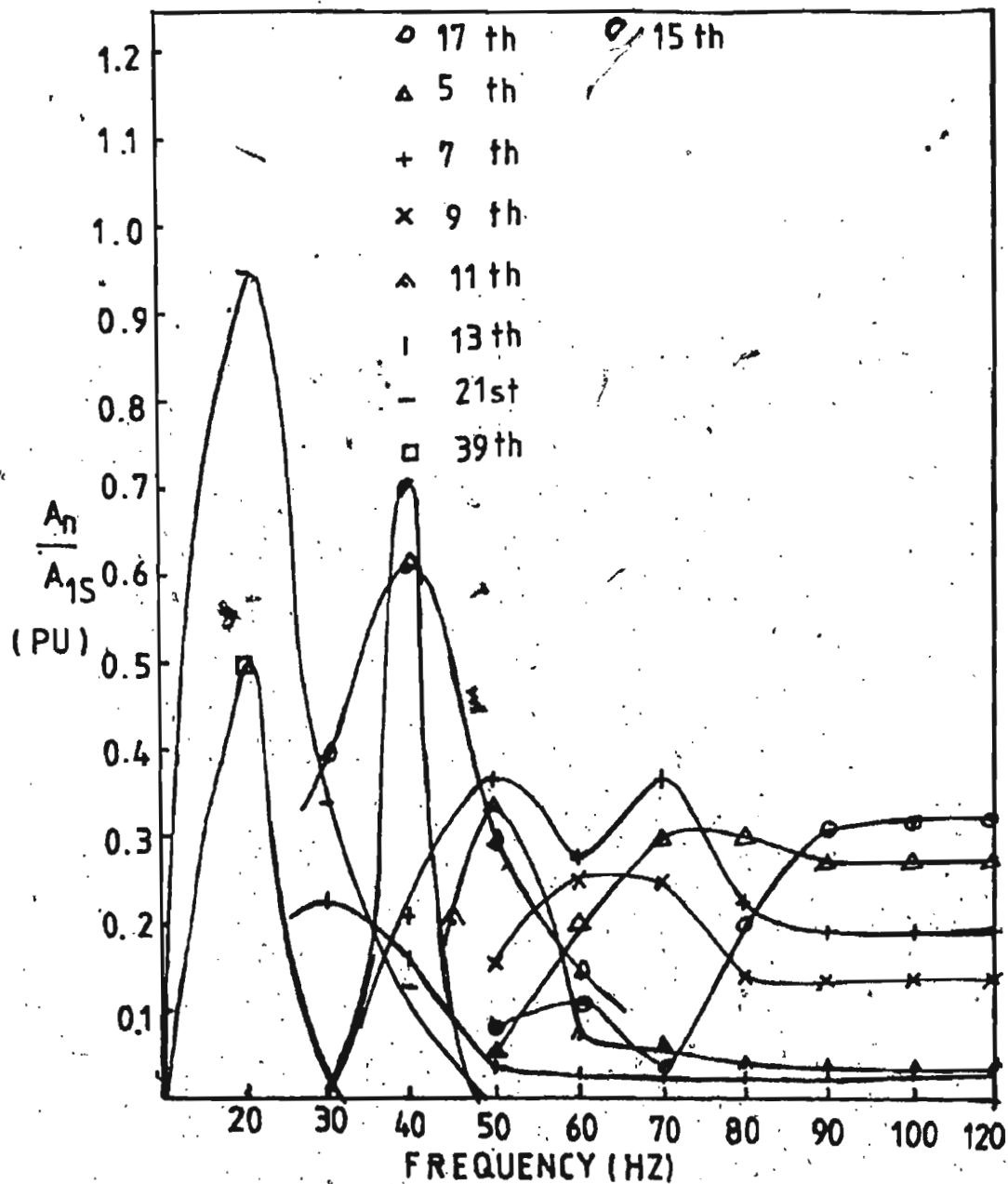


Fig. 2.18 Dominant harmonic contents of delta modulated inverter output at  $V_R = 6.75V$

the higher harmonics gradually decreases and the prominence of fundamental increases. It is quite evident in Figs. 2.17 and 2.18.

Another feature in delta modulation as indicated in section 2.3.1 is the harmonic contents of the modulated wave can be reduced at lower frequency of operation by changing the amplitude modulating signal  $V_R$ . This can be done at ease without further modification in circuit. The effect of change of  $V_R$  on the harmonic contents is shown in Fig. 2.17 and 2.18. It is evident from the Fig. 2.17 to 2.18 that the harmonic contents of the modulated wave are effected with the change in the value of  $V_R$ .

#### 2.4.4 Number of Commutations

Number of commutations in delta modulated inverter is determined by the ripple frequency of the triangular carrier wave, which in turn is dependent on the magnitude of the modulating sine wave once the control circuit parameters are specified. Number of commutation is associated with commutation losses in an inverter and the commutation takes place in every switching point of the modulated wave pulse. Usually the control circuit for the modulator is designed with maximum allowable number of commutation, which sets the values of  $R_2$ ,  $R_3$  and  $C$  of the control circuit of Fig. 2.4. However during operation, this number of commutation per second can be changed by modulating the  $V_R$  signal or in other

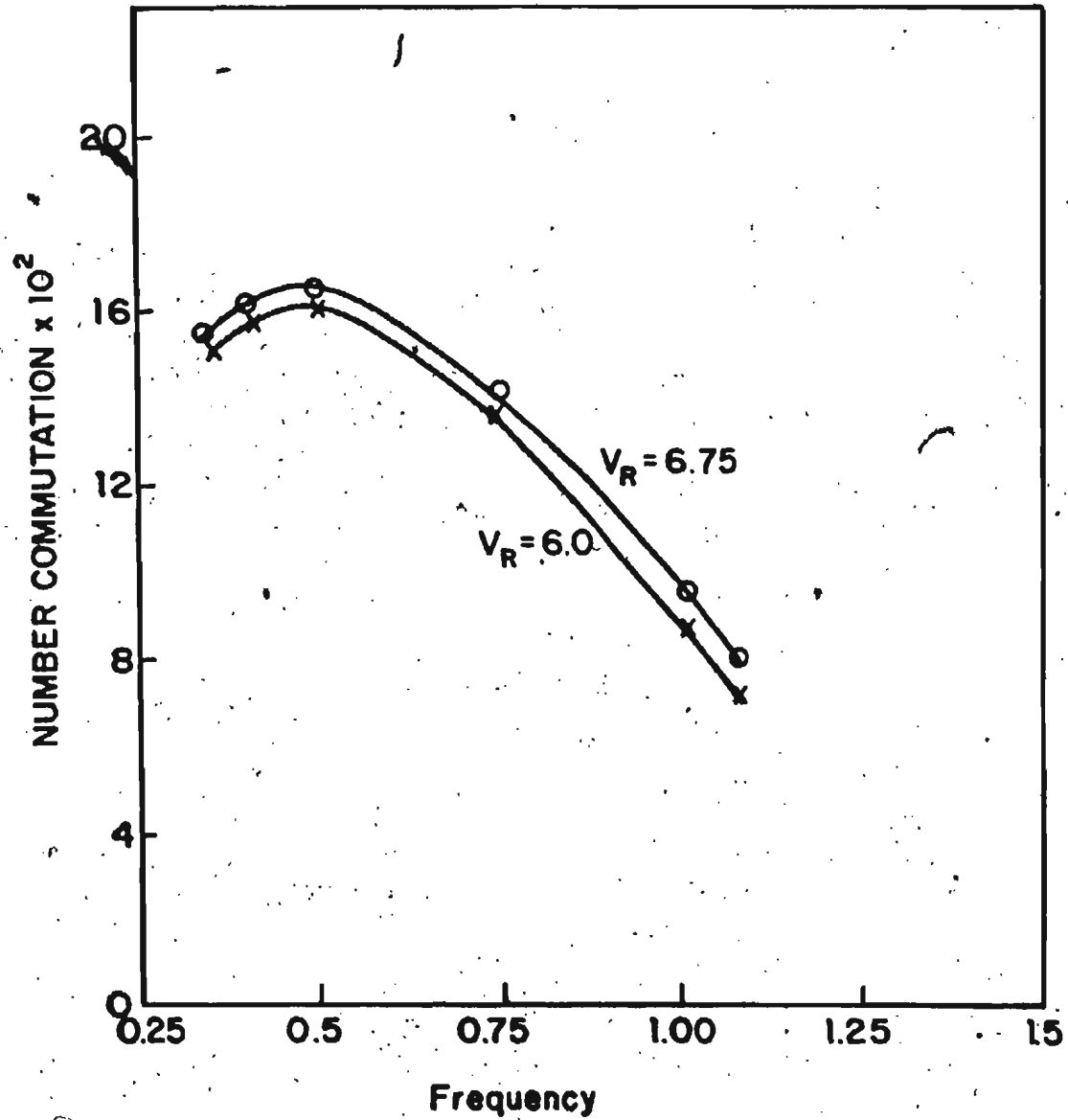


Fig. 2.19 Variation of number of commutation with frequency for various values of  $V_R$

words changing the modulation index. Number of commutation is largest when the frequency of operation of the inverter is low and it decreases as the frequency of operation of inverter goes up. Fig. 2.19 shows the variation of commutations as a function of modulating index. Thus the experimental results compare favourably with those obtained theoretically, as shown in Fig. 2.10.

## 2.5 Comparison of Delta Modulation with Sine Modulation

The commonly used modulation technique for the inverters at present is sine modulation. This method uses a reference sine wave and a carrier triangular wave to produce the required switching pulses for the thyristor of an inverter. A simple realization of the sine PWM is done. However in practice such control circuits require various complex modifications and additions to meet the needs of the loading nature of the inverter. Basically, sine modulation was introduced to reduce the harmonics at the output of the inverter. Practically the modulation index and the pulse number per half cycle determine the harmonics of the modulated wave. This is shown by Fourier analysis of the sine PWM. The Fourier coefficients of sine modulated wave is given (Appendix-E) as:



$$\begin{aligned}
 A_n &= \sum_{i=1,2,\dots}^N \frac{2E_{dc}}{\pi} \int \left[ \frac{2i-1}{2} \Delta + \frac{\delta_i}{2} \right] \sin(n\omega t) d\omega t \\
 &\quad - \left[ \frac{2i-1}{2} \Delta - \frac{\delta_i}{2} \right] \sin(n\omega t) d\omega t \\
 &= \frac{4E_{dc}}{n\pi} \sum_{i=1}^N \left\{ \sin\left[n\left(i-\frac{1}{2}\right) \frac{\pi}{N}\right] \sin n \frac{\delta_i}{2} \right\} \quad 2.5.1
 \end{aligned}$$

where

$N$  = Number of modulated pulses/half cycle

$\delta_i$  = pulse width of the  $i$ th pulse

$\Delta = \frac{\pi}{N}$  = distance between successive pulses

$E_r$  = maximum carrier wave voltage

$E$  = maximum reference sine wave voltage

$\theta_i$  = pulse location =  $\frac{(2i-1)\pi}{2N} = \frac{2i-1}{2} \Delta$

$w = \frac{E}{E_r}$  = modulation index

the pulse width of  $i$ th pulse is given by

$$\delta_i = \Delta w |\sin \theta_i| \quad 2.5.2$$

The detail derivation for sine PWM is given in appendix V. The Fourier coefficients expressions clearly indicate that the harmonic contents depend on the number of pulse/half cycle and the modulation index. The harmonic analysis is illustrated in Fig. 2.20 and 2.21 showing harmonics in sine modulated inverter with modulation index. The figures 2.20 and 2.21 show that there exists an optimum number of pulses/

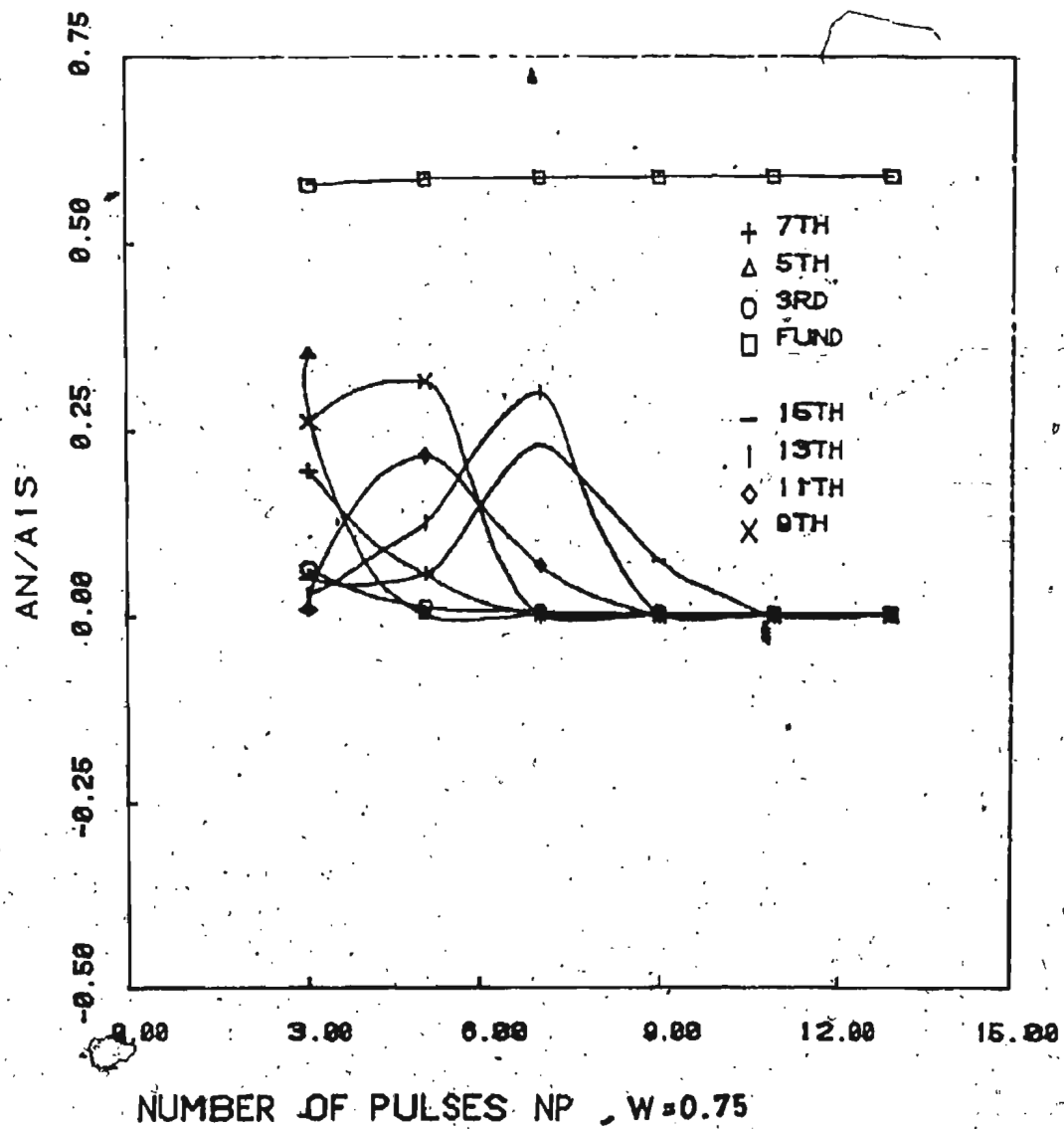


Fig. 2.20(a) Variation of harmonics in a sine modulated wave (modulation index = 0.75)

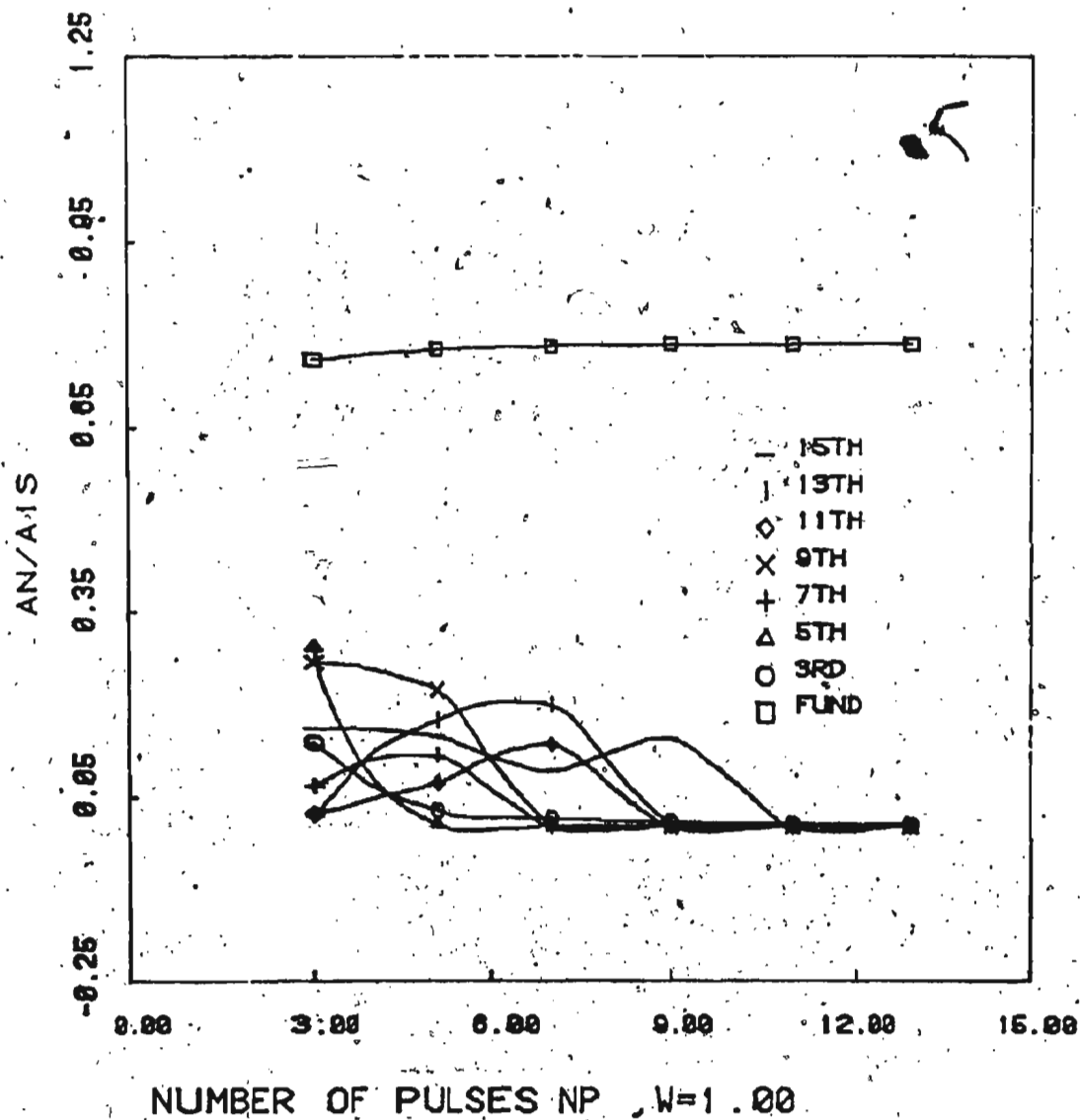


Fig. 2.20(b) Variation of harmonics in a sine modulated wave (modulation index = 1.00)

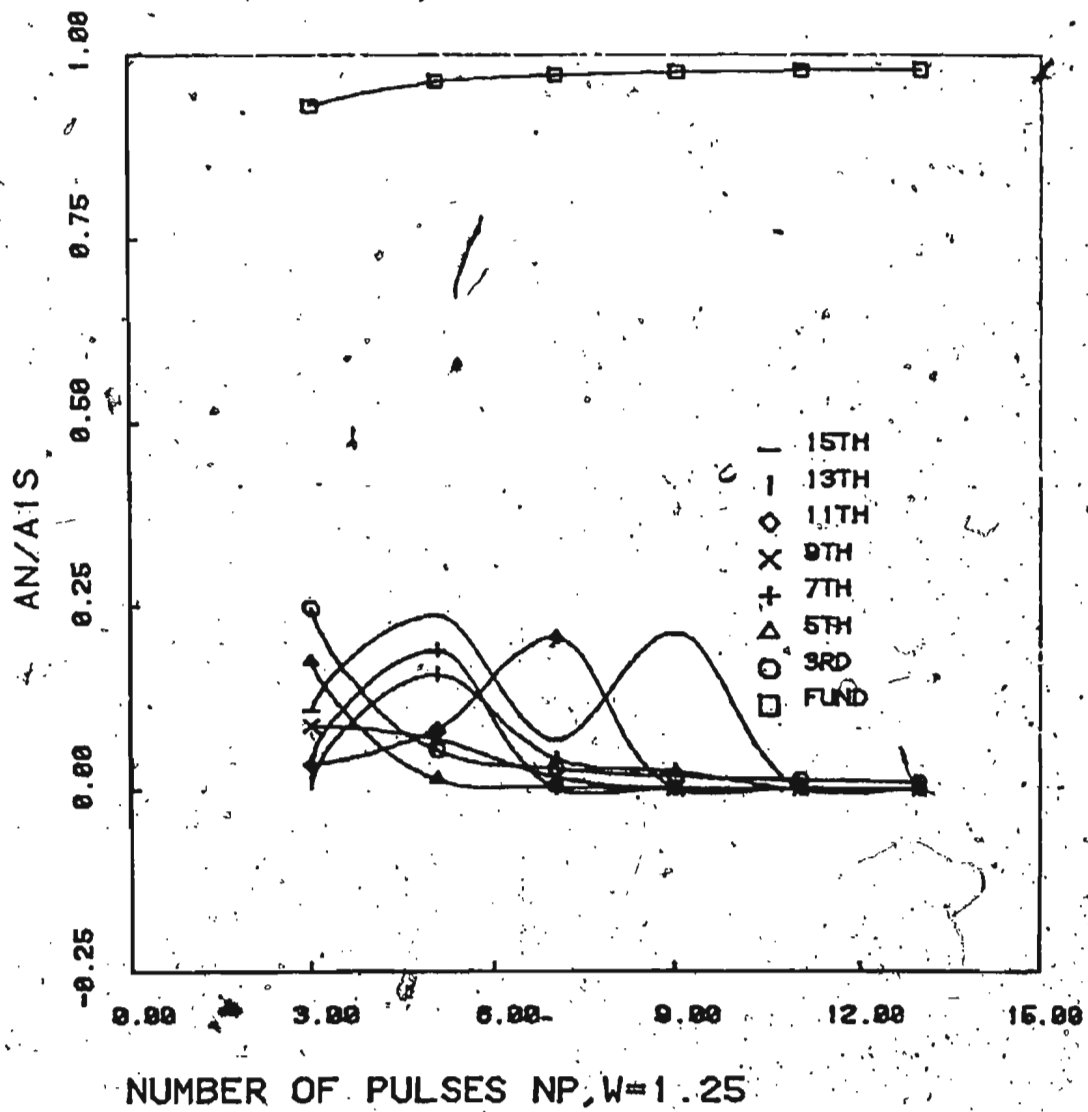


Fig. 2.20(c) Variation of harmonics in a sine modulated wave (modulation index = 1.25)

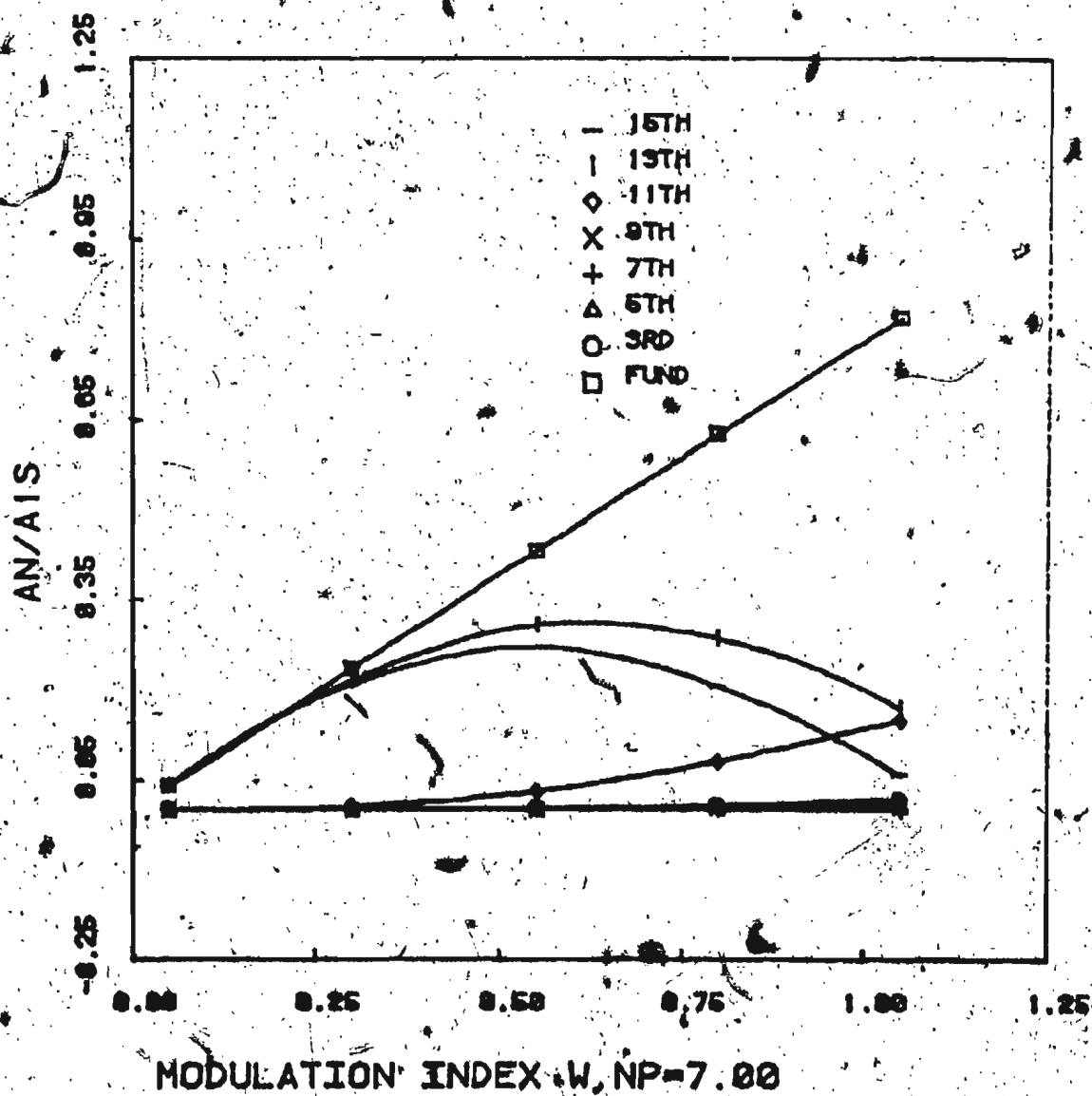


Fig. 2.21(a) Variation of harmonics in a sine modulated wave  
(Number of pulses = 7.00)

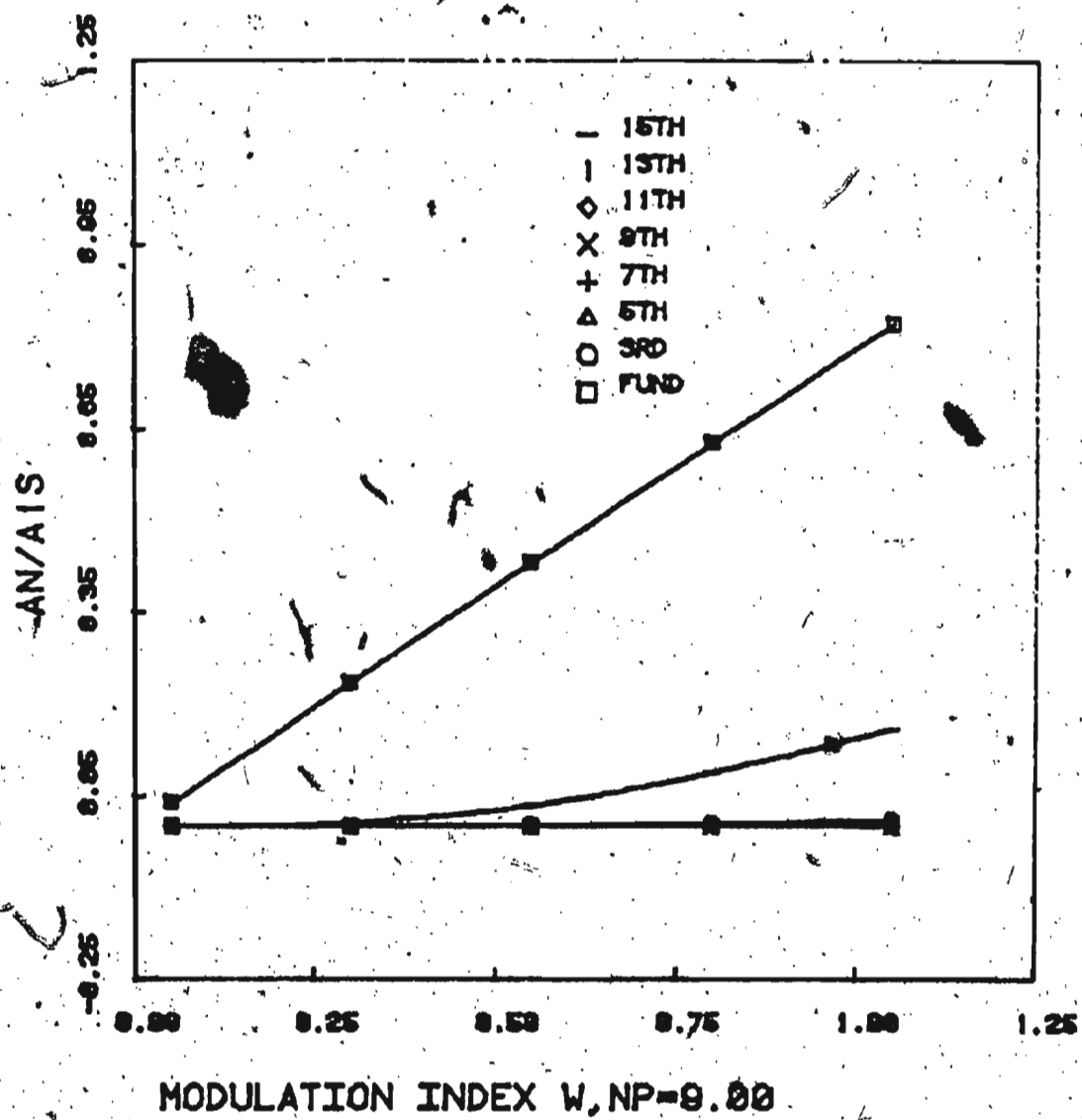


Fig. 2.21(b) Variation of harmonics in a sine modulated wave  
(Number of pulses = 9.00)

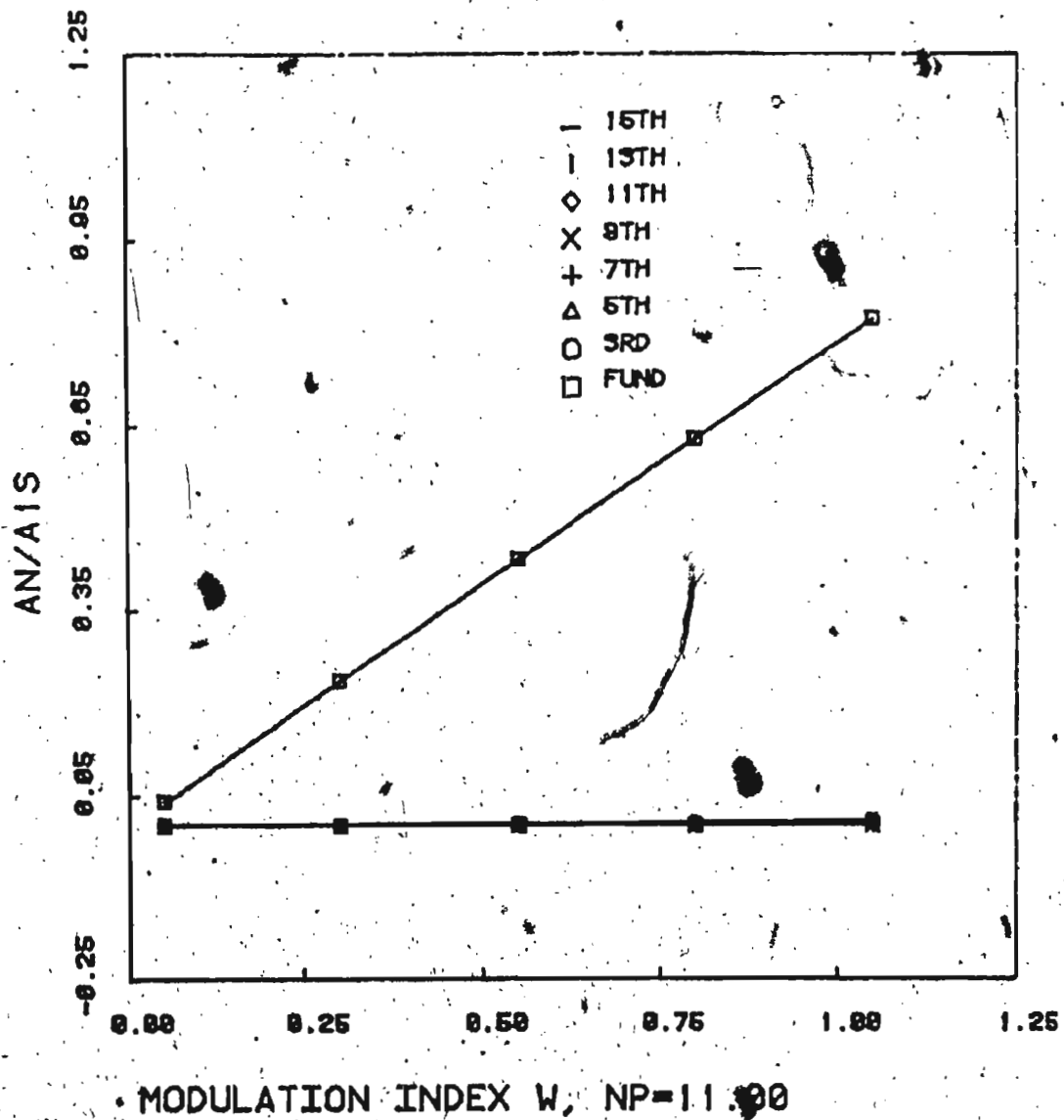


Fig. 2.21(c) Variation of harmonics in a sine modulated wave  
(Number of pulses = 11.00)

half cycle for a particular modulation index, which gives rise to the lowest harmonic contents at the output. Any other number of pulses per half cycle increase the harmonic contents at the output of the inverter. The number of pulses in a practical implementation is determined by the ratio of modulating wave frequency to the carrier wave frequency ( $f_r/f_c$ ). For a particular number of pulse per half cycle, this requires the ratio of  $f_r/f_c$  to be kept constant at certain value. As also evident from the harmonics plots in Fig. 2.21 the harmonic contents also depend on the modulation index  $m$ . At higher modulation index, the pulse width is no longer a function of the modulating wave at all the rising and falling edges of carrier wave. Consequently, the harmonic contents increases since the pulse widths do not continue to be the function of a sinusoid. The number of pulses and modulation index criterion necessitates additional control circuitry in the modulator to give a satisfactory operation. It is a standard practice in sine PWM to have two, and only two intersection of triangular carrier wave with sine modulating wave during each period of triangular wave. This implies a frequency limitation in sine modulation. For sine wave frequency less than the frequency of triangular wave more than two intersection occur in one time period of triangular wave and the generation of PWM by comparison of waveforms clearly breaks down. This requires



proper synchronization of the carrier triangular wave with the modulating wave in order to find a well defined cross over of carrier with modulating wave. This is achieved by changing the carrier wave frequency with sine modulating wave. In doing so, the condition of  $f_r/f_c$  ratio is set to be an integer number to avoid introduction of unwanted harmonics. All these requirements increase the circuit complexity in sine PWM. Furthermore, any special mode of operation, like the constant volts per hertz upto base frequency and constant power mode thereafter, requires special current and voltage controls to be added in the modulation circuits. Various control techniques were evolved to solve these and other requirements of sine modulation technique.

But in the case of delta modulation technique, it is already shown that most of these requirements are met by simple logic circuit implementation without additional control circuitry. Its inherent property of lower harmonic content at higher frequency operation, easy control of harmonic contents by modulating the sine reference signal ( $V_R$ ) and the inherent property of volts per hertz control, would make the delta modulation competitive with sine modulation techniques for applications in ac motor drives, particularly PM synchronous types. Delta modulation technique gives rise to higher harmonic contents at low frequency operation, but the dominant harmonics in such low

frequency operation are the higher harmonics beyond the 7th or above, whose magnitudes are usually low. Since the dominant harmonic frequencies are the high frequency ones, they can be easily filtered out. This is another advantage of delta modulation over sine modulation.

### CHAPTER 3

This chapter covers the basic operation of delta modulated inverter with passive loads. The analytical results obtained for delta modulated inverter in previous chapter are used in predicting performance of passive loads with inverter supply. The passive loads considered are resistive and R-L loads. Inverter equations are used to predict the load current, power, voltage and power factor. The validity of some of the features of delta modulated inverters are verified with passive load conditions. Theoretical results are verified experimentally for a single phase full bridge delta modulated inverter with passive R and R-L loads.

#### 3.1 Analysis of Delta PWM Inverter with Passive Loads

Like other inverters, the output of a delta modulated inverter is non-sinusoidal and contains harmonics. The harmonics together with the fundamental component, determine the performance of the loads under study. In delta modulated inverter, it is shown in the previous chapter that the harmonic contents are such that, at lower frequency of operation, the lower harmonics are insignificant and higher harmonics are dominant. For high frequency operation, the dominant harmonics are lower harmonics but at reduced

magnitude. The dominant harmonics at the output of the delta modulated inverter determines the current and power to a given passive or active load. For passive loads, the harmonics affect the current, voltage and power of the load and determine the waveshape of load current as well. However, the harmonic components have other implications when the load is active and dynamic.

### 3.1.1 Basic Equations for Passive Loads fed with Inverter

In chapter-2, the basic equations for the harmonic determination of delta modulated inverter output voltage, are developed. The voltage at the output of the inverter is given by the following equations:

$$V_o = \sum_{n=1,3,\dots}^{\infty} (A_n \cos n\omega_r t + B_n \sin n\omega_r t) \quad 3.1.1$$

(valid upto base frequency)

$$V_o = \sum_{n=1,3,\dots}^{\infty} \frac{4V_s}{n\pi} \sin n\omega_r t \quad 3.1.2$$

(valid beyond base frequency)

where the Fourier coefficients  $A_n$  and  $B_n$  are defined in equations (2.3.3) and (2.3.4).

Upto base frequency, the  $n$ th voltage harmonic is given by

$$V_{on} = (A_n^2 + B_n^2)^{1/2} \quad 3.1.3$$

For frequencies beyond the base frequency, the  $n$ th harmonic voltage is given by

$$V_{on} = \frac{4V_s}{n\pi} \quad 3.1.4$$

For passive loads with either R or R-L combination, the load current can be determined by using equations (3.1.1) to (3.1.4). The nth harmonic impedance of the load is given by

$$Z_n = R + n\omega L \quad 3.1.5$$

where R = resistance in ohm

n = harmonic number

$\omega = 2\pi f$ , the angular frequency (rad/sec)

L = inductance in henry

The load impedance value and the magnitudes of the harmonic voltages can be used to determine the load current and power delivered by the inverter to the load.

The current harmonics are given as:

$$I_{on} = \frac{V_{on}}{Z_n} \quad 3.1.6$$

The r.m.s. load current is given by

$$I_{rms} = \left( \frac{I_{01}^2}{2} + \frac{I_{02}^2}{2} + \frac{I_{03}^2}{2} + \dots + \frac{I_{on}^2}{2} \right)^{1/2} \quad 3.1.7$$

Real power to the load can be found by the equation

$$P_L = I_{rms}^2 R_L \quad 3.1.8$$

Also the harmonic current equation (3.1.6) can be used to determine the load current waveshape as:

$$i_o = \sum_{n=1}^{\infty} I_n e^{-jn\omega t} \quad 3.1.9$$

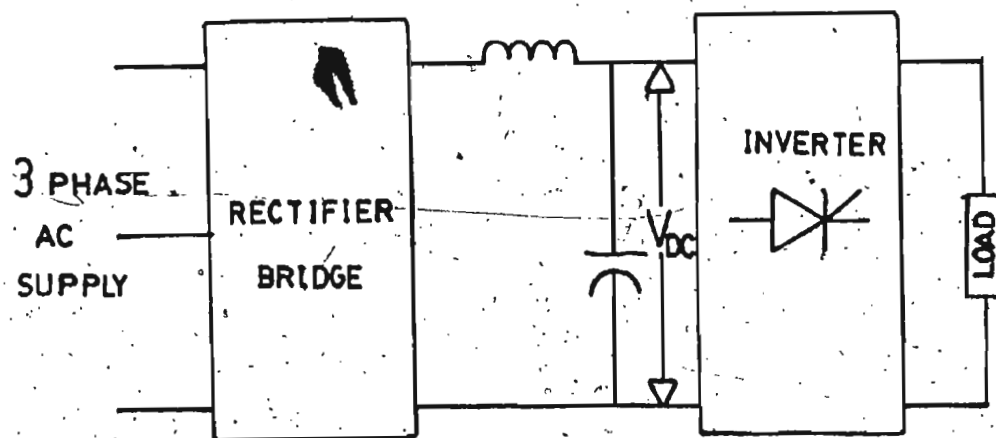


Fig. 3.1 Schematic diagram of an inverter with load

These equations are used in analysing the performance of R and R-L loads, fed by the delta modulated inverter. The results are verified experimentally.

### 3.2 Verification of Results with Resistive Load

For a resistive load, the impedance value in circuit of Fig. (3.10) is the resistance R, which is frequency independent. Hence the determination of resistive load performance becomes easy. Equations (3.1.3) to (3.1.7) give the expressions for the inverter output voltage and r.m.s. current to the resistive load [ $Z = R$ ].

Power consumed by the resistive load is

$$P_{\text{load}} = I_{\text{rms}}^2 R \quad 3.2.1$$

These equations together with harmonic current equations described in section 2.3.1 of chapter 2, were solved to find the resistive load behaviour with delta modulated inverter. Unlike other inverters, the current at lower frequency operation for resistive load is found to be higher. For resistive load, the higher harmonics near the ripple frequency of the carrier wave, contribute significantly towards the load current and power. As a result, at lower frequency of operation the current and power are higher. As the frequency of operation is increased, these higher harmonics are reduced in magnitude, whereas the

current and power due to the fundamental increases. These results are verified both by theoretical calculations and by experiments. The analytical results and the experimental results are given in Figs. (3.2) and (3.3) respectively. Corresponding numerical values of the results are included in Appendix VI. The results show a good agreement between the theoretical and experimental results. It validates the comments made so far for the resistive load behaviour fed from delta modulated inverter. The effect of change of modulation index ( $m$ ) is also shown on the plots. Since the load is resistive, the current has the same waveshape as the inverter output voltage. It has the same harmonic contents (current waveshapes for 50 Hz and 95 Hz operation is shown in oscillograph Fig. 3.4(a) and 3.4(b) for  $V_R = 5.5$  and  $V_R = 6.75$  respectively). The results show the general trend of increasing voltage, current and power upto base frequency and these become constant beyond the base frequency. Power factor is constant throughout the entire operation. Due to resistive load, its value is unity.

### 3.3 Verification of Results with R-L Load

The study of inverter with R-L load is important for further investigation of the performances of motor drives. Apart from some active dynamic source, the motor load to the inverter is a complex R-L load. The basic



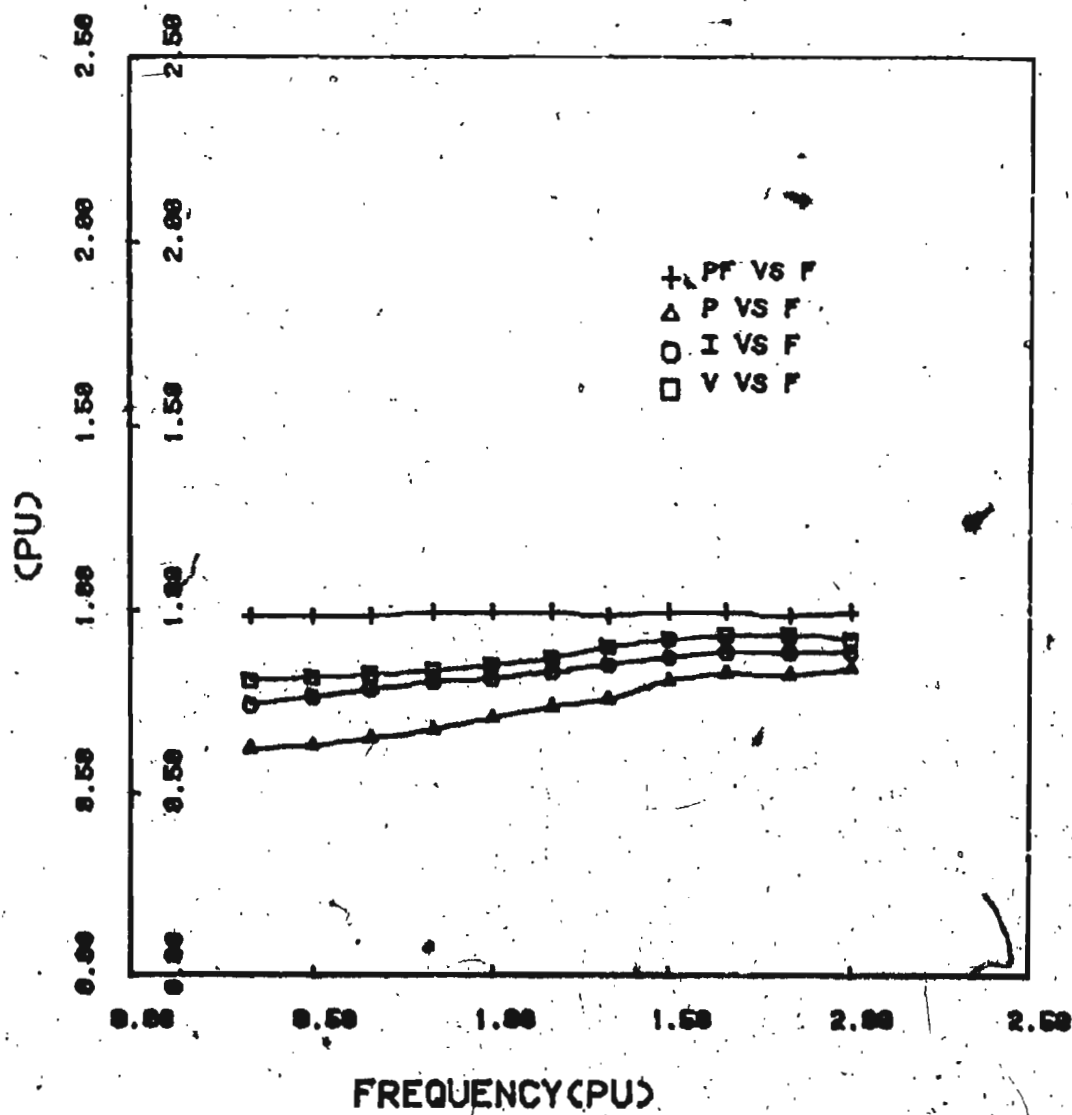


Fig. 3.2(a) Theoretical performance characteristics of R-load fed from DM inverter ( $V_R = 5.5V$ )

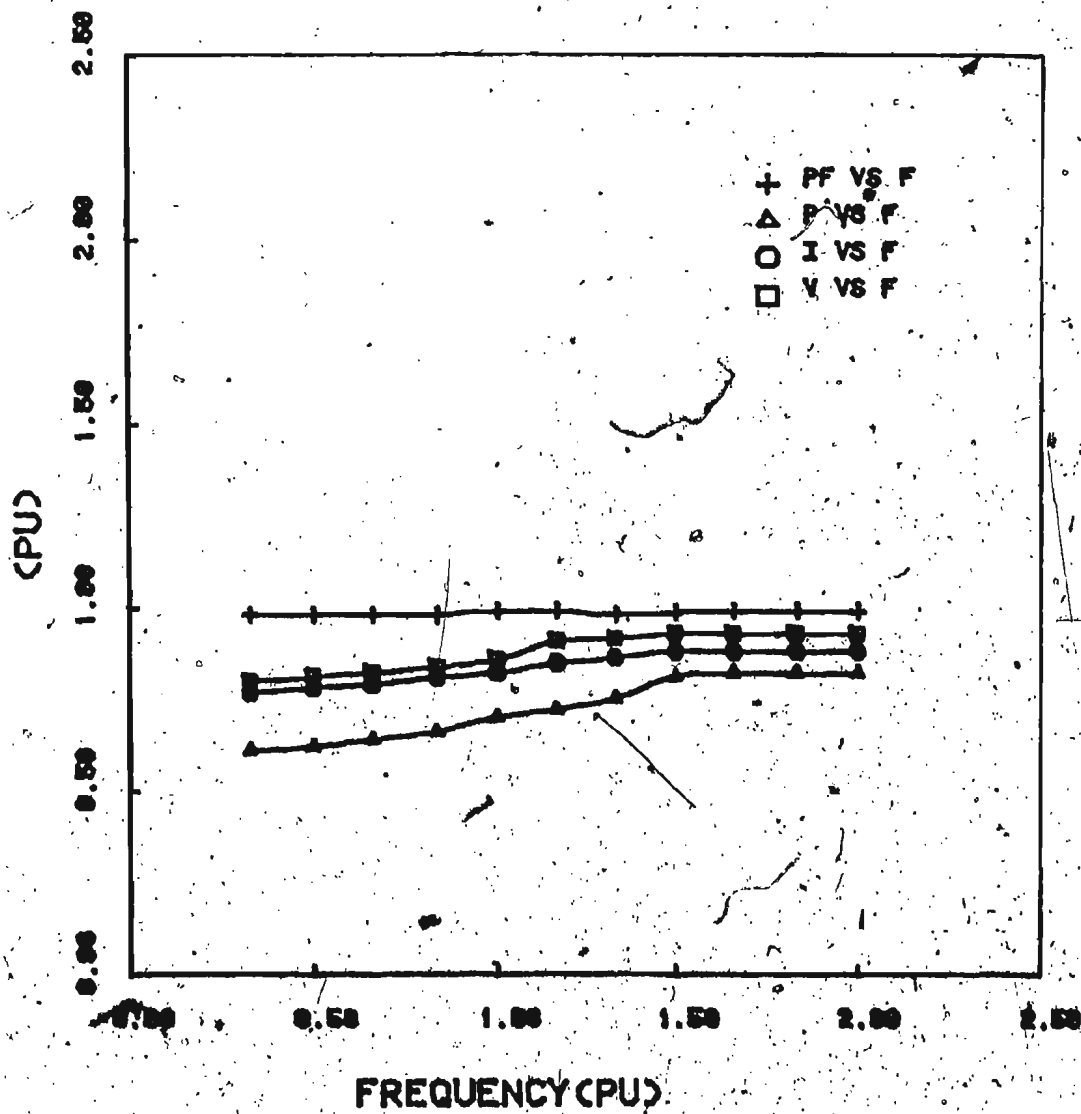


Fig. 3.2(b) Theoretical performance characteristics of R-load fed from DM inverter ( $V_R = 6.00V$ )

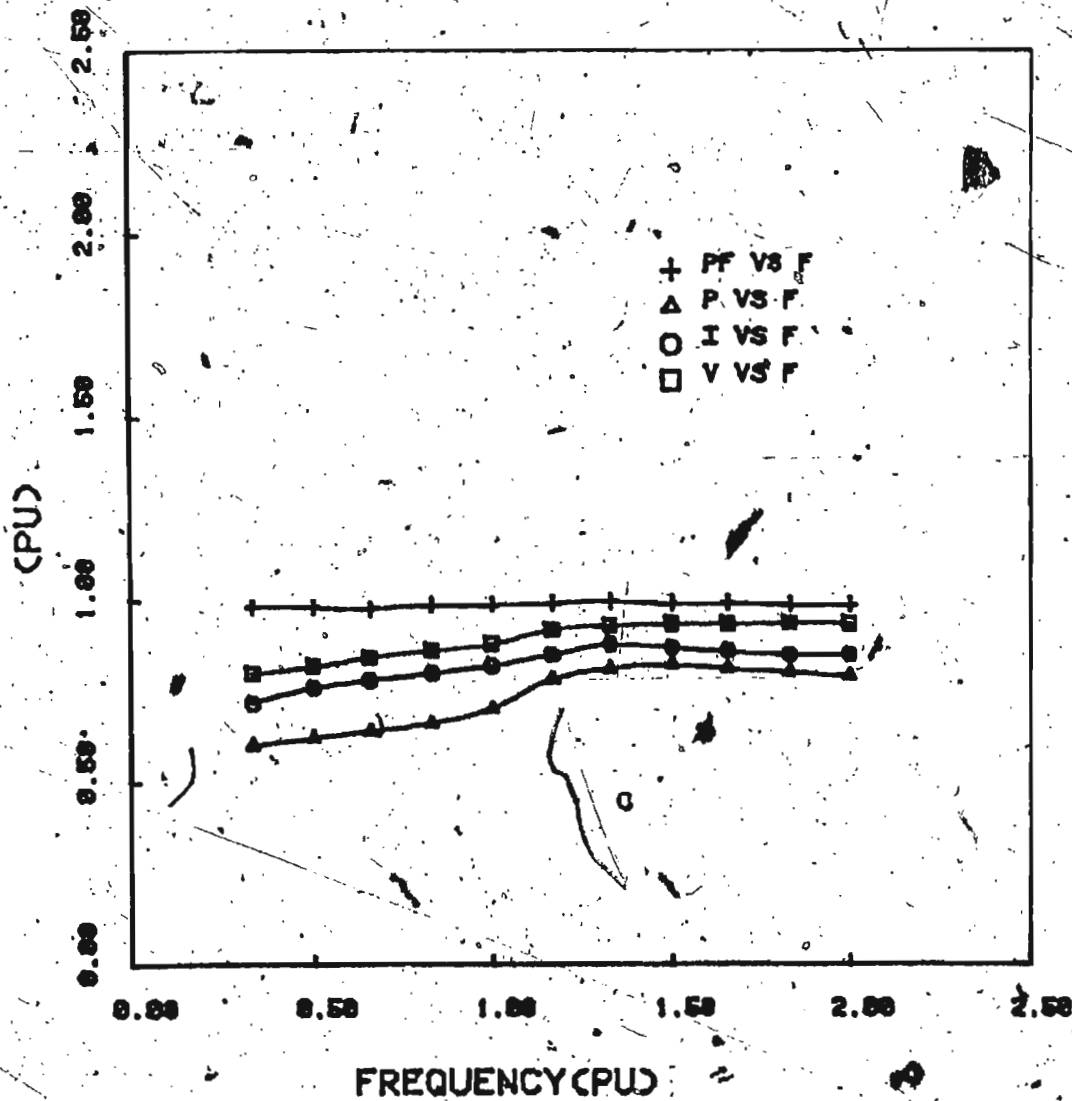


Fig. 3.2(c) Theoretical performance characteristics of R-load fed from DM inverter ( $V_R = 6.75V$ )

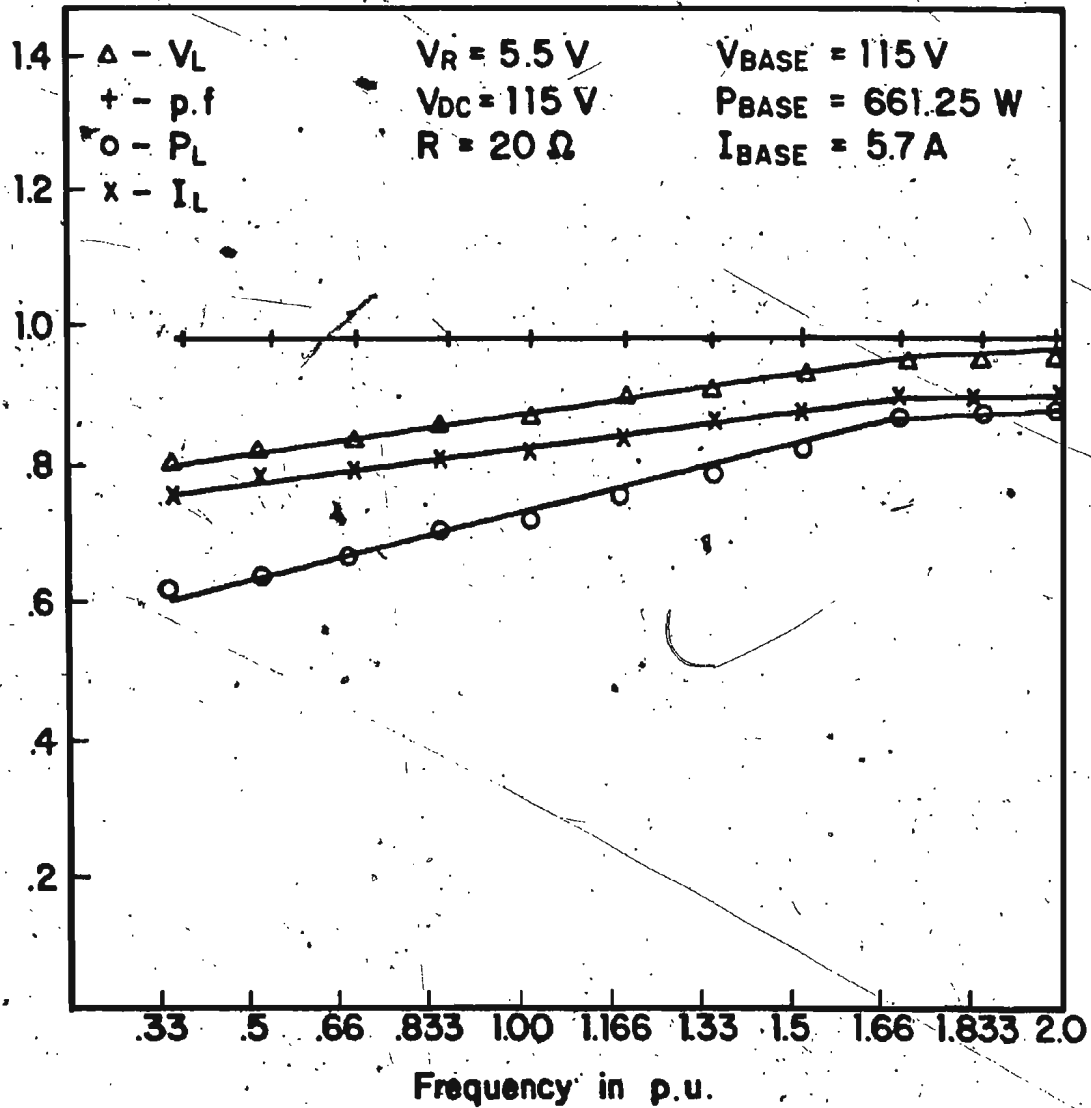


Fig. 3.3(a) Experimental performance characteristics of R-load fed from DM inverter ( $V_R = 5.5 \text{ V}$ )

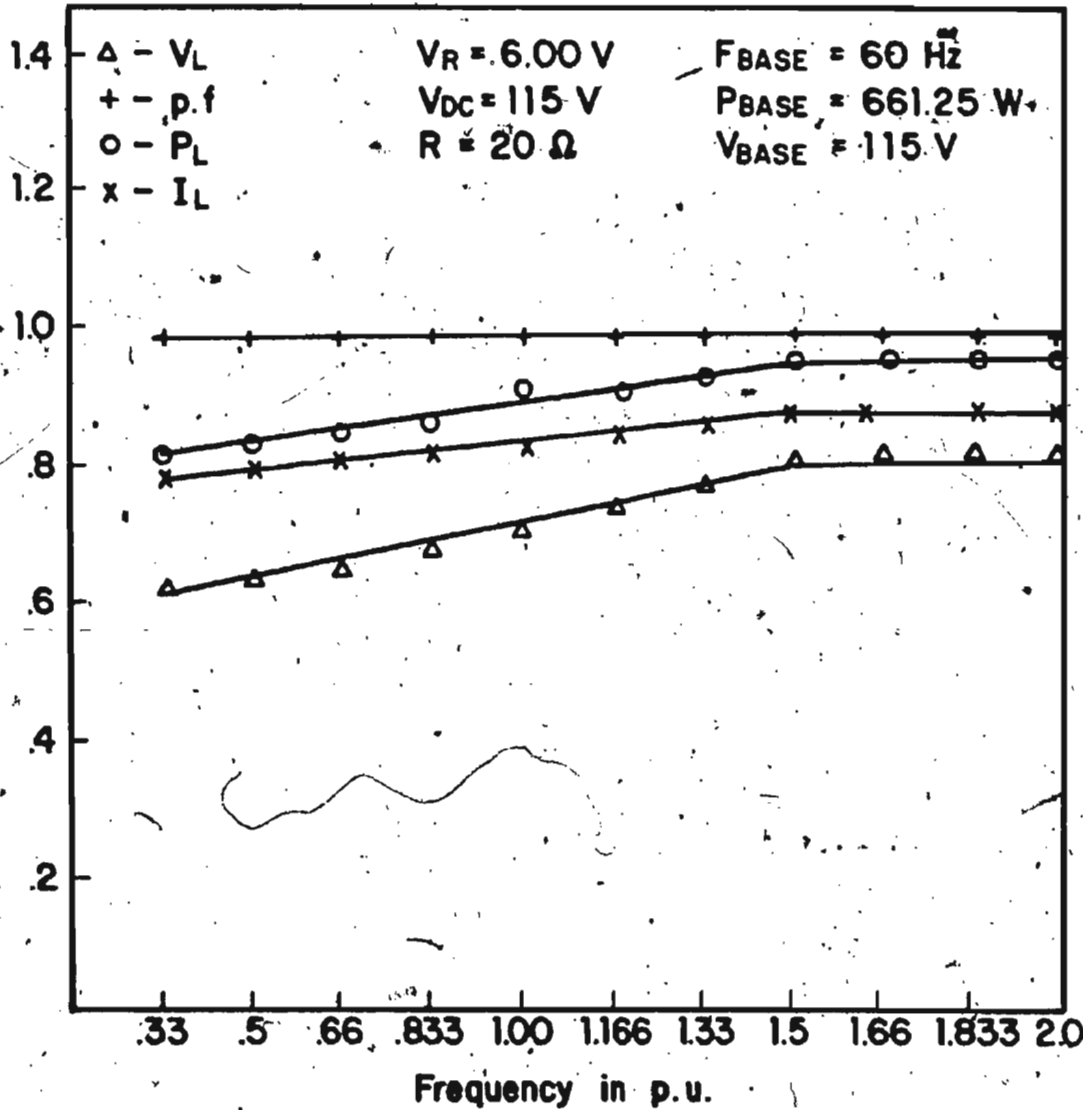


Fig. 3.3(b) Experimental performance characteristics of R-load fed from DM-inverter ( $V_R = 6.00 \text{ V}$ )

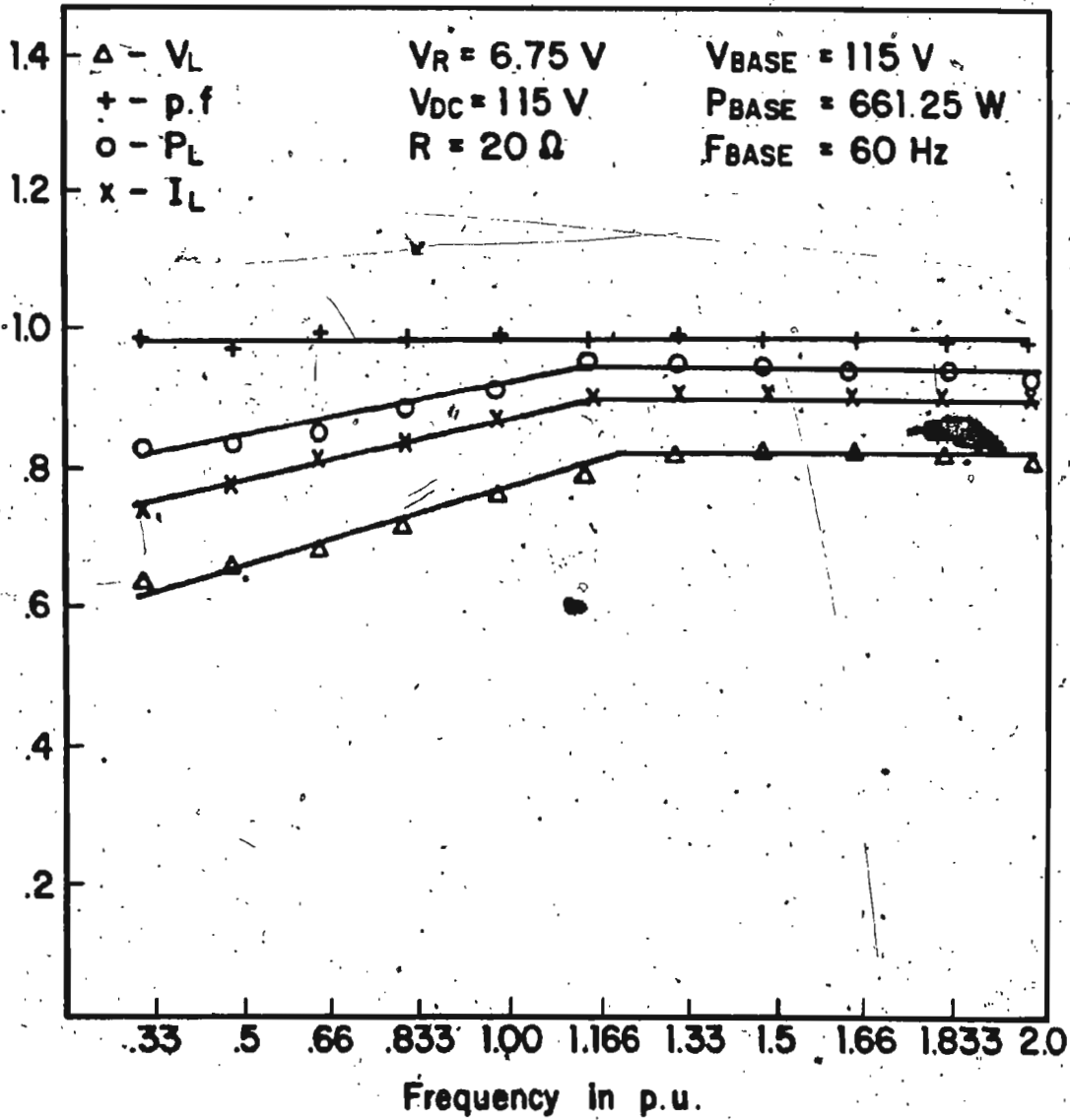
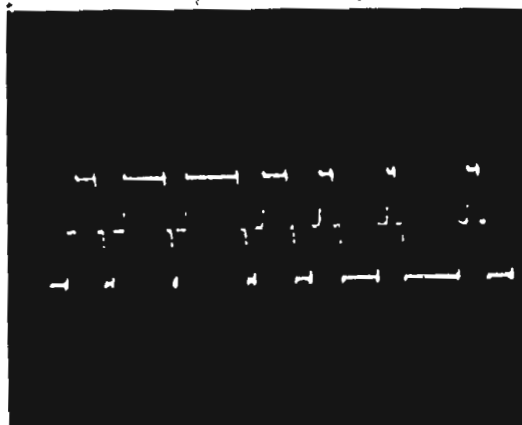


Fig. 3.3(c) Experimental performance characteristics of R-load fed from DM inverter ( $V_R = 6.75\text{V}$ )

$V_R = 5.5V$ 

50HZ

 $V = 5.5V$ 

95HZ

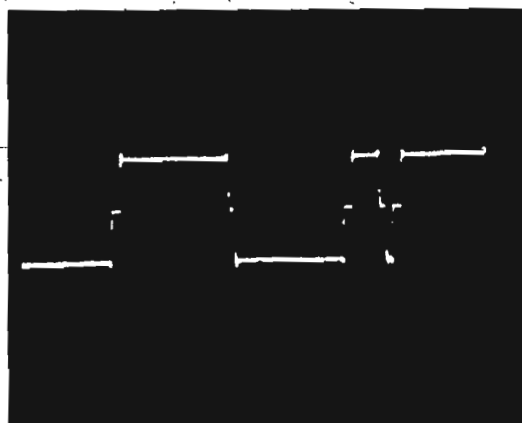
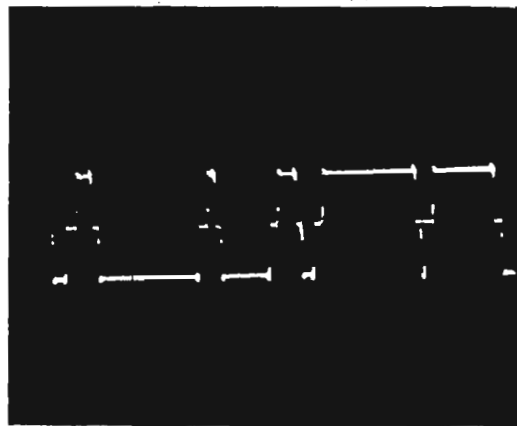


Fig. 3.4(a) Experimental load current waveshape of R-load ( $V_R = 5.5V$ ).

$V_R = 6.75V$   
50HZ



$V_R = 6.75V$   
95HZ



Fig. 3.4(b) Experimental load current waveshape of R-load  
( $V_R = 6.75V$ )



approach for such study is already outlined in section 3.1. The key equations for performance analysis of R-L loads are described in equation (3.1.1) to (3.1.9).

Inverter equations are solved to get the performance characteristics for R-L load. The plots of current and power to load characteristics as frequency changes are shown in Figs. 3.5(a) to 3.5(c) and 3.7(a) to 3.7(c). The current and power to the load increases upto base frequency and then start dropping down beyond base frequency.

The analytical results show that for the R-L load, the load current and active power follow the desired pattern required for a.c. motor drives. The higher harmonics with larger magnitude at low frequency of operation do not contribute much to the load current despite their high magnitude. The total impedance is dependent on the frequency of the harmonics. Since at lower frequency the dominant harmonics take place at higher frequencies (at or near the ripple frequency of the carrier wave), the current due to these harmonic are low as  $X_L$  of the load is large at high frequencies. This results in prominence of the fundamental component for the whole frequency range of operation. As a result the voltage seen by the load is mostly the fundamental voltage component which has a linear constant characteristic beyond the base frequency. The analytical results obtained

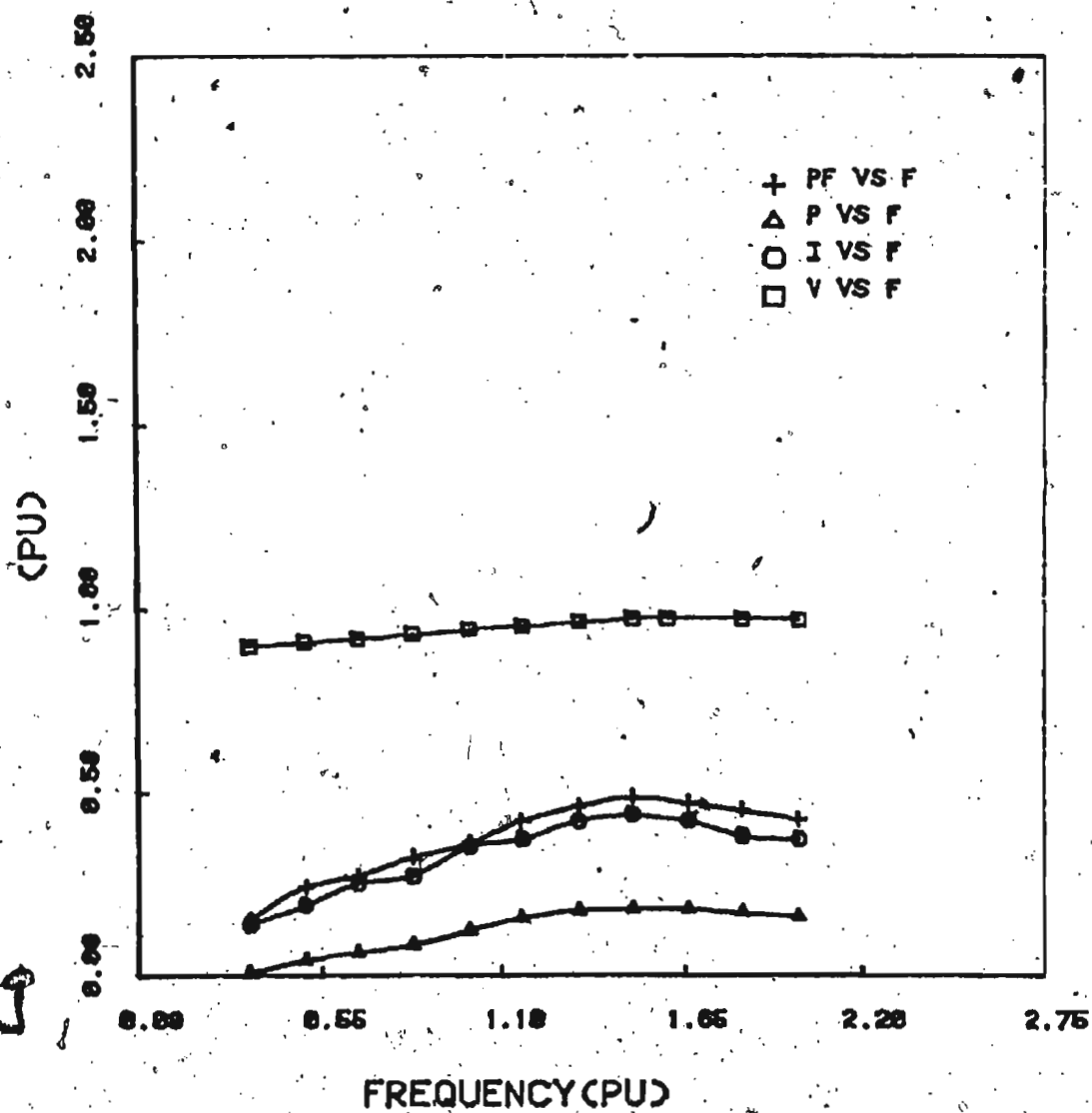


Fig. 3.5(a) Theoretical performance characteristics of R-L load fed from DM inverter ( $V_R = 5.5V$ )

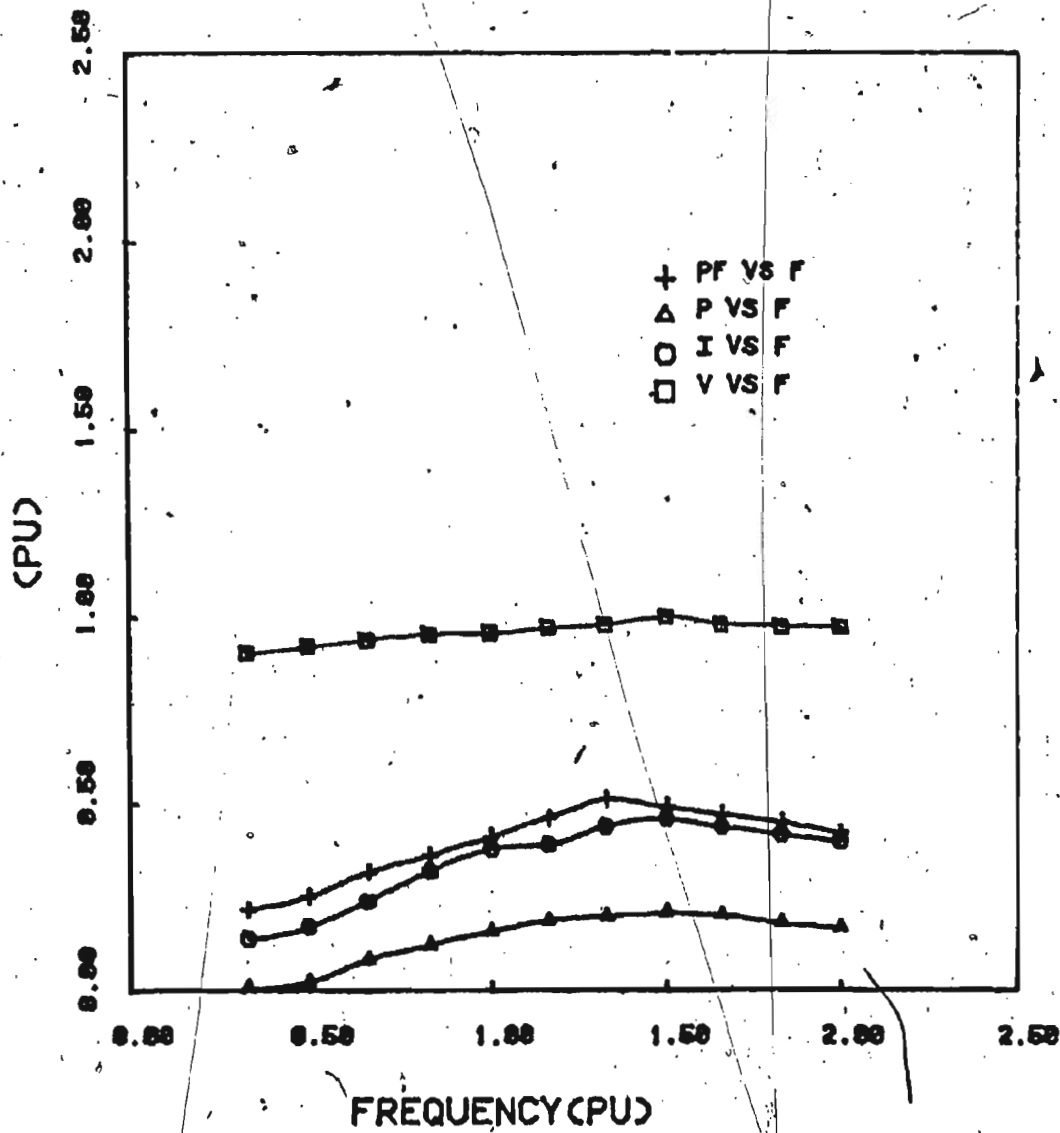


Fig. 3.5(b) Theoretical performance characteristics of R-L load fed from DM inverter ( $V_R = 6.00V$ )

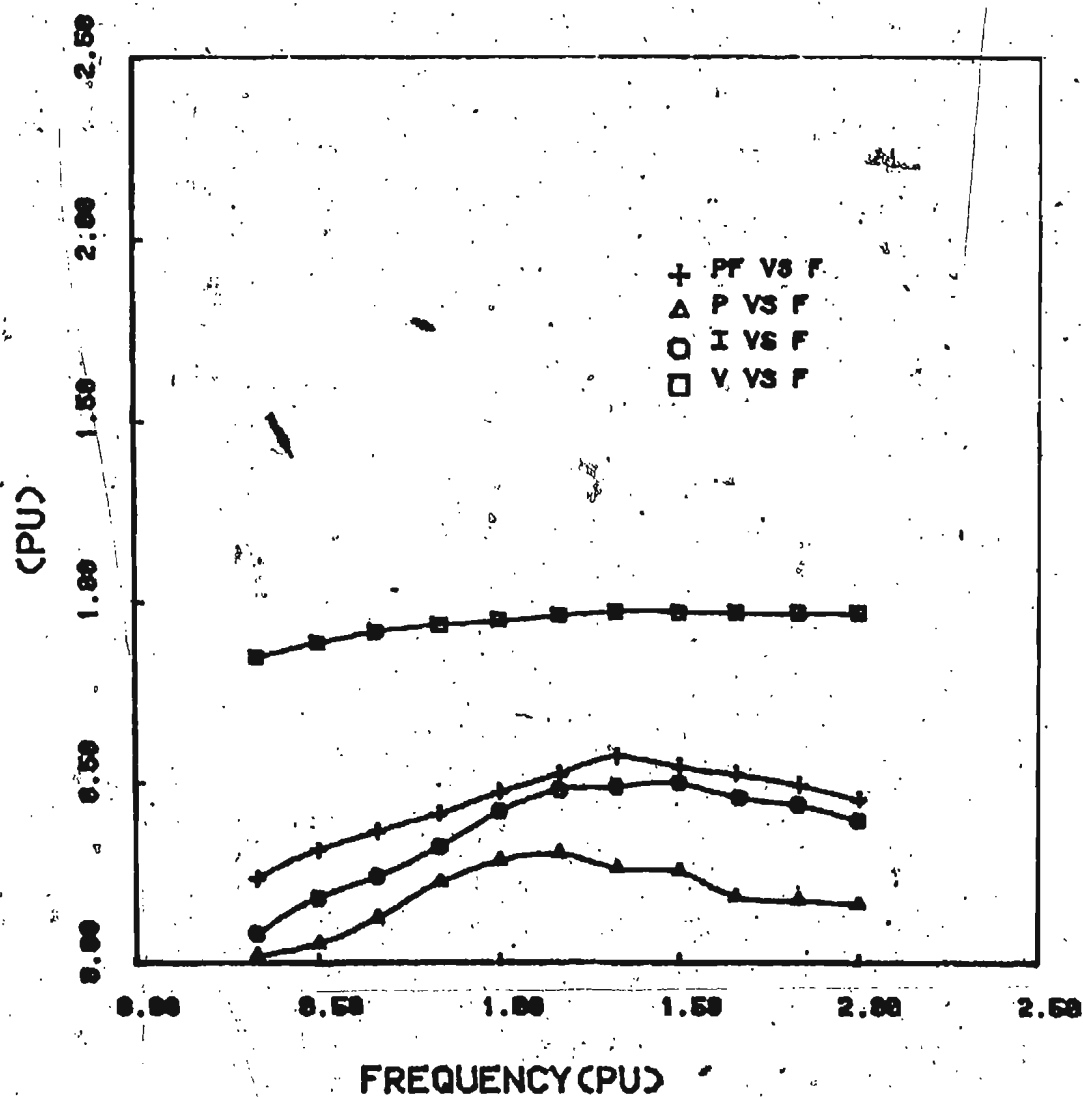
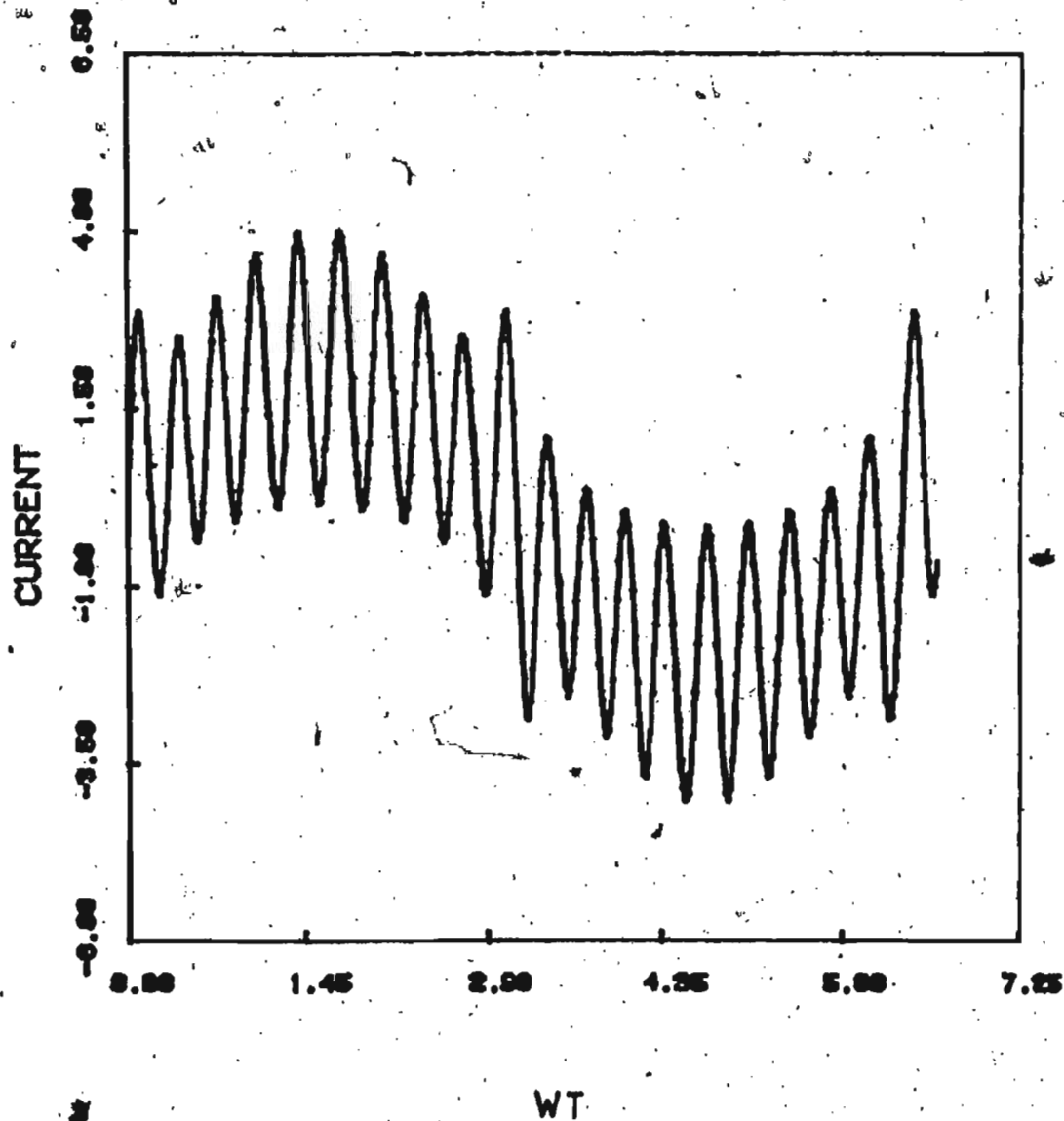


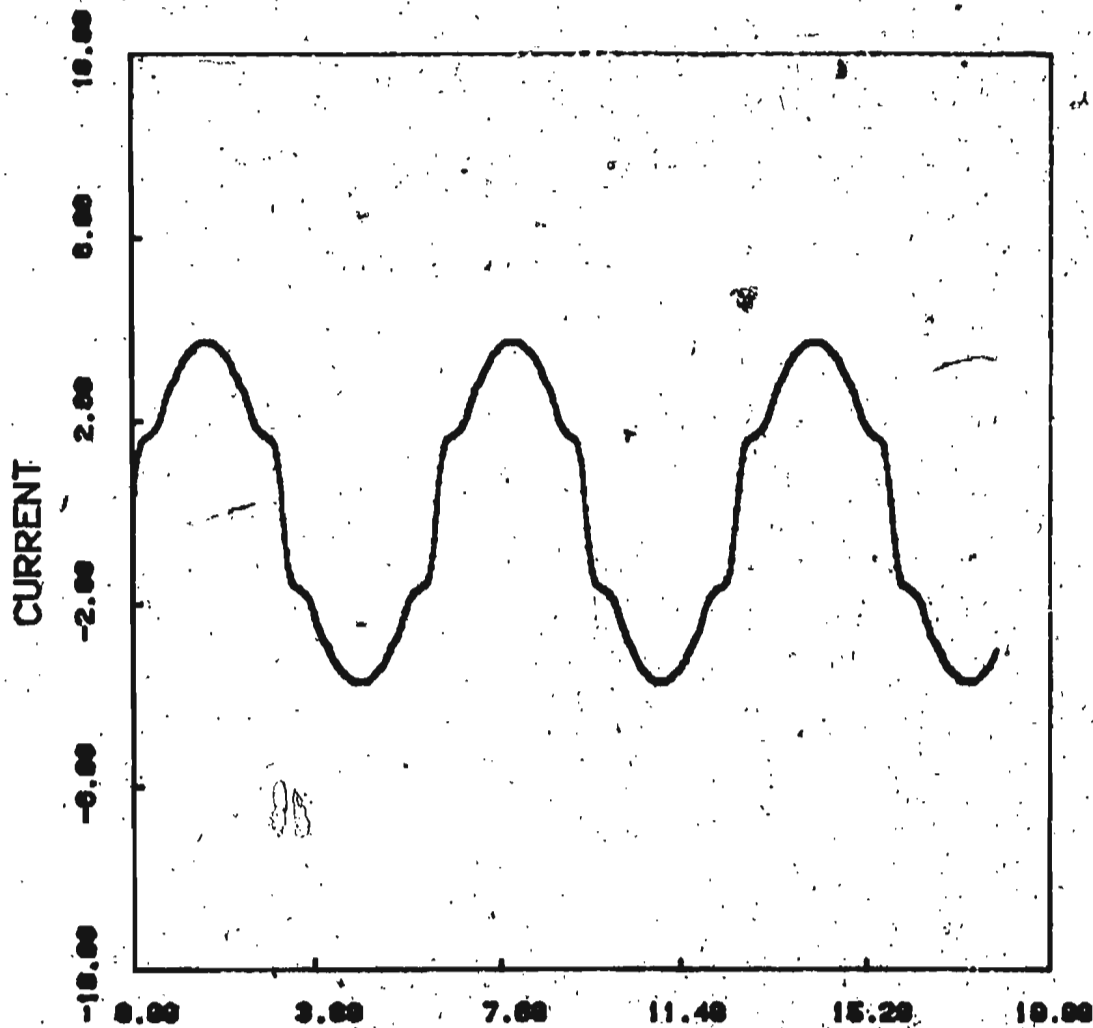
Fig. 3.5(c) Theoretical performance characteristics of R-L load fed from DM inverter ( $V_R = 6.75V$ )

Fig. 3.6(a) Theoretical current wveshape of R-L load fed from DM inverter



CURRENT WAVE SHAPE WITH R-L LOAD  $V_R=5.5V$   $F=50Hz$

Fig. 3.6(b) Theoretical current waveshape of R-L load fed from DM inverter



WT

• CURRENT WAVESHAPE OF R-L LOAD, F=95HZ  
VR= , DV=1.00V

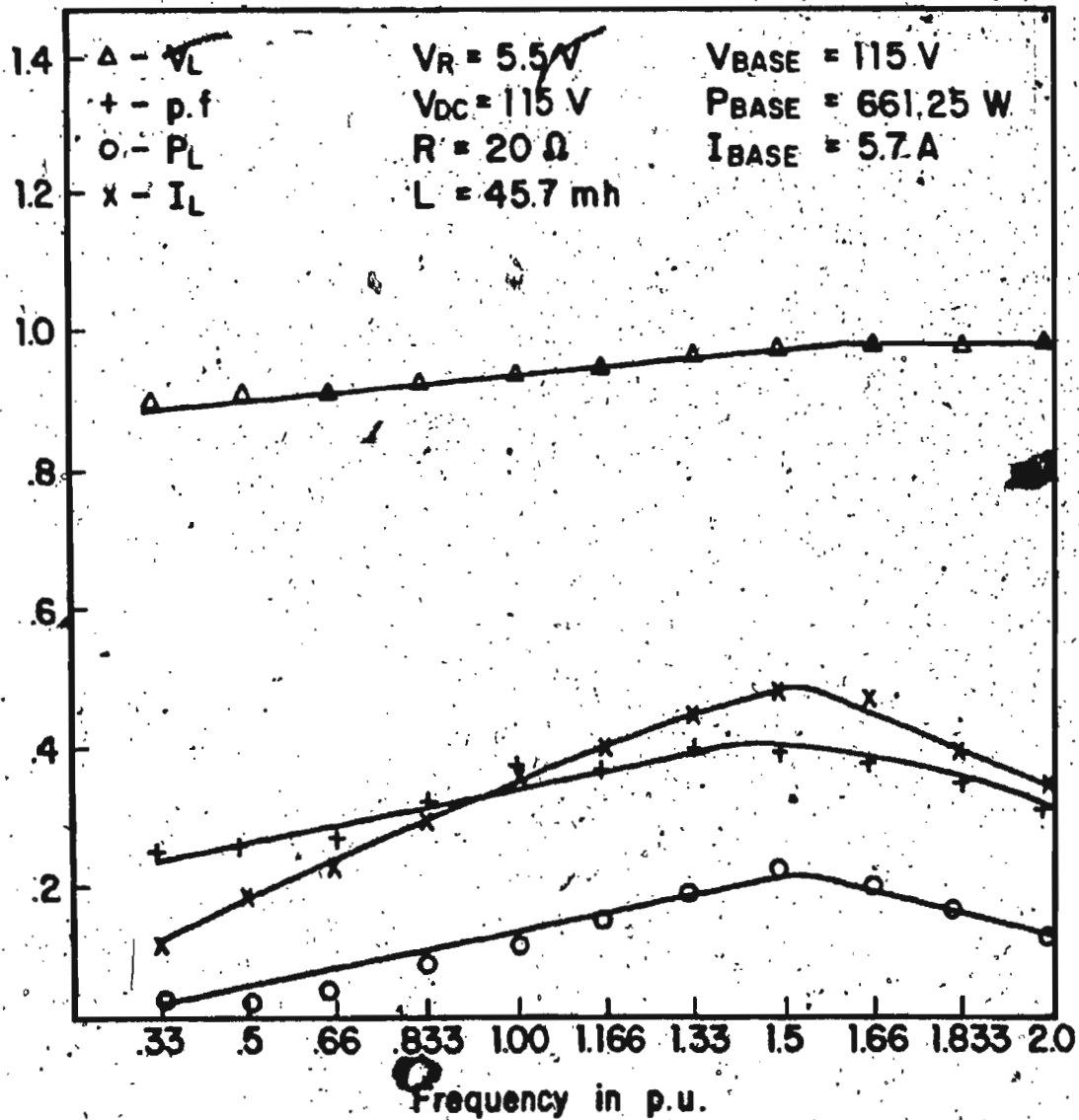


Fig. 3.7(a) Experimental performance characteristics of R-L load fed from DM inverter ( $V_R = 5.5V$ )

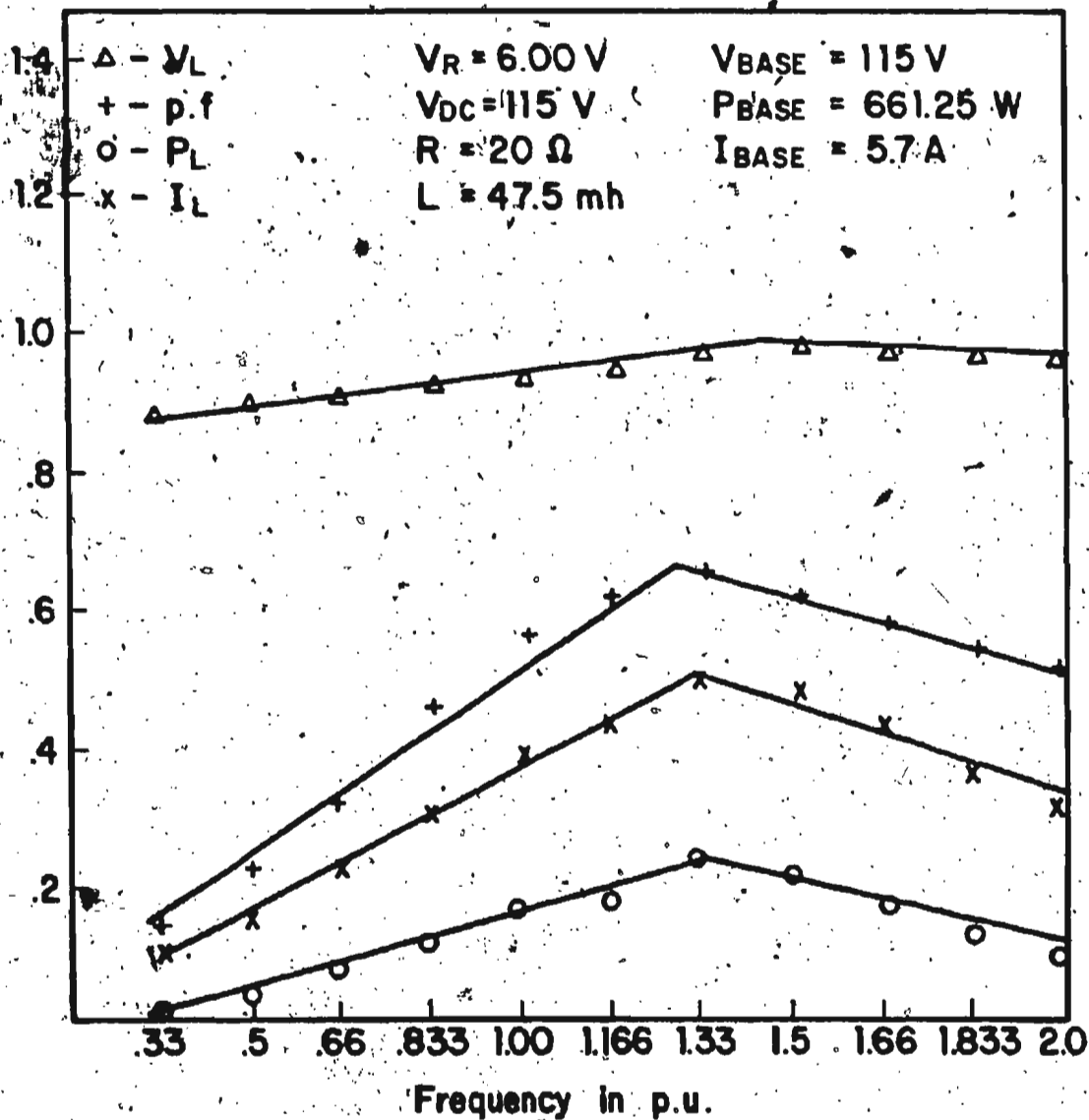


Fig. 3.7(b) Experimental performance characteristics of R-L load fed from DM inverter ( $V_R = 6.00 \text{ V}$ )



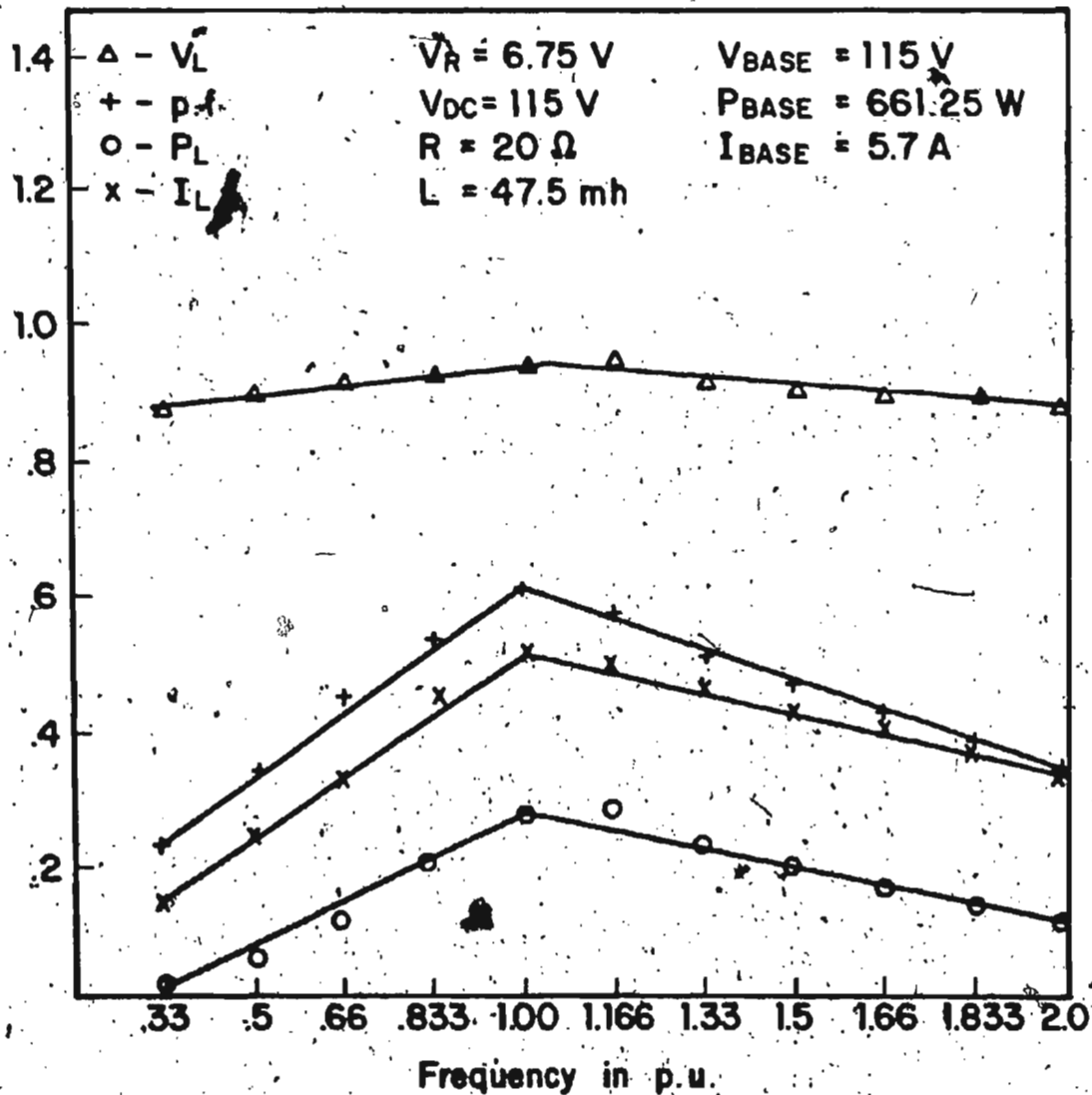
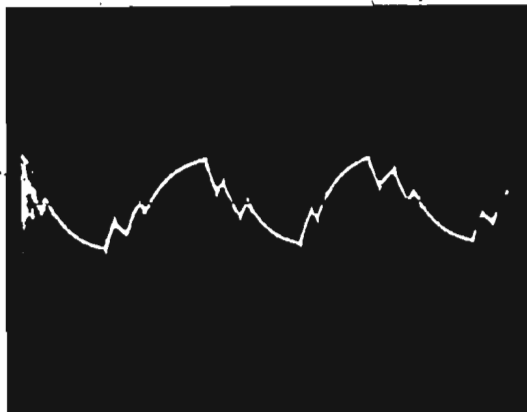


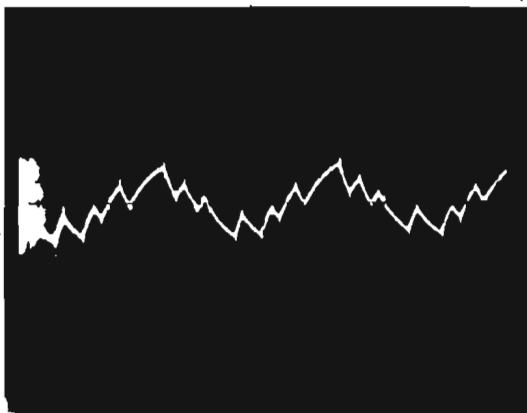
Fig. 3.7(c) Experimental performance characteristics of R-L load from DM inverter ( $V_R = 6.75 \text{ V}$ )

Fig. 3.8(a) Experimental current waveshape of R-L load at 50 Hz

$V_R = 6.75V$   
50 HZ



$V_R = 6.00V$   
50 HZ



$V_R = 5.5V$   
50 HZ

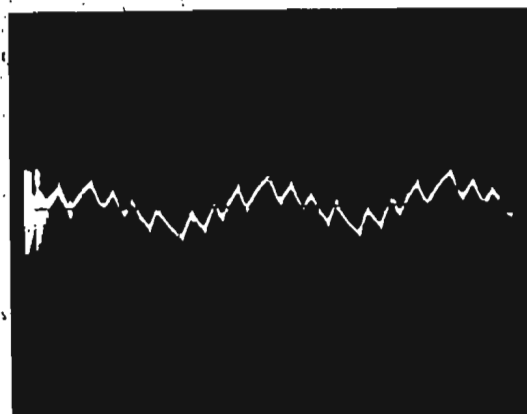
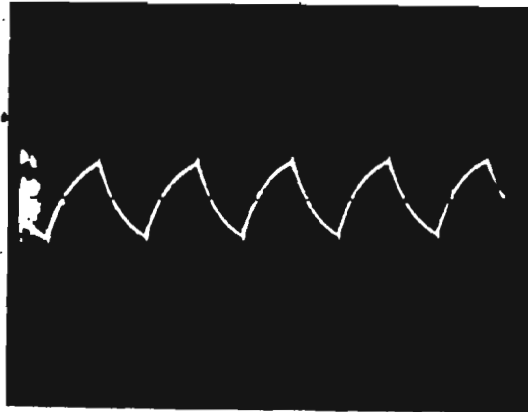
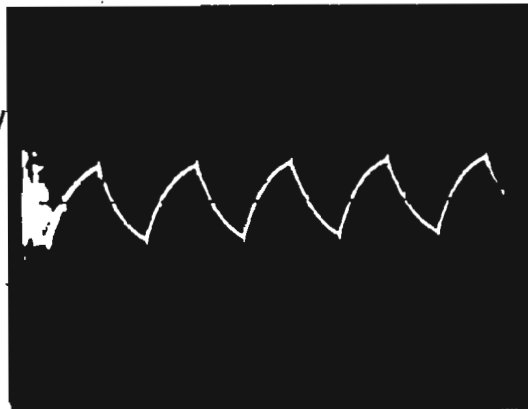


Fig. 3.8(b) Experimental current waveshape of R-L load at 95 Hz

$V_R = 6.75V$   
95HZ



$V_R = 6.00V$   
95HZ



$V_R = 5.5V$   
95HZ




from equations (3.3.1) to (3.3.3) are presented in Fig. 3.5(a) to 3.5(c) for 20 to 120 Hz of inverter operation for  $V_R = 5.5V$ ,  $6.50V$  and  $6.75V$  respectively. The results show that upto base frequency, the current and power to the load increase. These quantities drop down as frequency of operation is gradually increased beyond base frequency. This is because beyond base frequency the voltage has constant characteristics, whereas the impedance of R-L load increases with increase in frequency of operation. As a result, power to the load decreases together with current and power factor of the load. The effect of changing modulation index  $m$  in inverter is to change the base frequency of the inverter and also to change the harmonic characteristics of inverter output. So if with R-L load, the modulation index of inverter is changed, it is expected that the base frequency will change and the load current power and power factor will change too. The effect of changing ( $V_R$ ) is evident in results of the Figs. 3.5(a) to 3.5(c).

Since the voltage of the inverter output is modulated and the load is R-L, it is expected that the current waveshape of the R-L load will have a sinusoidal waveshape with prominent ripples sitting on it. This current wave has lower harmonic contents as well. Equation (3.3.4) is used to find the nature of the load current for  $V_R = 6.75V$  and  $5.5V$ . These are presented in Figs. 3.6(a) and 3.6(b)

respectively for 50 and 95 Hz of operation. The change in modulating index  $m$  (or  $V_R$ ) has the effect on current waveshapes. As  $V_R$  is increased, the ripples on the sine current waveshapes decreases, because of the lower number of switching of inverter gates in each cycle.

The above theoretical results are verified experimentally under the same conditions as specified in the analytical case. The Figs. 3.7(a) to 3.7(c) show the variations of the load current, power and power factor with variable frequency input to the load. The plots also show the effect of changing  $V_R$ . The numerical data for plots of Figs. 3.7(a) to 3.7(c) is included in Appendix VI. The experimental load current waveshapes are pictured for 50 and 95 Hz operation. These are shown in Figs. 3.8(a) to 3.8(b) for  $V_R = 5.5V, 6.00V$  and  $6.75V$  respectively. It is evident that the experimental results and analytical results are close enough. Variations in experimental results are due to the commutation interval between successive positive and negative pulses at the inverter output. The effect of commutation intervals were not considered in predicting the analytical results. However in practice, commutation intervals are always there in a thyristor inverter circuit.



## CHAPTER 4

The most versatile and reliable variable speed drives are the cage rotor induction motors whose speeds are controlled by variation of stator frequency. The common method of supplying a.c. motors now-a-days is by the static voltage converters and inverters. To meet the various requirements of the motors, the inverters require complex control circuits. The harmonics at the inverter output determine the steady state and transient performance of the motors. In this chapter, the operation of a single phase induction motor on a variable frequency supply with delta modulated inverter is examined. The analysis and experimental verifications of the steady state performance of single phase induction motors are based on full bridge delta modulated inverter supply.

### 4.1 Induction Motor as Variable Frequency Inverter Fed Drives

The majority of industrial drives are electric motors because they are controllable and readily available. In practice, most of these drives are induction motors. It has been the desire of manufacturers to vary the speed of induction motors by electrical means. This aim has been technically possible for some years due to advances in power electronics and now available at comparable cost and quality to alternate systems.

A standard induction motor is essentially a constant speed machine when supplied from the mains of fixed voltage and fixed frequency. The rotor speed  $N_r$  of induction motor is given by

$$N_r = \frac{(1 - s) 120f}{P} \text{ rpm} \quad 4.1.1$$

where

$f$  = frequency of supply c/s

$$s = \text{slip} = \frac{N_s - N_r}{N_s}$$

$P$  = number of poles

$N_s$  = synchronous speed

The relation for induction motor speed shows that a continuous speed variation is obtainable if the motor is supplied from a variable frequency supply. Also to maintain a constant torque, the flux should be maintained constant which can be achieved by a linear voltage variation with frequency.

There are basically three modes of operation of a.c. motors when operated from variable frequency variable voltage supply. These are

- Constant torque mode:

the flux is maintained constant, which requires a linear  $V/f$  variation.

- Constant power mode:

the voltage is raised as power factor drops.

- Constant voltage mode.

In fact, the control via frequency and voltage variation confers to the motor torque-speed characteristics, which are similar to those of d.c. motors (Fig. 1.2 of chapter 1) when the frequency and voltage are done in such a way that  $V/f$  is constant up to base frequency and remains constant beyond base frequency (Fig. 1.1 of chapter 1). In ordinary voltage source inverters or in current source inverters, the outputs are essentially square waves. To attain the desired torque speed characteristics in such inverter fed motors, it is usually required to provide additional control circuitry using feedback from the shaft of the motor to change the frequency and the voltage. The variation of voltage initiates a double conversion process in such inverters due to the additional voltage control, usually a controlled rectifier or a variable transformer added to the input side of the inverter. Also, since these inverters have high harmonics at their output, proper filters are required to eliminate dominant harmonics to reduce high frequency losses in the motors. On the other hand, the PWM technique eliminates the double conversion process by incorporating inherent voltage control techniques inside the inverter logic. Some basic PWM techniques now in use for a.c. motor drives are mentioned in section 1.3.1 of chapter 1. These PWM techniques have better harmonic elimination methods than the ordinary VSI and CSI's. With PWM technique, it is also



possible to attain any particular mode of motor operation. However, this can be achieved in commonly used sine PWM inverters by increasing the complexity of the controls. The proposed delta modulation technique has the unique characteristics of achieving the two of operating modes, the constant torque and constant voltage mode of motor drives without any additional control circuits. The constant V/f characteristics up to base frequency required for constant torque and constant power operation of a.c. motors, are inherent in delta modulated inverters. The following section analyze and verifies the results of performance of single phase induction motor fed from full bridge delta modulated inverter.

#### 4.2 Harmonic Equivalent Circuit of Single Phase Induction Motor

The equivalent circuit is derived from double revolving field theory. Since the inverter outputs contain harmonics, it is necessary to take into account the effect of all dominant harmonics in the motor performance. To do this, the basic approach is to replace the equivalent circuit of motors with their harmonic equivalent circuits. The modified harmonic equivalent circuit for single phase induction motor is given in Fig. 4.1 [36,37]

where  $k$  = harmonic number

$kX_2$  = kth harmonic reactance

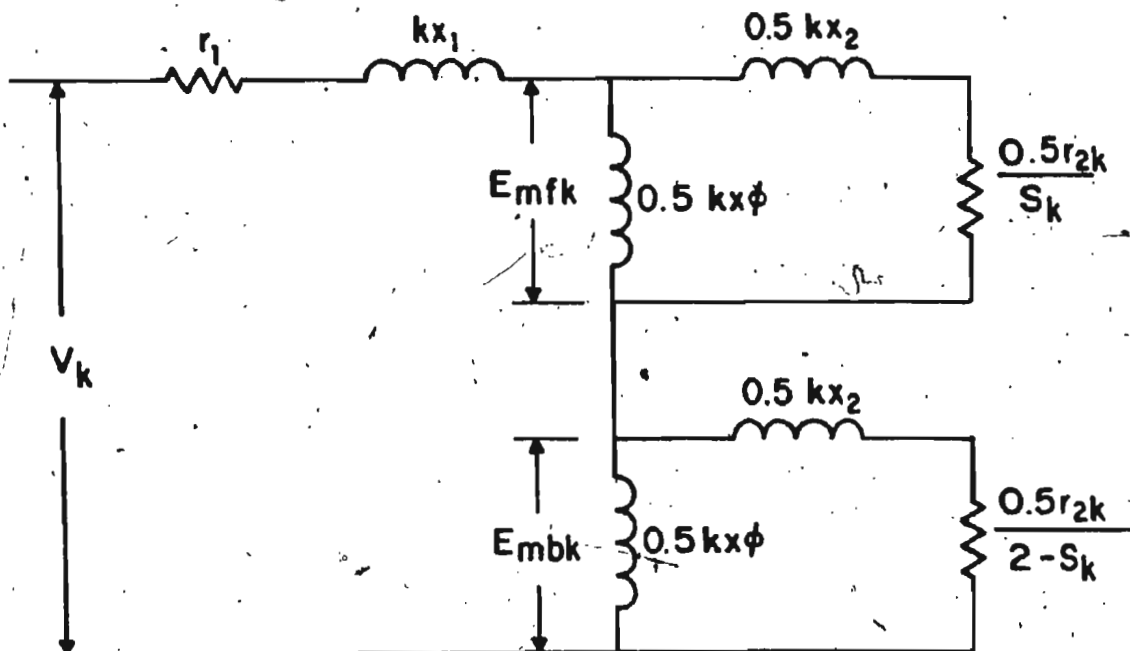


Fig. 4.1 Harmonic equivalent circuit of a single-phase induction motor

$r_{2k}$  = kth harmonic rotor resistance

$kX_1$  = kth harmonic stator leakage reactance

$$s_k = \frac{kn_1 - n_r}{kn_1}$$

$I_k$  = kth harmonic current

$V_k$  = kth harmonic voltage

$E_{mfk}$  = back emf due to forward rotating field due to kth harmonic voltage

$E_{mbk}$  = back emf due to backward rotating field due to kth harmonic voltage

The nature of variations of reactances, rotor resistance and slip due to variable supply frequency and harmonics are formulated in appendix A.

For the equivalent circuit shown in Fig. 4.1 the kth harmonic current is given by

$$I_k = \frac{V_k}{Z_{Tk}} \quad 4.2.1$$

where  $Z_{Tk} = Z_{fk} + Z_{bk} + r_1$

( $Z_{Tk}$ ,  $Z_{bk}$  and  $r_1$  are defined and formulated in appendix I).

If the equivalent circuit parameters for the motors are known, it is possible to determine the motor currents at various frequency of operation, for determining the steady state performance of 1-phase induction motors.

#### 4.3.1 Steady State Analysis of 1-Phase Induction Motor Fed from Delta Modulated Inverter

The following steady state analysis neglects the effects of pulsating torques produced in inverter fed motors due to interaction between flux produced by different harmonic currents.

The single phase induction motor model of Fig. 4.1 allows one to determine the fundamental harmonic currents to the motor (Eqn. 4.2.1) if the corresponding fundamental and harmonic voltages at the inverter output are known. The output voltages of the delta modulated inverter is defined in equations 3.1.1 to 3.1.4.

The developed power due to forward and backward revolving field of  $k$ th voltage harmonics are

$$P_{gfk} = I_k^2 * .5R_{fk} \quad 4.3.1$$

$$P_{gbk} = I_k^2 * .5R_{bk} \quad 4.3.2$$

The torques developed due to the  $k$ th harmonics given by

$$T_{dk} = \frac{1}{k\omega_g} (P_{gfk} - P_{gbk}) \quad 4.3.3$$

Internal power developed due to  $k$ th harmonic is

$$T_{dk} = (1-S_k) \omega_s T_{dk} \quad 4.3.4$$

Copper loss due to  $k$ th harmonic is

$$P_{cu} = S_k P_{gfk} + (2-S_k) P_{gbk} \quad 4.3.5$$

and input power due to kth harmonic is

$$P_{IK} = P_{dk} + S_k P_{gfk} + (2-S_k) P_{gbk} + I_k^2 r_l \quad 4.3.6$$

Solving equations (4.2.1) to (4.2.6), the responses to the individual harmonic voltages can be found for current, power and torque of the motors. The individual responses for fundamental and harmonics are superimposed to predict the steady state performance of single phase induction motor fed from delta modulated inverter. The details are given in (appendix A).

#### 4.3.2 Theoretical Results

The single phase induction motor model and theoretical analysis developed so far has been used to find the performance characteristics of two single phase induction motors of 1/4 and 1/2 hp ratings. The motor parameters used for analysis are listed in Appendix A.

Performance characteristics for the two motors are plotted in Figs. 4.2 to 4.7 for various modulation index. The general trends of these performance curves are as follows:- upto the base frequency, the motor current, power factor, developed maximum torque and efficiency increases with increase in frequency of operation. Beyond base the frequency, power factor, motor current and maximum power developed have almost constant profile with a small decreasing nature at high speed.

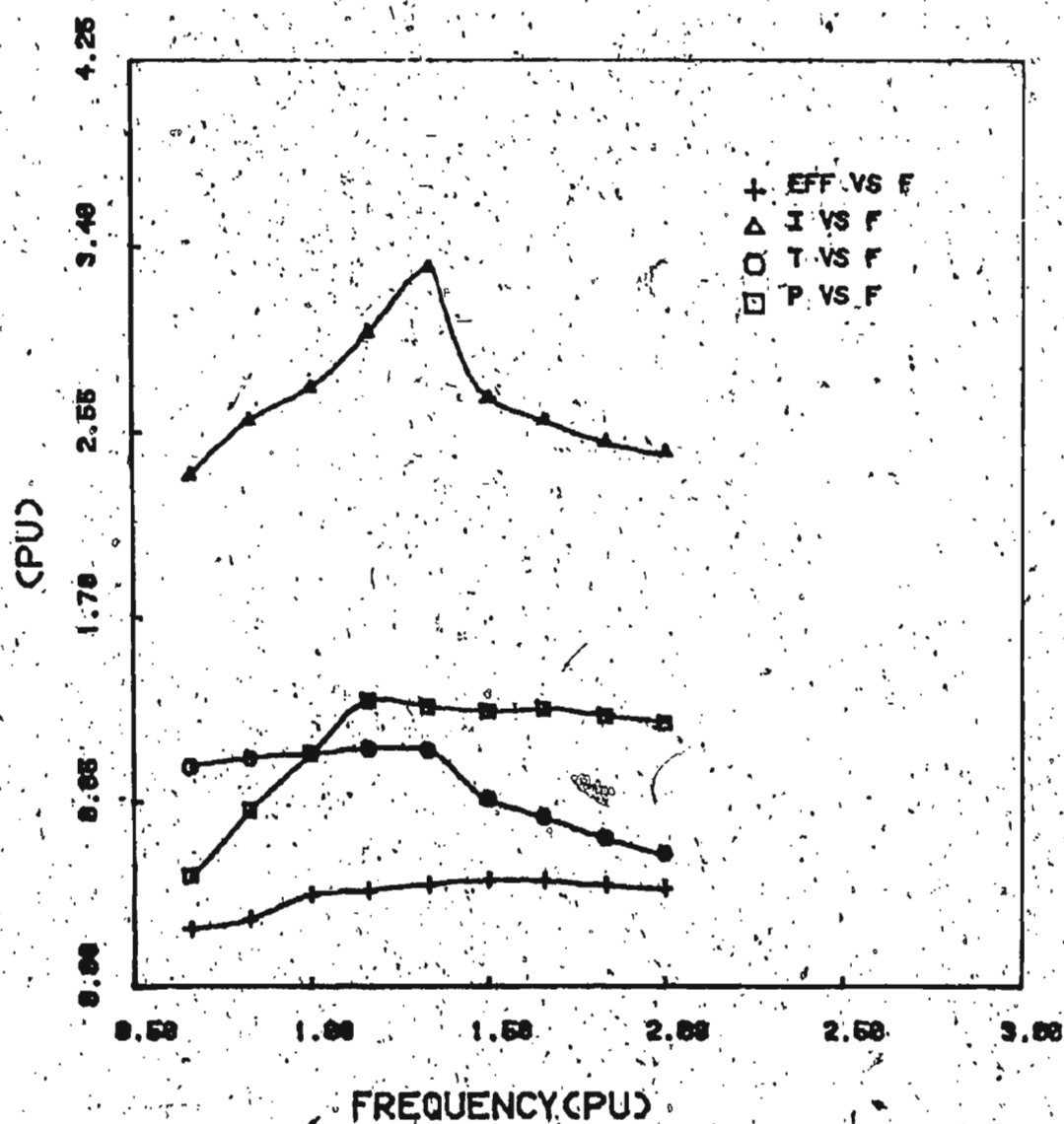


Fig. 4.3

Theoretical performance characteristics of a 1/4 hp, 1-phase induction motor fed from DM inverter ( $V_R = 6.75V$ )

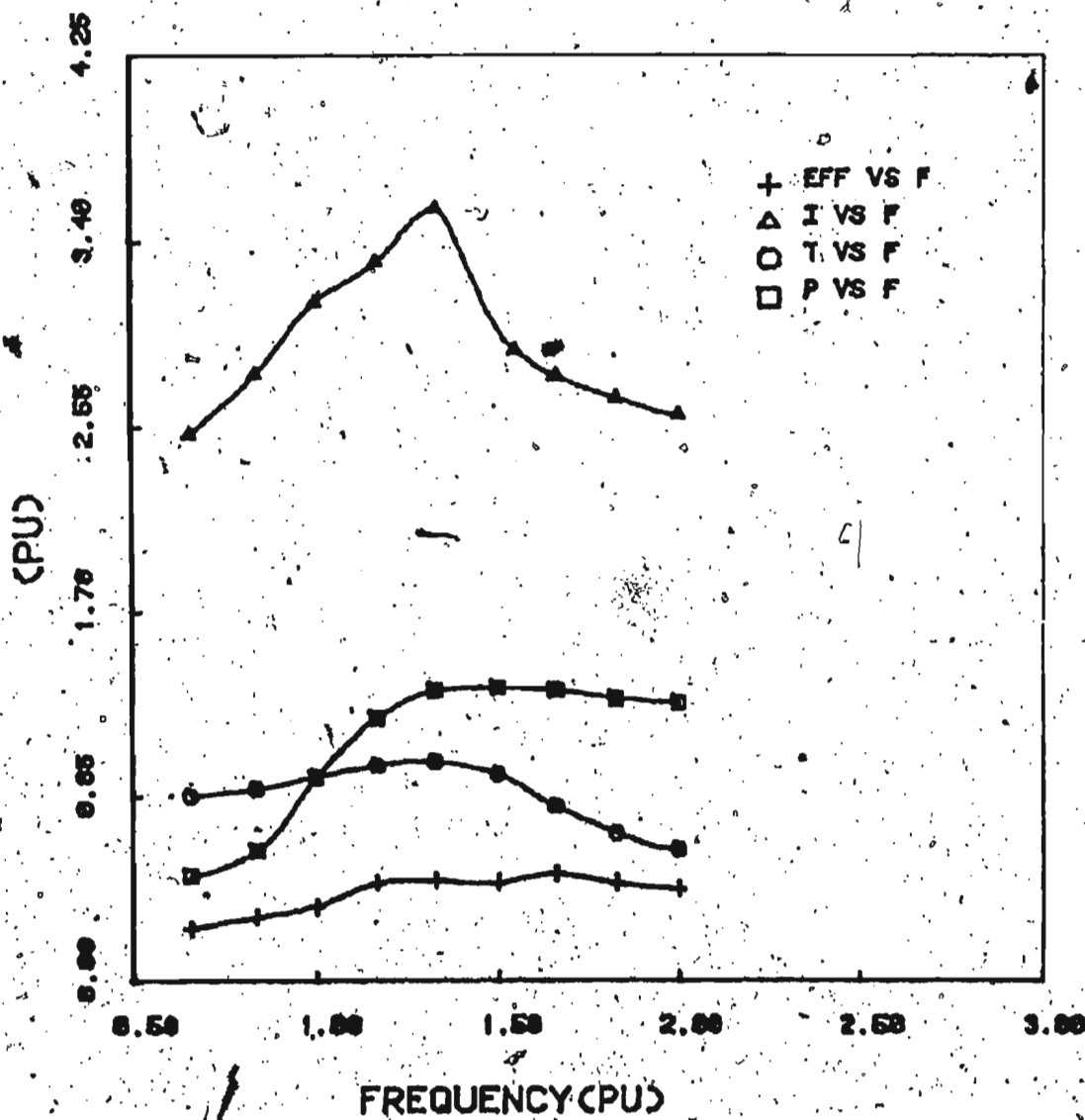


Fig. 4.2

Theoretical performance characteristics of a 1/4 hp, 1-phase induction motor fed from DM inverter ( $V_R = 5.5V$ )

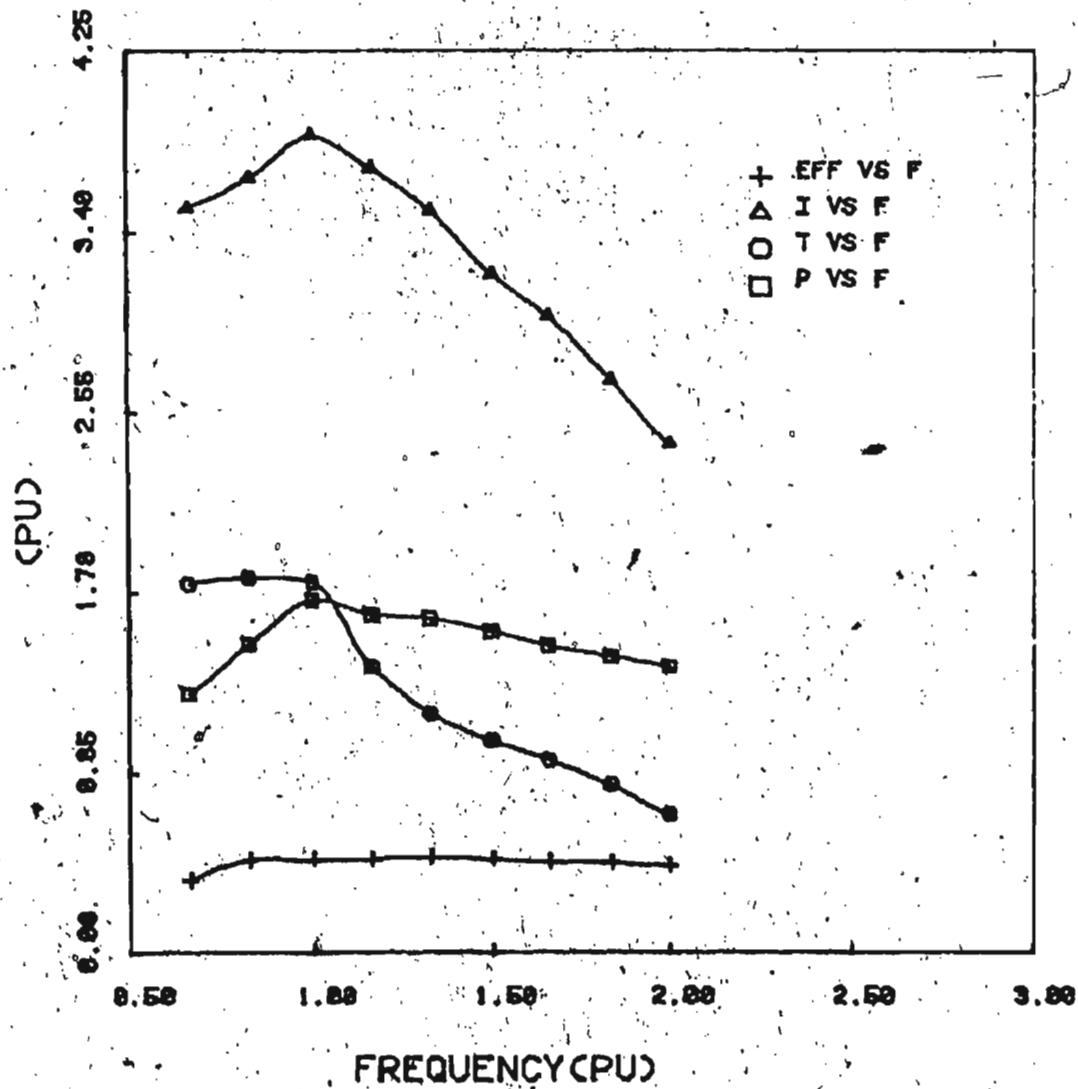


Fig. 4.4

Theoretical performance characteristics of a 1/4 hp, 1-phase induction motor fed from DM inverter ( $V_R = 7.5V$ )



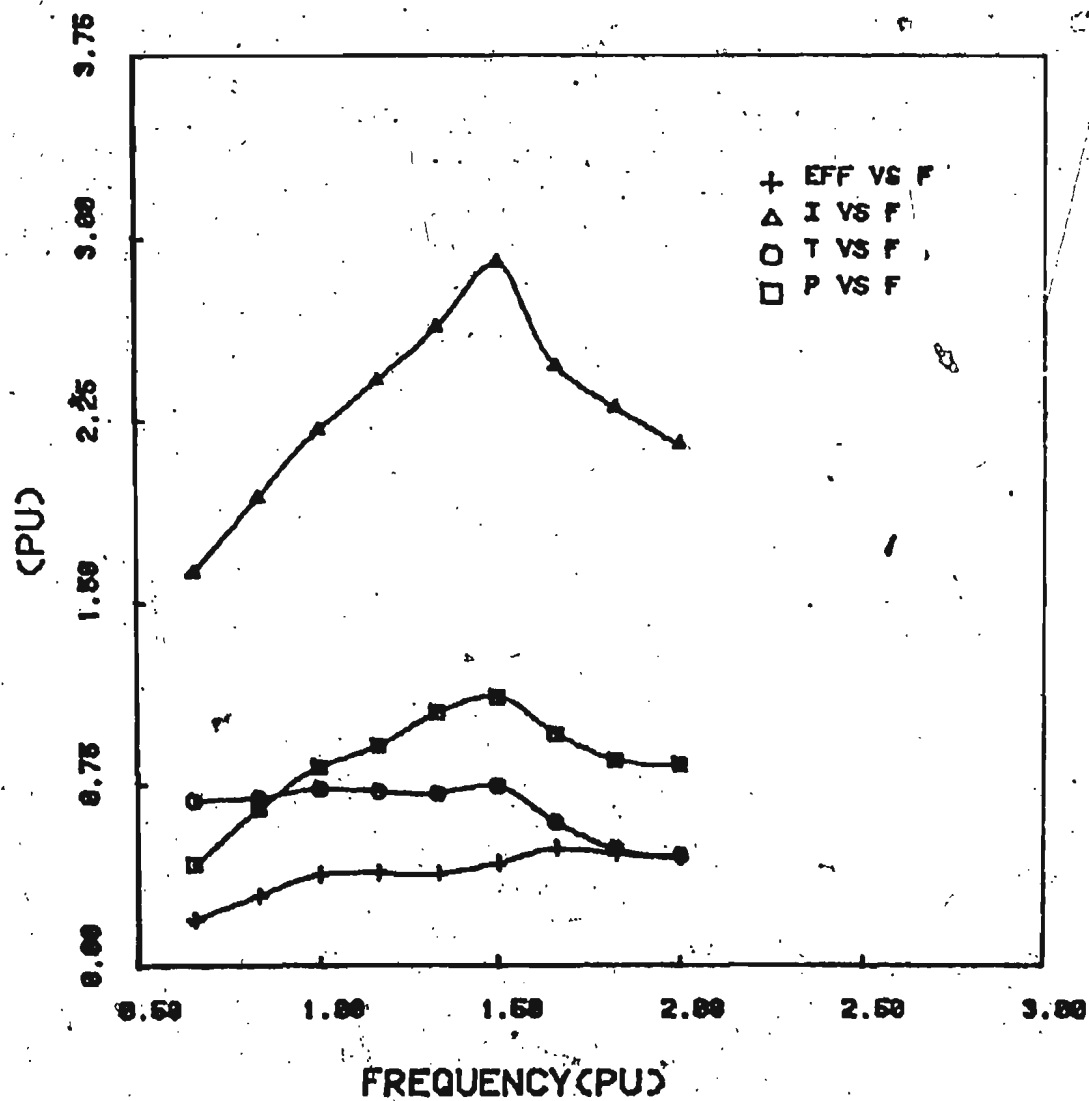


Fig. 4.5

Theoretical performance characteristics of a 1/2 hp, 1-phase induction motor fed from DM inverter ( $V_R = 5.5V$ )

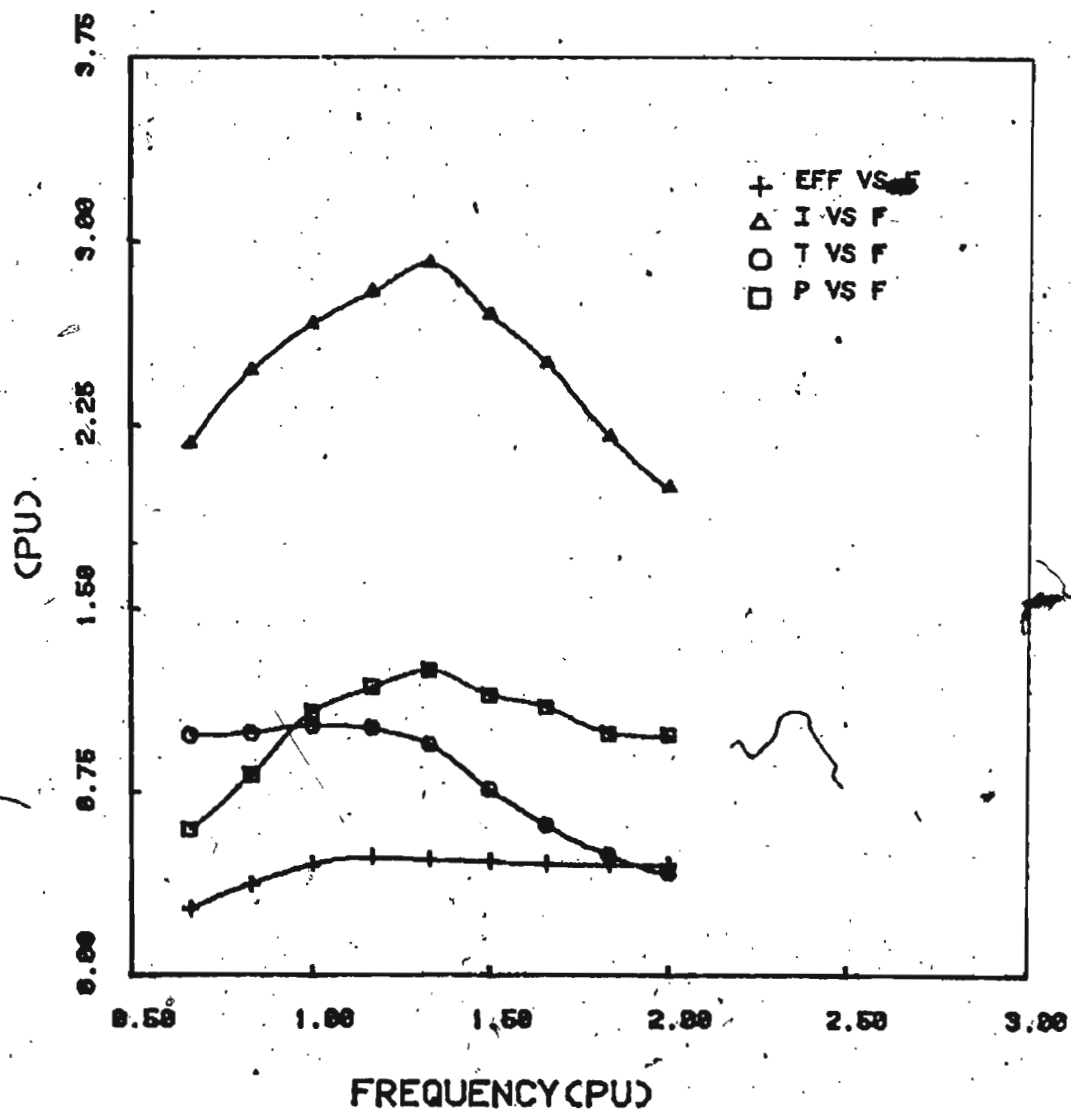


Fig. 4.6

Theoretical performance characteristics of a 1/2 hp, 1-phase induction motor fed from DM inverter ( $V_R = 6.75V$ )

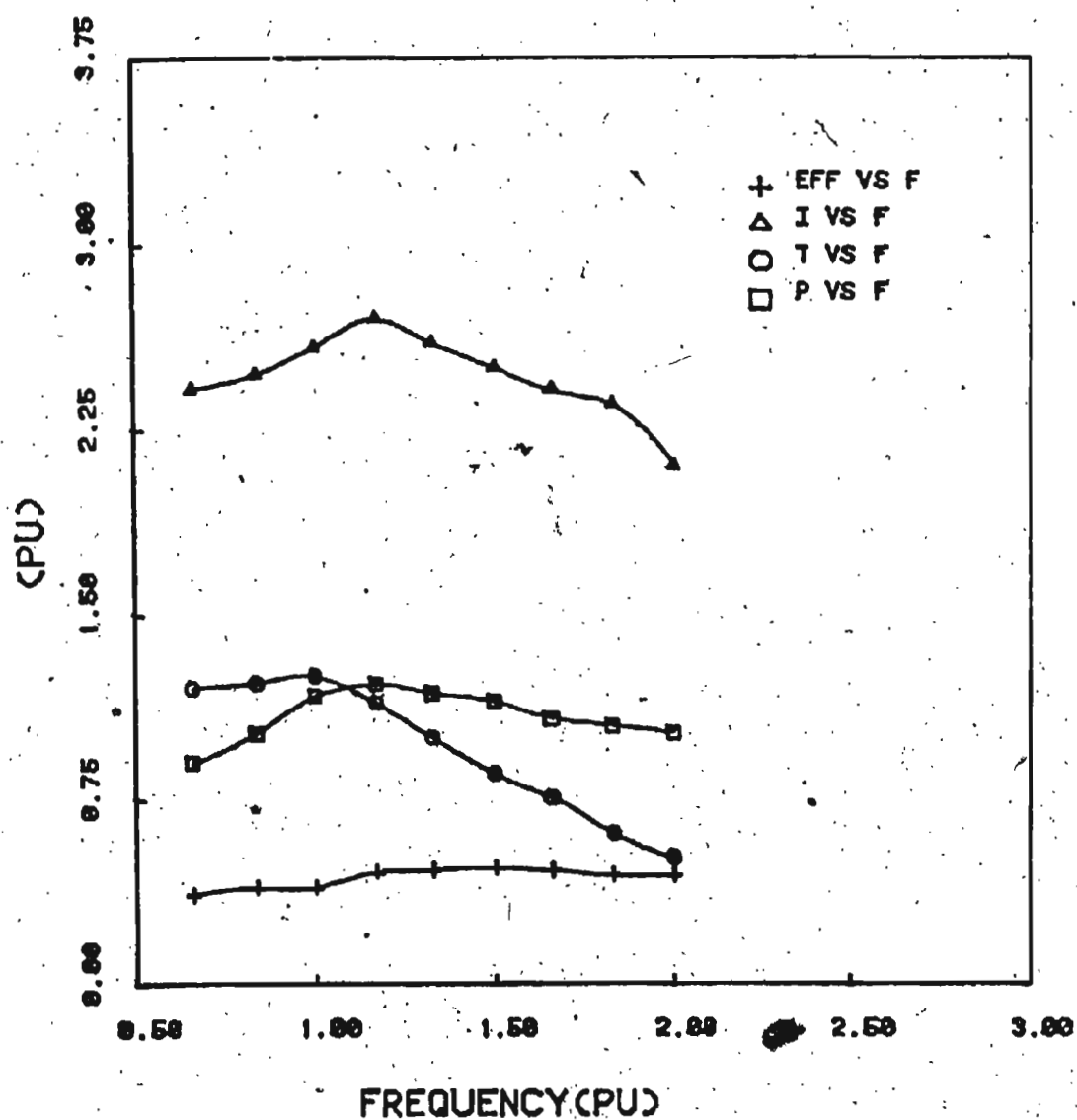


Fig. 4.7

Theoretical performance characteristics of a 1/2 hp, 1-phase induction motor fed from DM inverter ( $V_R = 7.5V$ )

On the other hand, the maximum torque developed at the airgap has constant characteristics upto the base frequency and decreases beyond the base frequency as frequency of operation increases. Speed variation of the motor though not shown in the characteristics curves, has a linear variation with frequency. The change in modulation index changes the base frequency of motor operation and that is evident from the various plots with different modulation index. As a result of change in the base frequency with modulation index, the range of motor operation on constant torque and constant power modes, changes too. The other effect of changing the modulation index is to change the harmonic behaviour of the inverter output voltage. This too is reflected in the plots for different power, torque, current and power factor values at the same operating frequency. The maximum developed torque, power factor and efficiency increase with the increase of modulation increase.

#### 4.3.3 Experimental Results

Two single phase induction motors of 1/4 and 1/2 hp, 60 Hz, 4-pole, 115V ratings were run from single phase full bridge delta modulated inverter. The steady state performance of the motors were obtained for variable frequency operations. The results are included in Figs. 4.8 to 4.13. Figs. 4.8 to 4.10 contain the results for the 1/4

hp motor while the plots of Figs. 4.11 to 4.13 contain the results of 1/2 hp motor. The performances are plotted for different modulation index at  $V_R = 5.5, 6.75, 7.5V$  in these plots, respectively. It is evident from the experimental results that the performance curves for motor current, power factor, minimum power developed and efficiency of the motor show good agreement with theoretical results. However, the maximum developed torque variations with frequency at low modulation index, show considerable variation with frequency at lower frequency of operation. From the experimental plots, we find that with lower modulation index with  $V_R = 5.5$  and  $6.75V$ , the maximum developed torque has an increasing trend at low frequency operation. It shows the desired constant torque upto base frequency at higher frequency of operation. Beyond the base frequency, the performance curve has the desired decreasing maximum developed torque as predicted for all modulation index. The linear increasing nature of maximum torque at low frequencies disappears to a certain level as the modulation index is increased. The variation of experimental torque characteristics at low frequencies for lower modulation index can be explained as: In theory, the delta modulated inverter output keeps a constant fundamental voltage to frequency characteristics upto base frequency. The analysis does not incorporate the commutation intervals provided between successive pulses at

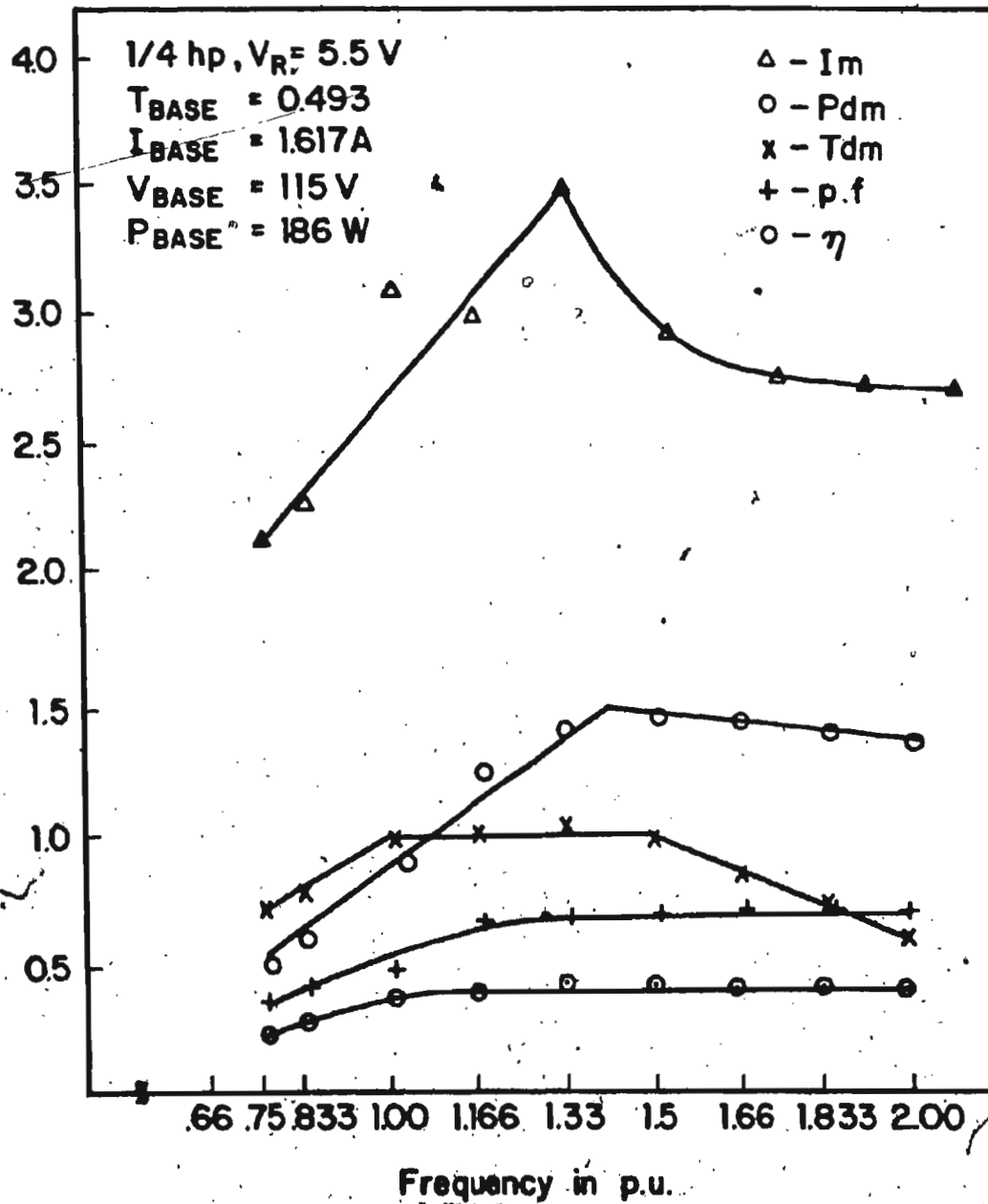


Fig. 4.8

Experimental performance characteristics of a 1/4 hp, 1-phase induction motor fed from DM inverter ( $V_R = 5.5$  V)

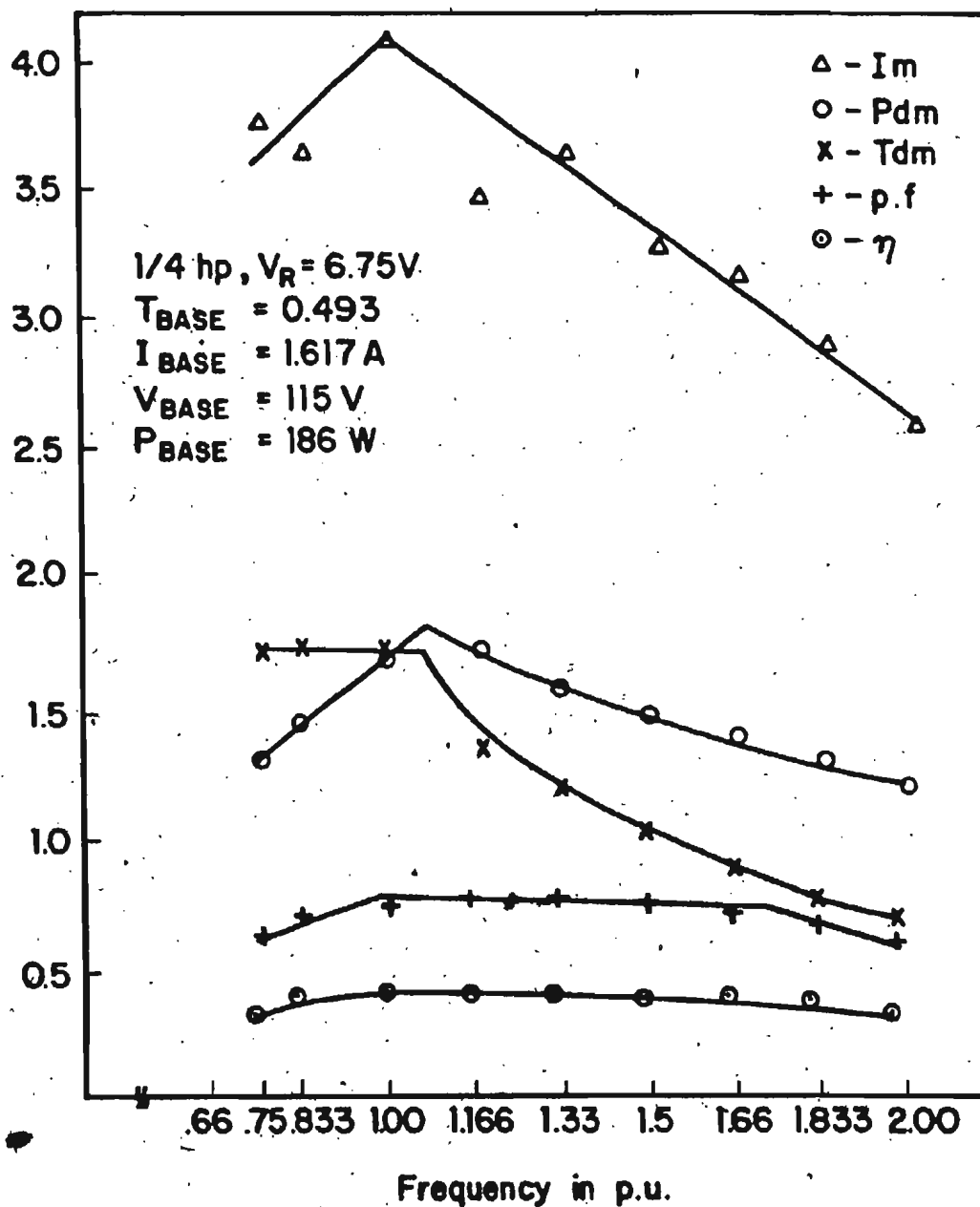


Fig. 4.9 Experimental performance characteristics of a 1/4 hp, 1-phase induction motor fed from DM inverter ( $V_R = 6.75V$ )

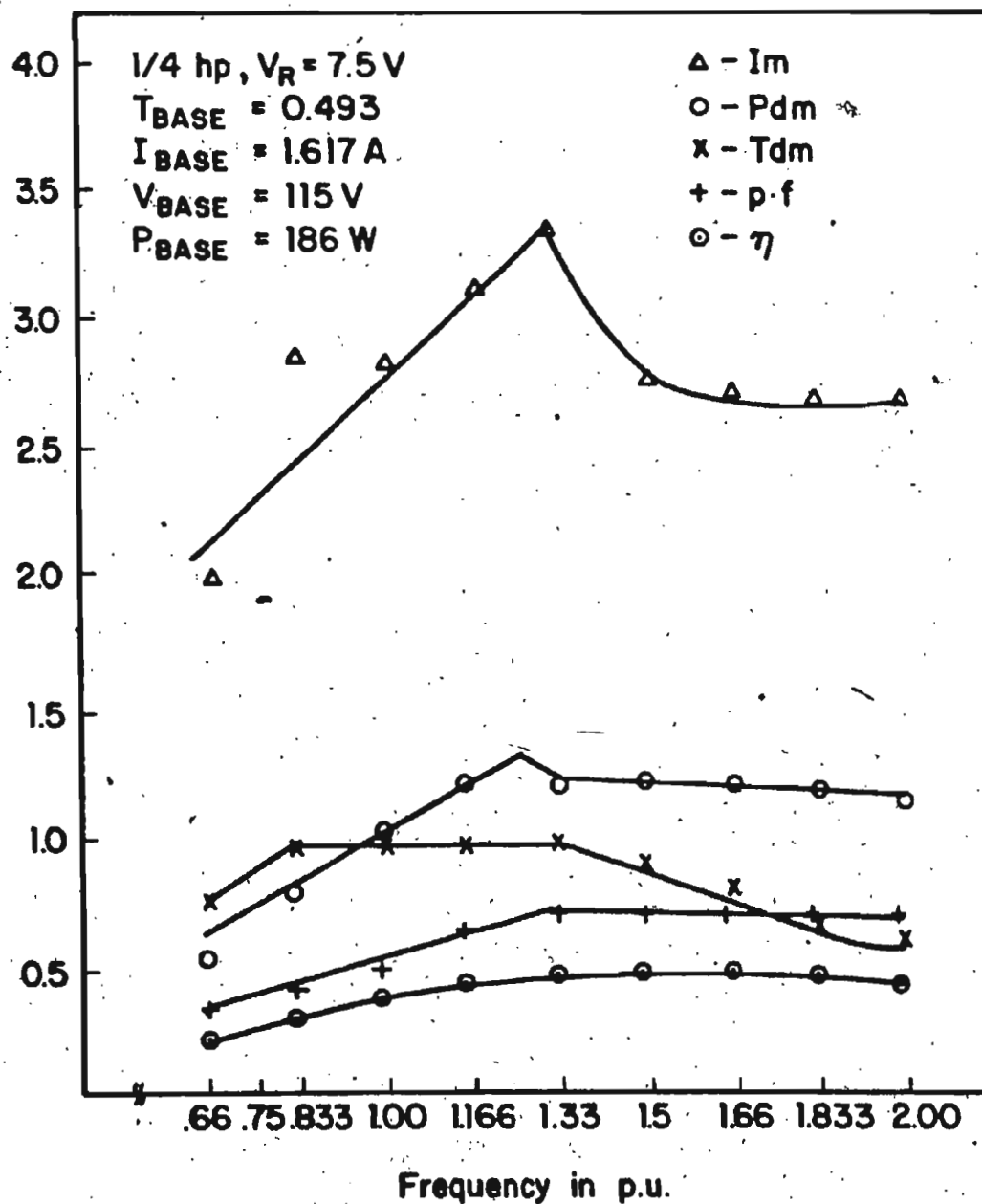


Fig. 4.10

Experimental performance characteristics of a 1/4 hp, 1-phase induction motor fed from DM inverter ( $V_R = 7.5$  V)



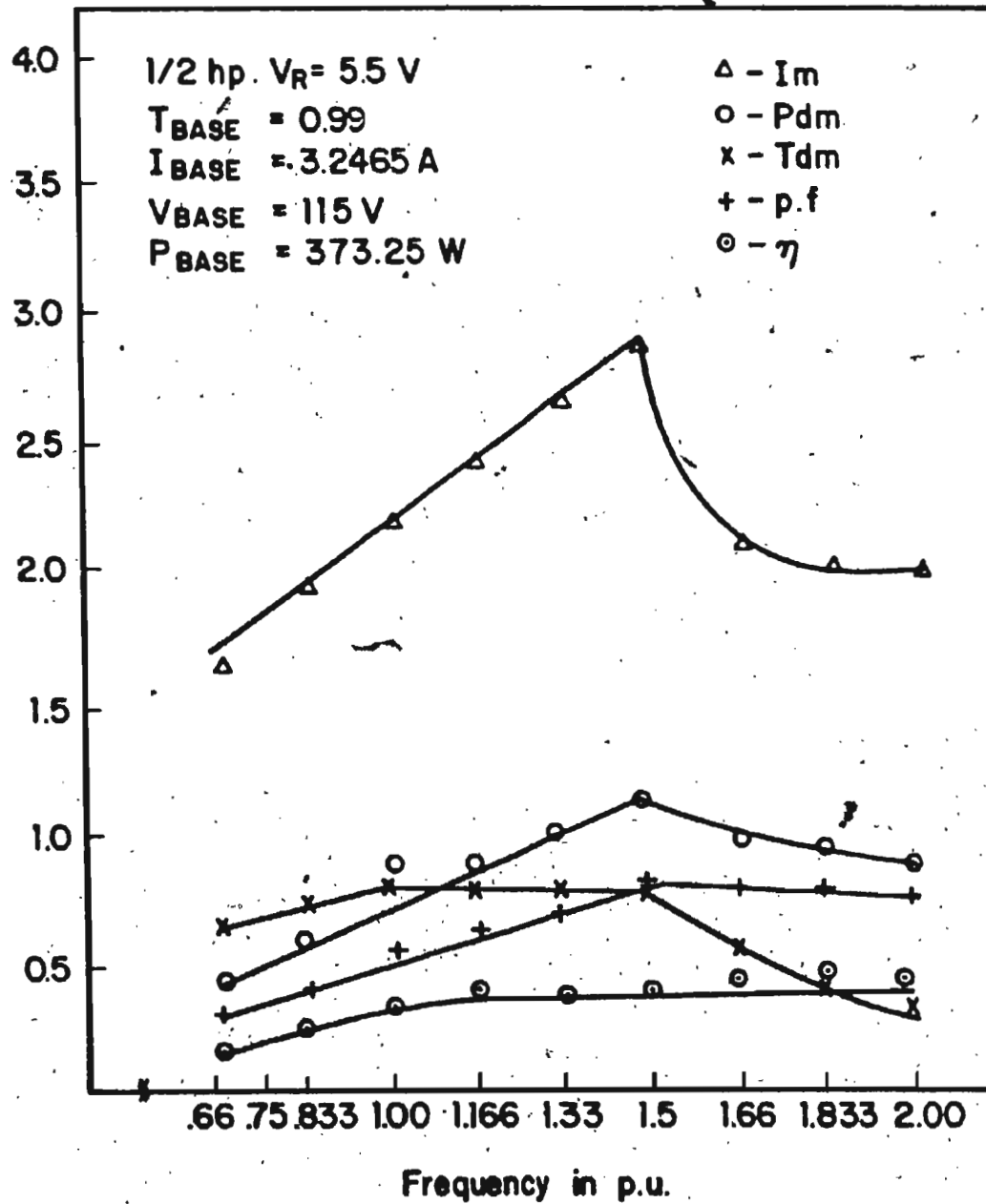


Fig. 4.11 Experimental performance characteristics of a 1/2 hp, 1-phase induction motor fed from DM inverter ( $V_R = 5.5 \text{ V}$ )

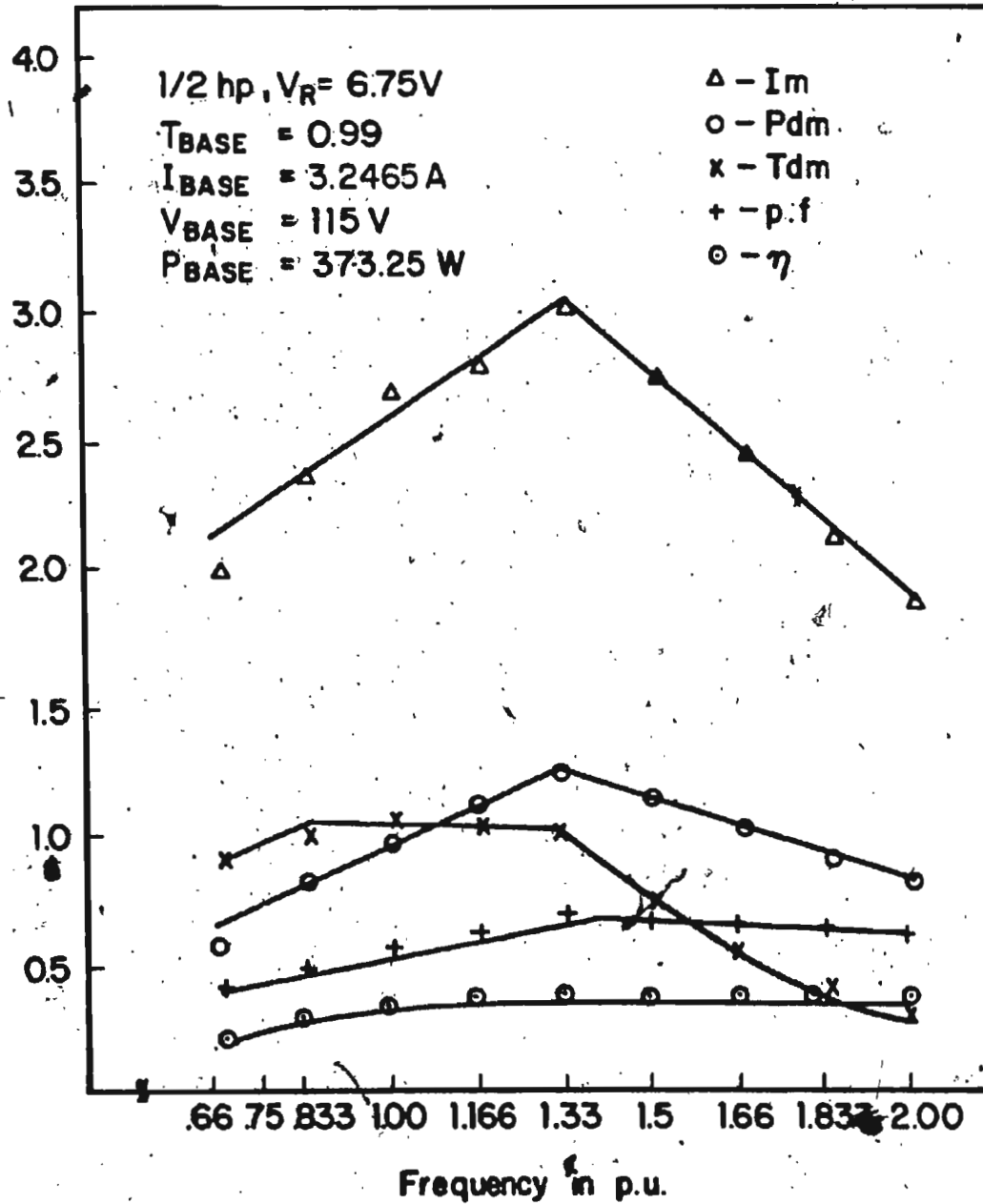


Fig. 4.12 Experimental performance characteristics of a 1/2 hp, 1-phase induction motor fed from DM inverter ( $V_R = 6.75V$ )

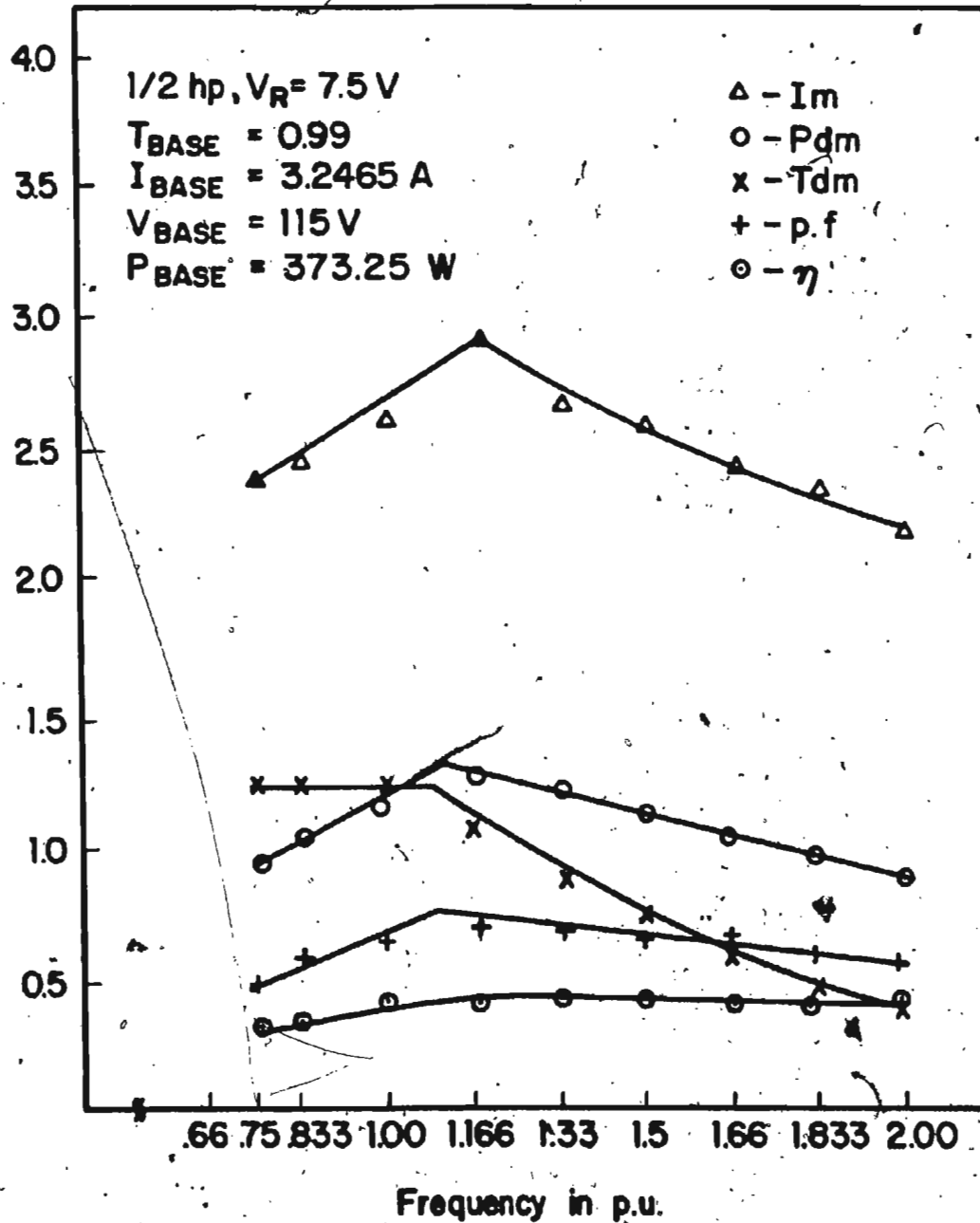


Fig. 4.13

Experimental performance characteristics of a  $1/2 \text{ hp}$ , 1-phase induction motor fed from DM inverter ( $V_R = 7.5 \text{ V}$ )

the inverter output. When the number of commutations is low the intervals do not affect the output voltage-to-frequency ratio significantly. The reason is, the voltage drop due to the commutation is insignificant. But as the number of commutation increases, the reduction of voltage due to the commutation intervals become significant. As a result, the inverter output could not maintain the constant  $V/f$  ratio in practical applications. It has been already stated in chapter 2 (section 2.2 and 2.4.4) that the commutation number per second is strictly dependent on the modulation index. The lower is the modulation index, the higher is the number of commutations. This is reflected in motor torque characteristics in practice. At lower modulation index for low frequency operation, the number of commutation is excessively high which results in lower voltage at the inverter output. This causes the motor torque characteristics to follow a increasing linear variation with change in frequency. As the frequency of operation is increased, the number of commutation decreases and the motor attains its desired constant torque characteristics and maintains this constant torque characteristics upto base frequency. When the modulation index is increased, the linear increase in torque characteristics disappears altogether due to lower number of commutations as shown in Figs. 4.9 and 4.11. This shows that if the motor

characteristics as predicted in the theoretical analysis is to be obtained, the modulation index should be kept high to a optimum value or the voltage variation at the input of the inverter has to be done with variation of frequency of operation. However, the first choice is the preferred one, because the second method will require a feedback from the motor to inverter input side. It thus involves a double conversion process, which is not desired in PWM inverters.

## CHAPTER 5

The requirements of a three phase delta modulated inverter logic are - a three phase sine reference wave generator, a delta modulator circuit for each phase and the proper logic circuits for production of gating signals for the thyristors of the three phase inverters. The three phase sine reference wave generator was designed and built for such an inverter logic. It consists of a square wave generator, the output of which is fed to a ring counter to produce a three phase square wave. The three phase square wave is converted to constant amplitude triangular wave through a DCAS and an integrator circuit. It is then passed through FETs to give the desired 3-phase sine modulating wave. The modulator circuits are the same as used in single phase implementation. The sine modulating waves are fed to all three modulator circuits to produce the switching signals which are processed by logic circuits to get the gating signals. This chapter gives a description of each section involved in a 3-phase delta modulation logic implementation.

### 5.1 Three Phase Delta Modulation Circuit Design and Implementation

Developments of single phase delta modulated logics are extended in developing a three phase delta modulator, the design and implementation of which are described in the

following sections. Essentially a three phase modulator for delta modulation consists of three phase reference wave generator, the three modulation circuits and the logic circuits for three phases to produce the required gating signals for the thyristors of 3-phase inverters. The important factors in a three phase modulation are to generate constant amplitude three phase sine wave to feed the modulation circuits, choice of maximum number of commutation to ensure proper thyristor operation in 3-phase inverter, synchronising the modulated wave and carrier wave and finally, the choice of  $120^\circ$  to  $180^\circ$  conduction modes of the inverter switches.

## 5.2 Three Phase Sine Reference Wave Generator

Many methods of producing three phase sine wave generator were put forward in the past [38-45]. In most cases the techniques use analog circuitry in which a single phase signal of fixed frequency  $\omega_0$  is generated. This signal is modulated by two or three phase square wave signals of a frequency  $\omega$  higher than  $\omega_0$  by the desired frequency so that the modulated signal has frequency components  $(\omega \pm \omega_0)$ ,  $(3\omega \pm \omega_0)$  ..... etc. Using low pass filter, all the high frequencies are filtered out, leaving only the signal of the desired frequency  $(\omega - \omega_0)$ . The hybrid method of generating low frequency sine wave signal is reported in reference [45].

A completely digital method is reported in reference [41]. The digital method uses a PROM containing values of  $\sin x$  for 32 steps between 0 to 90 degrees. The programmed values along with other digital signals are used to produce a digital sine wave. The scheme however, is expensive and complicated. For the present purpose, a hybrid circuit for producing sine waves proposed in reference [39] is designed and implemented. The circuit is simple and there are fewer components when compared to methods in reference [38-43]. In the present scheme, a three phase square wave of variable frequency is generated first. Each square wave is used to produce a constant amplitude triangular wave which is then shaped to a sine wave characteristic of the drain current of a FET for a drain voltage variation between zero and pinchoff.

Fig. 5.1 gives the block diagram of the scheme used. The scheme has three distinct sections. A  $V/f$  converter generates the variable frequency square wave. From the square wave the 3-phase square wave is generated by the circuit illustrated in Fig. 5.2.2, the logic development of which is shown in Table 5.1 and 5.2. The last section in the scheme uses a DCAS and an integrator circuit to convert the square waves to a constant amplitude triangular wave. The triangular waves are shaped to the desired sine wave by FETs. No attempt has been made in the present implementation to



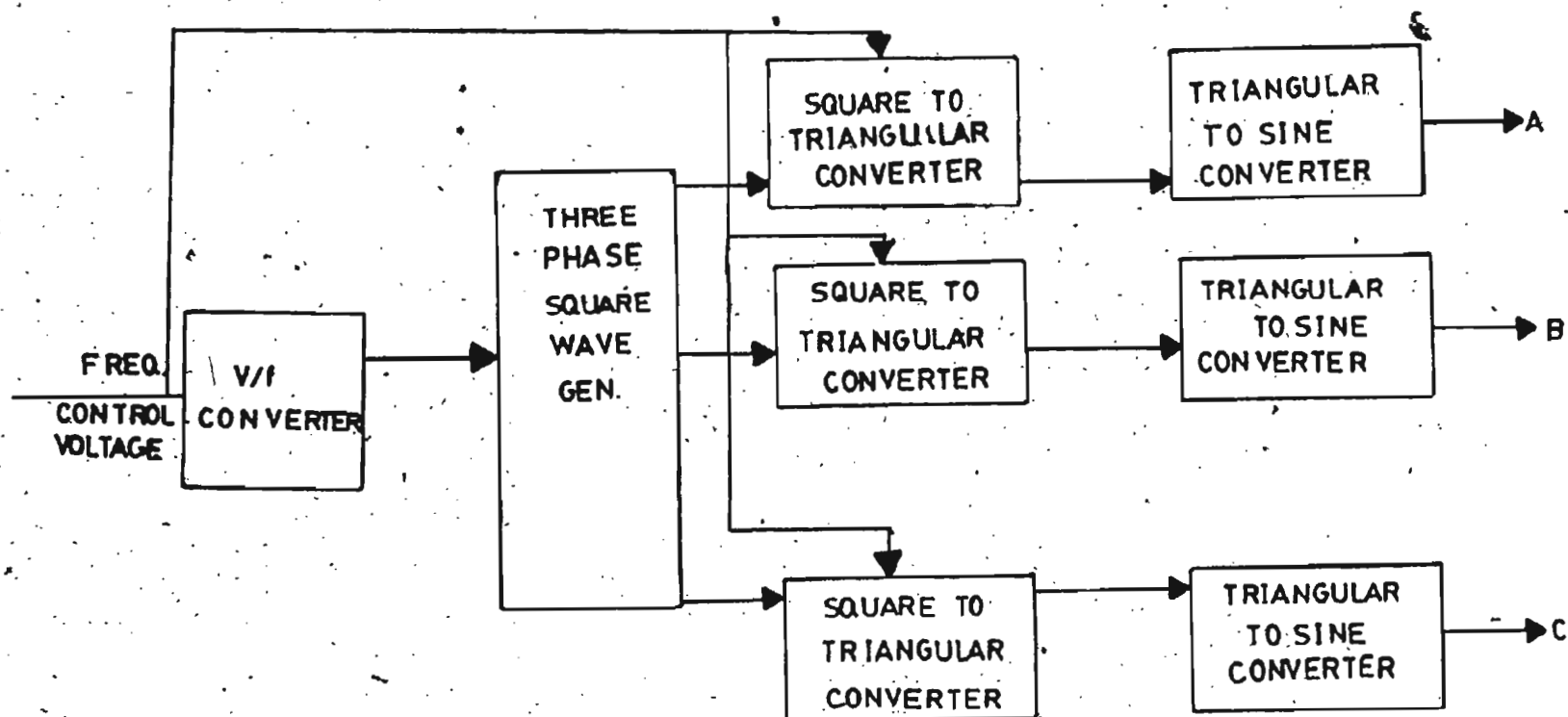


Fig. 5.1 Block diagram of a 3-phase sine wave generator

control the amplitude and phase sequence of the reference waves, which however can be accomplished easily as described in reference [37]. The practical implementation circuit is included in Appendix F. The outputs of the circuits are illustrated in Fig. 5.4 for 60 hz operation.

### 5.2.3 Modulator and Logic Circuits

For three phase implementation, the modulation circuit is the same as that of single phase implementation circuit. Three identical circuits same as Fig. 2.4 were built and fed from the 3 phase sine reference wave generator. The resultant output at the modulator circuits are shown in Fig. 5.4. However, the switching waveforms of the inverter are generated by using a different logic circuit for the three phase inverter. In single phase inverter circuit, every alternate pulse of the modulated wave was used to switch on a pair of thyristors. But in three phase inverter circuit, the logic is developed in such a way that the pulses in one half cycle is used to switch on a pair of the thyristors. The timing diagram of the signals for main and commutation thyristors are shown in Fig. 5.5, and the logic circuit diagram is shown in Fig. 5.6. The practical circuit for implementing the logic diagram is given in Fig. A.7 of Appendix E. The switching signals after modulating with high frequency pulses, are illustrated in Fig. 5.7.

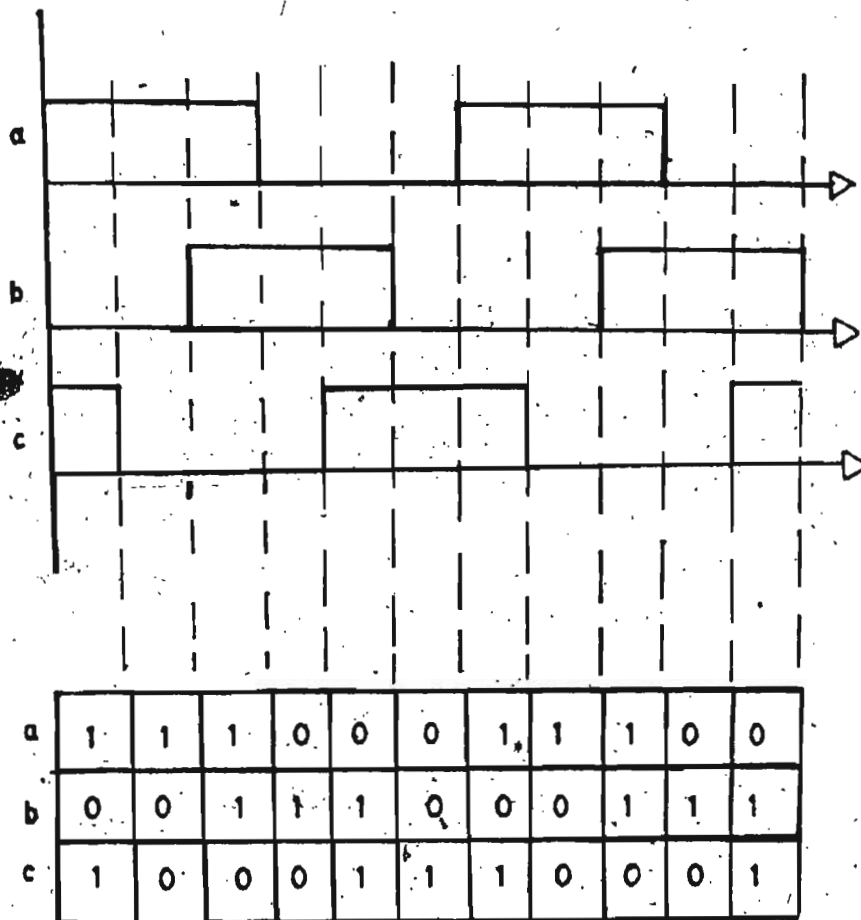


Fig. 5.2 States of 3-phase square wave

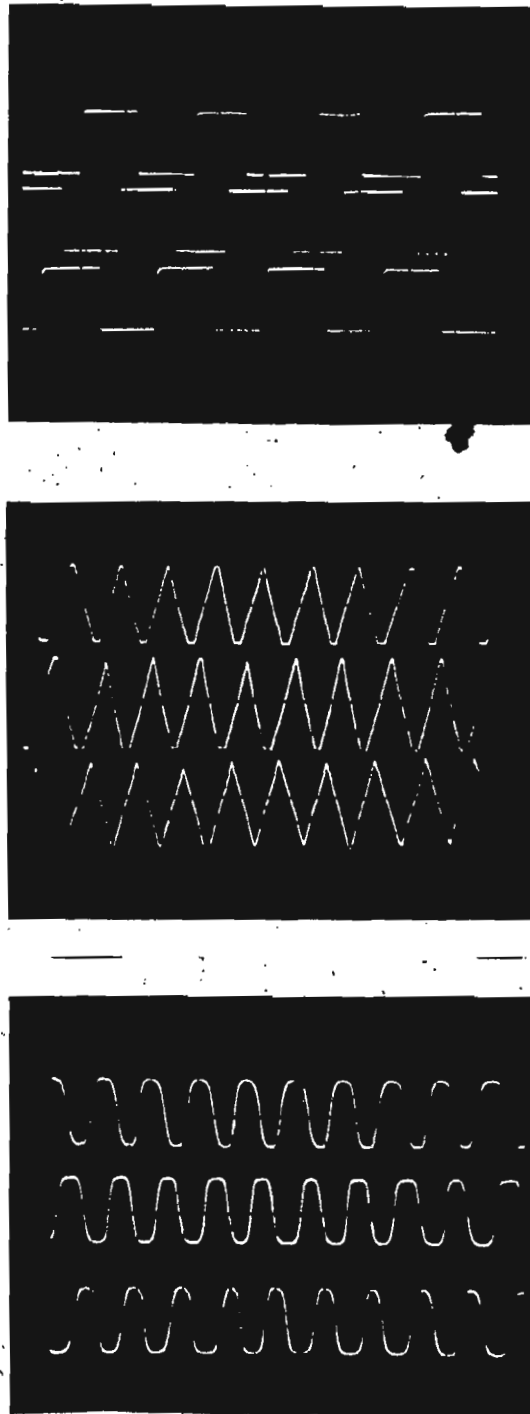


Fig. 5.3

Waveshapes of different sections of sine  
reference wave generator

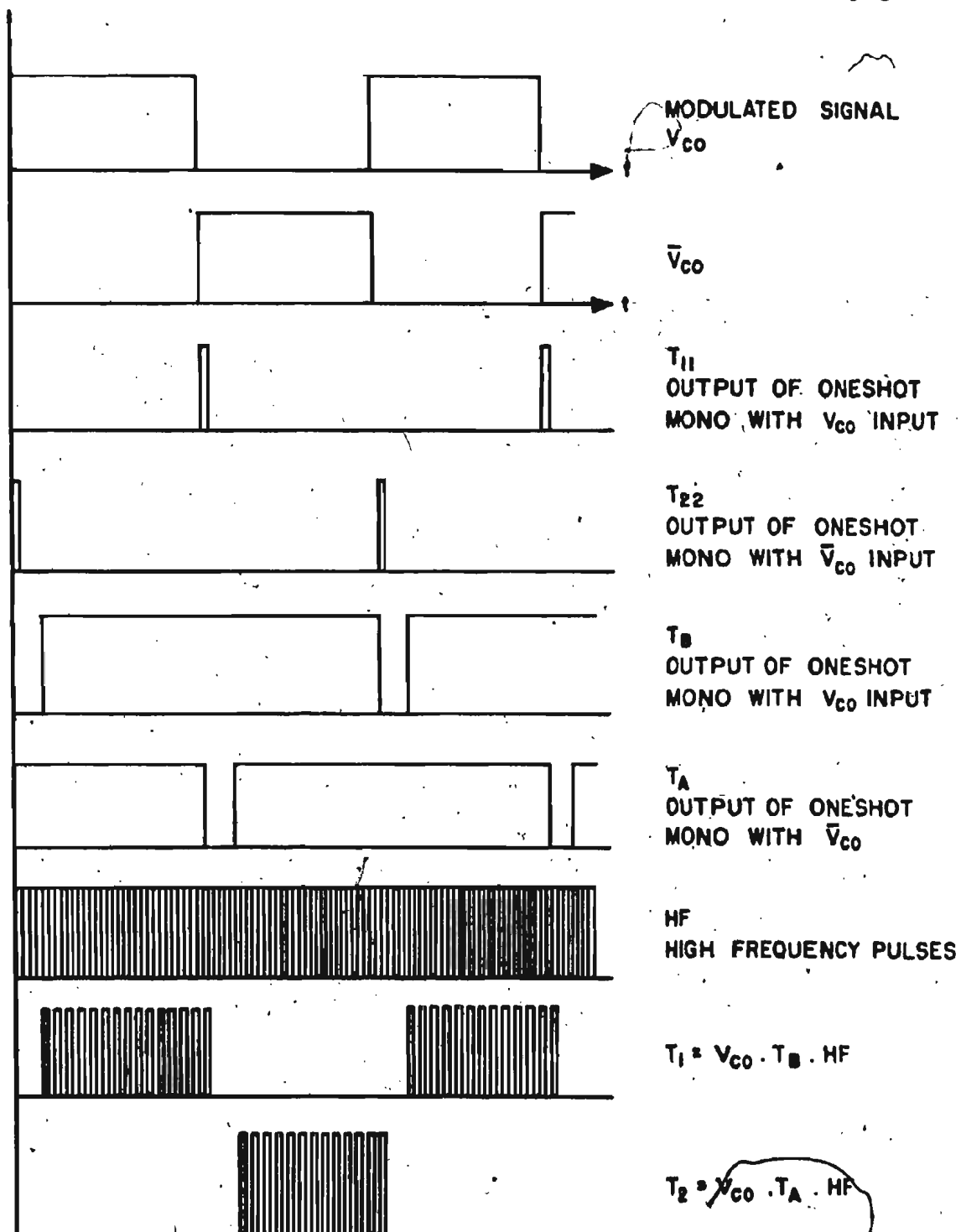


Fig. 5.4 Timing diagram of 3-phase delta modulated wave generation



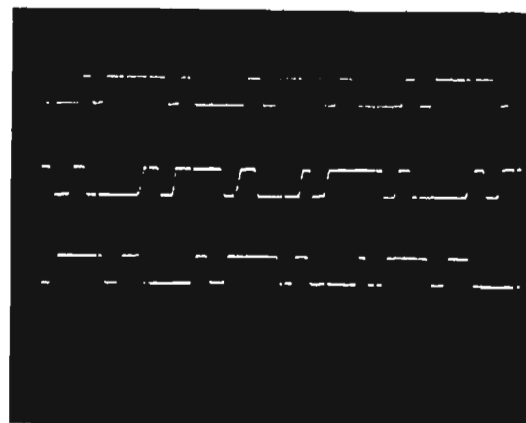


Fig. 5.6

Output waveshapes of a 3-phase delta modulation circuit

The logic circuits designed and developed for the three phase application was successfully tested by running a 3 phase bridge inverter. Detailed study of the loading of a three phase inverter is under way. It is however considered beyond the scope of this thesis.



CHAPTER 6SUMMARY AND CONCLUSIONS

In this thesis an analysis and implementation of the delta modulated inverter has been carried out. The analysis includes a study of delta modulation technique for inverters and the application of the delta modulated inverter to passive and induction motor loads. The features of delta modulation, namely easy implementation, lower harmonics at the output of the inverter, transition of  $V/f$  characteristics from multiple pulse mode to single pulse mode, easy harmonic and commutation control have been verified theoretically and experimentally for a single phase delta modulated inverter. A Fourier analysis was done for the delta modulated wave. It has been found in the study that the harmonic behaviour of delta modulated inverters are such that at the inverter output, the harmonic voltages are high at low frequency operation and low at high frequency operation. However, at low frequency operation, the dominant harmonics are higher orders; and at high frequency operation, the dominant harmonics are lower order. As a consequence, when the DM inverters are used for R-L load or motor dynamic loads, higher harmonics in the load currents are attenuated. This is because the harmonic reactances for higher order harmonics at low frequency operation are high and for lower order

In analog circuit implementation, the above features definitely give delta modulation an upper hand over the conventionally used sine PWM technique. A brief comparison of sine PWM with the proposed delta modulation scheme has been made. In analog implementation, though delta modulation has an edge over sine modulation, it is yet to be determined whether this will be the same when delta modulation is implemented with the help of microcomputers.

The analysis of delta modulation has been used in predicting the performance of passive and motor dynamic loads with inverter supplies. The passive loads considered are resistive and R-L loads. For passive load performance, inverter equations are used to predict load current, power, voltage and power factor. The validity of the features of the delta modulated inverters are verified experimentally with passive loads.

In the study of the motor performances with delta modulated inverter supply, single phase induction motor performance in the steady state mode using a delta modulated inverter has been studied. To meet various requirements of motor drives, conventional VSI, CSI and sine PWM inverters require complex control circuits. Harmonics at the inverter output influence the steady state and transient performance of such drive systems. Single phase induction motor performance for two 1/4 and 1/2 hp motors have been analyzed and verified experimentally. The analysis and verification

A

harmonics at high frequency operation are high. This high reactance value at different dominant harmonics limits the harmonic load current. The theoretical results of the harmonic behaviour of the delta modulated inverter output was verified experimentally with a spectrum analyser.

It has been shown theoretically and experimentally that the modulator output voltage has an inherent fundamental voltage-to-frequency variation, which is essential for ac motors to have characteristics like dc motor i.e. - constant torque and constant power operation with variable frequency supply.

The variation of the level of modulating sine wave signal on the harmonic contents of the inverter output has been studied. With low modulating signal level at the input of the modulator, an increase in number of pulses causes increase in the harmonic content, whereas the high modulating signal level at the input of the modulator decreases the number of pulses per cycle, which causes a reduction in the harmonic content at the inverter output. This ensures an easy way of controlling the harmonics at the DM inverter output. A changing modulating signal also has the effect of changing the number of commutations in inverter operation. The maximum number of commutations per cycle in the inverter, depends on the modulating signal level besides other circuit parameters.

of steady state performance included determination of motor current, power, power factor and efficiency at variable frequency operations. The analysis showed that the delta modulation technique provides certain features like V/f variation, harmonic content and ease of analog implementation which would make it a very useful technique for inverter motor drives. The successful experimental study of single phase motors with delta modulated inverters indicate that delta modulation is unique in variable speed drives. It has been found that motor performances with delta modulated inverters is comparable to those with sine PWM drives using additional control circuitry for harmonic and V/f controls. Discrepancies in torque-speed characteristics at low frequency operation with low modulating signal level has been explained.

Finally, the study describes the analog implementation of a three phase delta modulation circuit for generating switching waveforms for a three phase inverter. The requirements of 3 phase inverter logics are a sine reference wave generator, a modulator circuit for each phase and a proper logic circuit for producing switching waveforms for the main and commutation thyristors of a three phase inverter. The three phase sine reference wave generator was designed and built for such an inverter logic. It consists of a square wave generator, the output of which is fed to a

ring counter to produce a 3 phase square wave. The three phase square wave is converted to a constant amplitude triangular wave through a DCAS and an integrator circuit and then passed through FETs to give the desired three phase sine modulating wave. The modulator circuit consists of three identical 1-phase modulator circuits. The sine modulating waves are fed to all three modulator circuits to produce the switching waveforms which are processed by logic circuits to get the proper gating signals. The three phase delta modulation circuit was used to run a three phase inverter. The testing of the three phase ac motors fed from the 3-phase delta modulated inverter is beyond the scope of this thesis.

The theoretical and experimental load current waveshapes have been compared for an R-L load. The load current wave shapes are of particular interest in designing the commutation circuit of the inverters and choosing the filter sizes at the output of the inverter.

#### RECOMMENDATION FOR FUTURE WORKS

The present work contains the analysis and analog implementation of delta modulation for inverters with passive and single phase induction motor loads. Design and implementation of a three phase circuit for a three phase inverter has been completed. But a detailed study of three phase inverters with loads has not been presented. With

these points in mind future work in the area may be stated as, follows:-

(a) A detailed study is to be made of the delta modulation technique for three phase inverters is to be done. The study may include delta modulated inverter fed passive and active loads. Active loads can be either induction motors or synchronous motors. Besides providing constant power profile in ac motor characteristics in variable speed operation, the V/f ramp characteristics would provide good starting characteristics for synchronous type ac machines. This is especially needed for synchronous machines using permanent magnets as their excitation.

(b) Steady state analysis has been done for 1-phase induction motors. The study may continue with the steady state analysis of three phase ac motors and their transient behaviour when fed from delta modulated inverters.

(c) A comparison of delta modulation with sine modulation technique has been made on the basis of analog implementation only. No attempt has been made to implement delta modulation for inverter operation with microcomputers. The complexities and requirements involved in microprocessor implementation can be undertaken in the future, and after that only the meaningful comparison of delta modulation with the sine modulation technique can be established.

(d) As load is applied to an inverter output, harmonic distortion of the input current at the dc side is introduced in the system. This input current waveshape is important in designing effective filters for the input side of the inverter.

(e) Inverter applications are not limited to variable speed drives only. They have wide use in induction heating and UPS systems etc. In the UPS system, delta modulation for inverters may be attractive for their excellent low order harmonic attenuation and low commutation rates for high modulation index values. This possibility for delta modulated inverters for use in other applications should be studied and explored in detail.

REFERENCES

1. King, K.G., "Variable Frequency Thyristor Inverters for Induction Motor Speed Control", Direct Current, February 1965, pp. 125.
2. Kirnick, A., and Heinrich, "Static Inverter with Neutralization of Harmonics", Trans. AIEE, Vol. 81, May 1962, pp. 59-68.
3. Turnbull, F.G., "Selected Harmonic Reduction in Static DC-AC Inverters", Trans. AIEE, Vol. 83, July 1964, pp. 374-378.
4. Schonung, A., and Steimmler, H., "Static Frequency Changer with Subharmonic Control in Conjunction with Reversible Speed AC Drives", Brown Boveri Review, Aug/Sept. 1964, pp. 555-577.
5. Mokrytzki, B., "Pulse Width Modulated Inverters for AC Motor Drives", IEEE Trans. on IA, Vol. IGA - 3, Nov./Dec. 1967, pp. 493-503.
6. Adams, R.D. and Fox, R., "Several Modulation Technique for PWM Inverters", IEEE Trans. on IA Vol. 3, No. 5, Sept./Oct. 1972, pp. 636-643.
7. Bowes, S.R., "New Sinusoidal Pulse Modulated Inverter", Proc. of IEE, Vol. 122, No. 11, 1975, pp. 1279-1285.
8. Kliman, G.B. and Plunkett, A.B., "Development of a Modulation Strategy for a PWM Inverter Drive", IEEE Trans. in IA, Vol. IA-15, No. 1, Jan./Feb. 1979, pp. 72-79.
9. Trevor, Grant and Thomas Barton, "Control Strategies for PWM Drives", IEEE Trans. on IA, Vol. IA-16, No. 2, March/April 1981, pp. 211-215.
10. Bowes, S.R. and Mount, M.J., "Microprocessor Control of PWM Inverters", IEE Proc. pt-B, Vol. 128, 1981, pp. 293-305.
11. Grant, D.A. and Saidner, R., "Ratio Changing in Pulse Width Modulated Inverters", IEE Proc., Vol. 128, pt. B, No. 5, Sept. 1981, pp. 243-248.
12. Bowes, S.R. and Clements, R.R., "Microprocessor Based PWM Inverters", IEE Proc., Vol. 129, pt. B, No. 1, Jan. 1982, pp. 1-17.



13. Green, R.M. and Boys, J.T., "Implementation of Pulse Width Modulated Inverter Modulation Strategies", IEEE Trans., on IA, Vol. IA-18, No. 2, March/April 1982, pp. 138-145.
14. Cook, B.J., Cantoni, A. and Evans, R.J., "A Microprocessor Based, 3-Phase Pulse Width Modulator, IEEE Ch. 1682-4/82/0000-0375, 1982, pp. 375-383.
15. Pollman, A., "A Digital Pulse Width Modulator Employing Advanced Modulation Technique", IEEE Ch. 1682-4/82/0000-0116, 1982, pp. 116-121.
16. Bowes, S.R. and Clare, J.C., "PWM Inverter Drives", IEE Proc., Vol. 130, pt. B, No. 4, July 1983, pp. 229-240.
17. Buck, F.D., Gistellinck, P., Backer, D.D., "Optimised PWM Inverter Driven Induction Motor Losses", IEE Proc., Vol. 130, pt.-B, No. 5, Sept. 1983, pp. 310-320.
18. Zubeck, J., Abbondanti, A., Nordby, C.J., "Pulse Width Modulated Inverter Motor Drives with Improved Modulation", IEEE Trans. on IA, IA-11, NO. 6, 1975, pp. 695-703.
19. Patel, H.S. and Hoft, R.G., "Generalized Technique of Harmonic Elimination on Voltage Control in Thyristor Inverter", Part-I, IEEE Trans. on IA, 1973, pp. 310-317.
20. Patel, H.S. and Hoft, R.G., "Generalized Technique of Harmonic Elimination on Voltage Control in Thyristor Inverter", Part-II, IEEE Trans. on IA, IA-10, 1974, pp. 666-673.
21. Buja, G.S. and Indri, G.B., "Optimal Pulse Width Modulation for Feeding AC Motors", IEEE Trans. on IA, IA-13, 1977, pp. 38-44.
22. Nonaka, S. and Okada, H., "Methods to Control Pulse Width of Three Pulse Inverters", Journal of IEE Japan, Vol. 86, July 1972, pp. 71-79.
23. Bedford, B.D. and Hoft, R.G., "Principles of Inverter Circuits", John Wiley and Sons Inc., 1964.
24. Buja, G.S., "Optimum Output Waveforms in PWM Inverters", IEEE Trans. on IA, Vol. IA-16, No. 6, Nov./Dec. 1981, pp. 830-836.

25. Dewan, S.B. and Forsythe, S.B., "Harmonic Analysis of a Synchronized Pulse Width Modulated 3 Phase Inverter", IEEE Trans. on IA, Vol. IA-10, Jan./Feb. 1974, pp. 117-122.
26. Huang, I.B. and Lin, W.S., "Harmonic Reduction in Inverters by Use of Sinusoidal Pulse Width Modulation", IEEE Trans. on Control Instrumentation, Vol. IECI-27, No. 3, Aug/1982, pp. 201-207.
27. Bowes, S.R. and Bird, B.M., "Novel Approach to Analysis of Modulation Processes in Power Converters", Proc. IEE, Vol. 122, No. 5, May 1975.
28. Ziogas, P.D. and Photiadis, P.N.D., "An Exact Input Current Analysis of Ideal Static PWM Inverters", IEEE Trans. on IA, Vol. IA-19, No. 2, March/April 1983, p. 281-295.
29. Jackson, S.P., "Multiple Pulse Modulation in Static Inverter Reduces Selected Output Harmonics", IEEE Trans. on IA, IGA-64, 1970, pp. 357-360.
30. Ziogas, P.D., "The Delta Modulation Technique in Static PWM Inverters", IEEE Trans. on IA, March/April 1981, pp. 199-204.
31. Jones, D., "Delta Modulation for Voice Transmission", Electronic Engineering, Jan. 1978, pp. 49-51.
32. Misha, Schwartz, "Information, Transmission Modulation and Noise", McGraw-Hill, 1980, pp. 140-155.
33. Cattermole, K.W., "Principles of Pulse Code Modulation", London ILIFFE Books Ltd., 1969, pp. 198-218.
34. Carlson, A.B., "Communication Systems, An Introduction to Signals and Noise in Electrical Communications", 2nd Edn., McGraw-Hill, p. 326-331.
35. Walden, J.P., Turnbull, F.G., "Adjustable Voltage and Frequency Polyphase Sine Wave Generator", IEEE IA Conference Record, 1974, pp. 1015-1020.
36. Murphy, J.M.D., "Thyristor Control of AC Motors", Pergamon Press, 1973.
37. Fitzgerald, A.E., Kingsley, C. and Kusko, A., "Electric Machinery", 3rd Edn., McGraw-Hill, 1971.

38. Ramamurthi, V.P. and Bellamkunda, Ramaswami, "A Novel Three Phase Reference Sine Wave Generator for PWM Inverters", IEEE Trans. on Ind. Electronics, IE-29, Aug./1982, pp. 235-240.
39. Parasuram, M.K. and Ramaswami, B., "A Three Phase Sine Reference Wave Generator for Thyristorized Motor Controllers", IEE Trans. on Industrial Electronics and Control Instrumentation, Vol. IECI-23, No. 3, August 1976, pp. 270-276.
40. Ben Zion Kaplan, "A Versatile Voltage Controlled Three Phase Oscillator", IEEE Trans. on Industrial Electronics and Control Instrumentation", Vol. IECI-26, Aug./1979, pp. 192-195.
41. Samir, K. Datta, "A Novel 3-Phase Oscillator for Speed Control AC Motors", IEEE Trans. on Industry and General Applications, Jan./Feb. 1971, pp. 57-60.
42. Clarke, D.J. and Paresh C. Sen, "A Versatile Three Phase Oscillator", IEEE Trans. on Industrial Electronics and Control Instrumentation, Vol. IECI 24, Feb. 1977, pp. 312-316.
42. Peterson, W.E., "FET Converts Triangle to Sines", Electronics Aug. 31/1970, pp. 69-71.
43. R.D. Middlebrook and Richer, "Nonreactive Filters Converts Triangular Wave to Sine Wave", Electronics, March 8/1965, pp. 96.
44. J.G. Graeme, G.E. Tobey and L.P. Huelsman, "Operational Amplifier Design and Applications", New York, McGraw-Hill, 1971, pp. 385-391.
45. J.P. Walden and F.G. Turnbull, "Adjustable Voltage and Frequency Polyphase Sine Wave Signal Generator", IEEE Trans. on IA, Vol. IA-12, No. 3, May/June 1976, pp. 312-316.
46. Dewan, S.B. and Straugen, A., "Power Semiconductor Circuits", Wiley Interscience, 1974.
47. Gyugy and Pelly, "Static Power Frequency Changers - Theory, Performance and Applications", John Wiley and Sons.
48. Bowes, S.R. and Clements, R.R., "PWM Inverter Drives", Proc. IEE, Vol. 130, pt. B, No. 3, May 1983, pp. 149-160.

## APPENDIX-A

## Single Phase Induction Motor Model for Inverter Drives:

Most static frequency converters generate an output voltage waveform with significant harmonic contents. So it is customary to replace the conventional a.c. motor models by their harmonic equivalent circuits to analyse the performance of motors theoretically. The basic analysis for single phase (run with main winding only) induction motors uses an equivalent circuit derived from double revolving field theory of operation. The equivalent circuit for sinusoidal input voltage may be modified for harmonic voltages and currents. The equivalent circuit may be adapted for  $k$ th harmonic voltage and current as shown in Fig. 4.1 which is redrawn in Fig. A.1.

where

$k$  = harmonic order

$I_k$  =  $k$ th harmonic current

$V_k$  =  $k$ th harmonic voltage

$r_1$  = stator resistance

$kx_1$  = stator leakage reactance due to  $k$ th harmonic current

$r_{2k}$  = rotor resistance due to  $k$ th harmonic

$kx_2$  =  $k$ th harmonic leakage reactance of the rotor

$E_{bfk}$  = back emf due to  $k$ th forward revolving field

$E_{bbk}$  = back emf due to  $k$ th backward revolving field

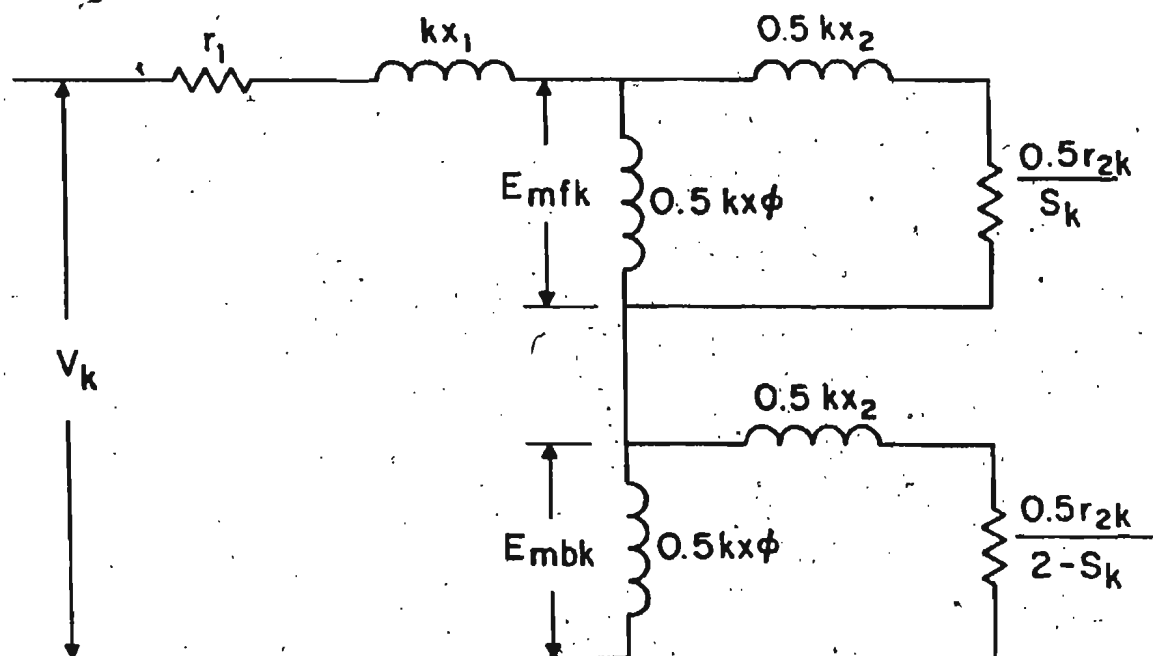


Fig. A.1 Harmonic equivalent circuit of 1-phase induction motor.

$s_k$  = slip of kth harmonic field

$$= \frac{k n_1 - n}{k n_1}$$

$n_1$  = fundamental frequency

$n_2$  = actual frequency of the rotor

Once the harmonic equivalent circuit parameters are known, the harmonic currents, torque and power can be found readily. If  $V_k$  be the harmonic voltage then

$$I_k = \frac{V_k}{Z_{TK}}$$

where

$$Z_{TK} = Z_{fk} + Z_{bk} + r_1$$

$Z_{fk}$  = kth harmonic impedance to forward revolving field

$$= \left( \frac{r_2}{s_k} + jkx_2 \right) \parallel jx_\phi$$

$$= R_{fk} + jX_{kf}$$

$Z_{bk}$  = kth harmonic impedance to backward revolving field

$$= \left( \left( \frac{r_2}{2-s_k} \right) + jkx_2 \right) \parallel jkx_\phi$$

$$= R_{bk} + jX_{kb}$$

Torques and power developed due to harmonic currents are given by

$$T_{fk} = \frac{1}{K\omega_s} P_{gfk}$$

$$P_{gfk} = I_k^2 \cdot 5R_{fk}$$

$$T_{bk} = \frac{1}{K\omega_s} P_{gbk}$$

$$T_{fk} = \sum_{k=1}^n T_k$$

$$P_d = \sum_{k=1}^n P_{kd}$$

$$P_I = \sum_{k=1}^n P_{Ik}$$

$$P_O = P_d - W_c$$

$$\text{efficiency } \eta = \frac{P_O}{P_I}$$

$$\text{shaft torque } T_s = \frac{P_O}{(1-S_1)\omega S_1}$$

$$\text{power factor p.f.} = \frac{P_O}{VI}$$

If the harmonic voltages and the actual slip of the motor is known, the steady state performance i.e. P, T, I, V and efficiency at variable frequency operation can be found using the equations developed so far. However the model does not take into account the skin effect of increasing frequency on the rotor resistance. A correction factor ranging from 2-3 can be used for skin effect. Moreover simplification can be achieved by considering slip due to high frequency harmonic field equal to 1 which is a fairly good approximation [36]. The effect of pulsating torque are also neglected in this model for simplifying calculations.

## APPENDIX-B

Delta Modulation, Circuit Implementation and Logic Circuit for Producing Gating Signals for Thyristors of the Inverter:

Delta modulation technique for the PWM Inverter requires a very simple circuit implementation, provides smooth transition between PWM and single pulse mode of operation and offers constant voltage per hertz operation without the need of additional circuit complexity. This method utilises a sine reference waveform and delta shaped carrier waveform is allowed to oscillate within a defined window extending equally above and below the reference wave. The maximum window width and the maximum slope of carrier wave determines the maximum switching frequency of the inverter switches.

Some of the voltage waveforms associated with the modulation technique are illustrated in Fig. 2.2. Fig. 2.4 shows their respective circuit implementation. The modulated signal can be processed through a logic circuit illustrated in Fig. 2.12 to produce the signals of timing diagram of Fig. 2.11 of chapter 2.

In Fig. 2.2  $V_I$  is the modulated wave generated by comparing reference sine wave ( $V_R$ ) with carrier wave ( $V_F$ ).  $V_s$  is the d.c. logic power supply voltage.

Fig. 2.4 depicts a circuit capable of producing the waveforms of Fig. 2.2.



Operation of the circuit can be explained as follows: Sine wave  $V_R$  is supplied to the input of comparator  $A_1$ , carrier wave  $V_F$  is generated by the integrator  $A_2$  as follows: whenever output  $A_2$  exceeds the upper or lower window boundary (preset by  $R_2/R_3$ ), comparator  $A_1$  reverses the polarity of  $V_I$  at input of  $A_2$ , this action reverses the slope of carrier  $V_F$  at the output of  $A_2$ , thus forcing  $V_F$  to oscillate around the reference waveform  $V_R$  at ripple frequency  $\omega_r$ . This forced oscillation ensures that the fundamental component of  $V_F$  and reference wave  $V_R$  have the same amplitude.

Since integrator  $A_2$  is also a low pass filter

$$V_{Fn} = \frac{V_{In}}{n(R_1 C) \Omega_r}$$

where  $V_{Fn}$  and  $V_{In}$  are  $n$ th harmonic of  $V_F$  and  $V_I$  modulated waveform respectively.

$$\text{Also, } V_{F1} = V_R$$

$$\text{therefore } V_{F1} = \frac{V_I}{R_1 C \Omega_r} = V_R$$

$$\text{or } \frac{V_{cl}}{\Omega_r} = V_R (R_1 C)$$

Since the amplitude of  $V_R$  is constant and independent of  $\Omega_r$ , the ratio  $\frac{V_I}{\Omega_r}$  is also constant and independent of  $\Omega_r$ . This is true until  $\Omega_r = \Omega_{rp}$  at which  $V_I$ .

Fig. A.2 Actual circuit connection for logic circuits producing gating signals of 1-phase bridge inverter

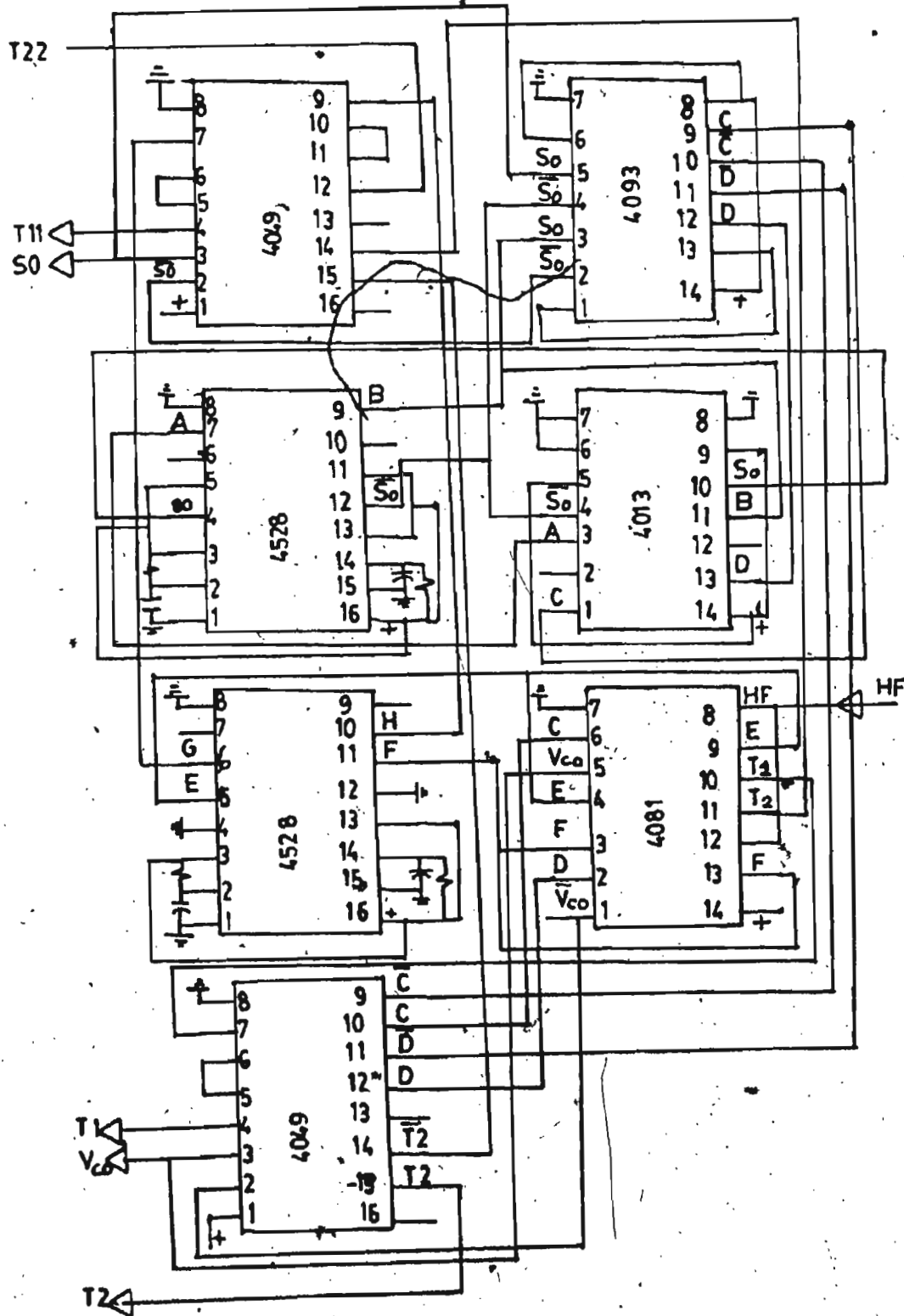
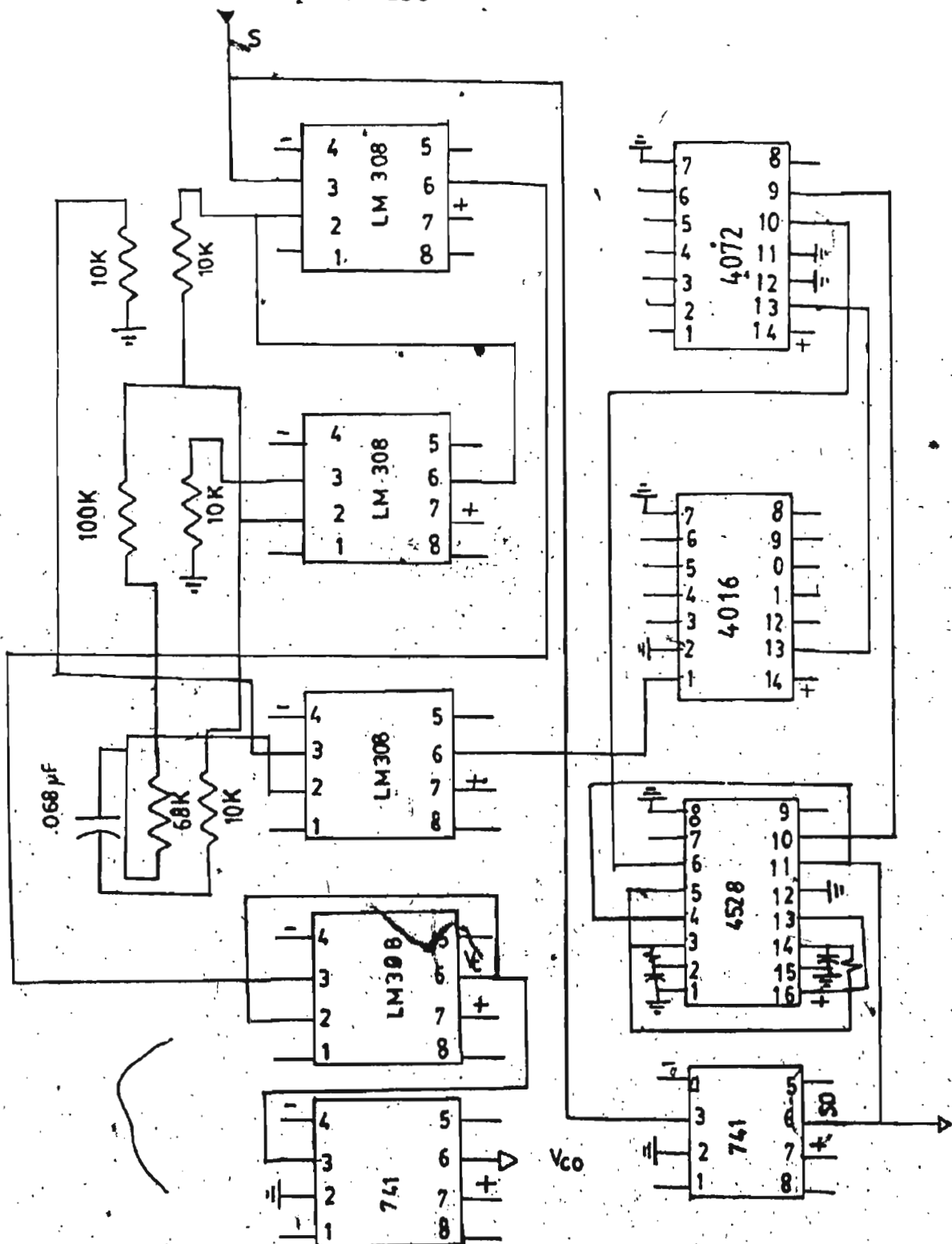


Fig. A.3 Actual circuit connection for delta modulator, 1-phase use



becomes a square wave of frequency  $\Omega_r$ . After this  $V_1$  remains constant.

The actual circuit connection of logic circuits is shown in Fig. A.2. and actual connection diagram for delta modulator circuit is shown in Fig. A.3.

## APPENDIX-C

## Fourier Analysis of Delta Modulation with Sine Input:

The generation of delta modulated signals for pulse width modulated inverter is depicted in the Fig. A.4 of Appendix B. We define the following

$$\Delta V = \frac{R_2}{R_3} V_s$$

$R_2$  and  $R_3$  are circuit constants

$V_s$  is the logic power supply voltage

$\omega_r$  = ripple frequency of triangular wave

$\Omega_r$  = frequency of sine wave

then the equations of different waves of Fig. 2.2 are given by

the sine wave is  $= V_R \sin \Omega_r t$

upper envelope is  $= +\Delta V + V_R \sin \Omega_r t$

lower envelope is  $= -\Delta V + V_R \sin \Omega_r t$

when  $\Omega_r = \Omega_{rb}$  (break frequency),  $\omega_r$  becomes a train of square wave only. So after break frequency

$$V_o = \sum_{n=1,3,\dots} \frac{4V_s}{n\pi} \sin n \Omega_r t$$

where harmonics are given by

$$V_{on} = \frac{4V_s}{n\pi}$$

For frequencies less than break frequency the harmonics of pulse train can be found as follows:

Slope of triangular carrier wave is always constant, determined by the R.C. combination of the integrator. Let this slope be  $A$ . In the first step we have to determine the pulse width  $\delta_1$ ,  $\delta_2$  and so on before we can carry out the analysis.

Pulse Width Determination for 1st Pulse:

We have

$$\Omega_r = 2\pi f_{\Omega r}$$

$$\Delta V + V_R \sin \Omega_r t_1 = A t_1$$

or,

$$t_1 = \frac{\Delta V + V_R \sin \Omega_r t_1}{A}$$

$$\delta_1 = \Omega_r t_1$$

For other pulses

$$t_i = \frac{2\Delta V + A t_{i-1}}{A} + \frac{V_R \sin \Omega_r t_{i-1} - V_R \sin \Omega_r t_i}{A(-1)^i}$$

solving these equations, the pulse termination time  $t_1$ ,  $t_2$ ,  $t_i$  are found out.

and in  $\omega_r t$  scale

$$\delta_1 = \Omega_r t_1$$

$$\delta_2 = \Omega_r t_2$$

$$\delta_i = \Omega_r t_i$$

[where  $\delta_1 - \delta_i > \pi$  gives last pulse termination for the half cycle].

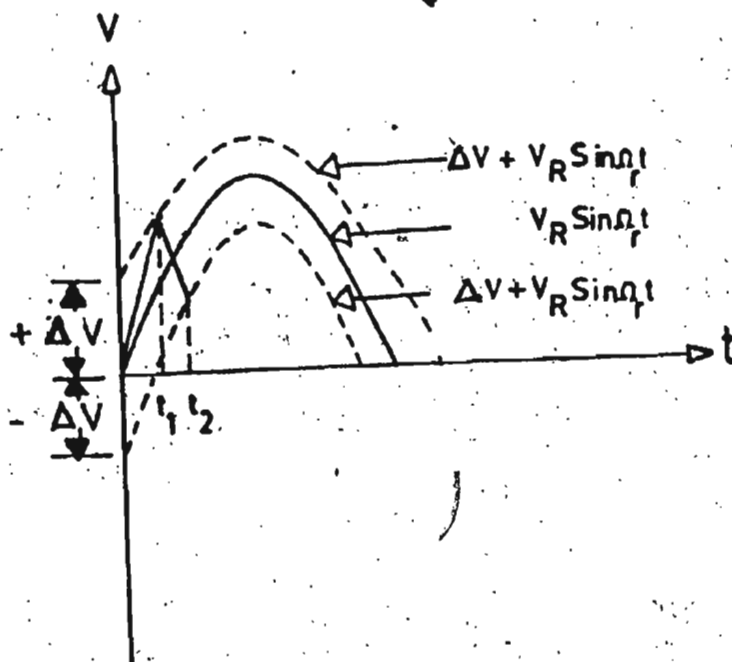


Fig. A.4

Illustration of pulse position determination of  
delta modulated wave

Once the pulse positions are known, the fourier analysis can be carried out.

Fourier Analysis:

Let  $N_p = i$  = number of pulses/half cycle

then

$$A_1 = \frac{2V_s}{\pi} \sum_{i=1}^{N_p} (-1)^{i+1} \int_{\delta_{i-1}}^{\delta_i} \cos \omega t \, d(\omega t)$$

$$= \frac{2V_s}{\pi} \sum_{i=1}^{N_p} (-1)^{i+1} ((\sin \delta_i - \sin(\delta_{i-1} - \delta_c)))$$

Similarly,

$$A_3 = \frac{2V_s}{3\pi} \sum_{i=1}^{N_p} (-1)^{i+1} (\sin 3\delta_i - \sin 3(\delta_{i-1} - \delta_c))$$

In general,

$$A_n = \frac{2V_s}{n\pi} \sum_{i=1}^{N_p} (-1)^{i+1} (\sin n\delta_i - \sin n(\delta_{i-1} - \delta_c))$$

and

$$B_n = \frac{2V_s}{n\pi} \sum_{i=1,2,3,\dots}^{i=1,2,3,\dots} (-1)^{i+1} (\cos n(\delta_{i-1} - \delta_c) - \cos \delta_i)$$

$$V_{on} = \sqrt{(A_n^2 + B_n^2)}$$



## APPENDIX D

## Fourier Analysis of Sine PWM Inverter Output:

The generation of sine modulated signals for the pulse width modulated inverter is explained in Fig. A.5, whenever the carrier triangular wave crosses the reference sine modulating wave signal a pulse is produced and its duration is as long as the carrier wave magnitude remains higher than the modulating wave signal level.

## Pulse Width Determination:

Let

$N$  = number of modulating pulses for each cycle

$\delta_i$  = pulse width of  $i$ th pulse

$\Delta = \frac{\pi}{N}$  = distance between successive pulse

$E_r$  = maximum carrier wave voltage

$E$  = maximum reference (modulating) sine wave voltage

$\theta_i$  = pulse location

$W = \frac{E}{E_r}$  = modulating index

We know  $\delta_i = E_i$

also  $\delta_i = \frac{1}{E_r}$

$$E_i = E \sin \theta_i = \frac{E_r}{E} E \sin \frac{(2i-1)}{2N} \pi$$

$$\text{or } E_i = W E_r \sin \frac{(2i-1)}{2N} \pi = E_r W | \sin \theta_i |$$

$$\delta i = \Delta \frac{E_i}{E_r} = \Delta \frac{E}{E_r} | \sin \theta_i |$$

$$= w | \sin \theta_i |$$

When number of pulses are kept constant (pulse width) is linearly dependent on modulating index  $w$ .

#### Fourier Analysis:

Once the pulses' width and their positions are determined, a fourier series expansion of modulated wave can be obtained.

Since the pulse train is an odd periodic function, the inverter output waveform can be represented by a fourier series as

$$V_{ab} = \sum_{n=1,3,\dots}^{\infty} A_n \sin(n\omega t)$$

where

$$A_n = \frac{2}{\pi} \int_0^{\pi} E_{dc} \sin(n\omega t) d\omega t$$

for the  $i$ th pulse pairs

$$A_n = \frac{2}{\pi} \int_{\frac{2i-1}{2}\Delta - \frac{\delta_i}{2}}^{\frac{2i-1}{2}\Delta + \frac{\delta_i}{2}} E_{dc} \sin(n\omega t) d\omega t$$

for  $N$  number of pulses, the resultant fourier coefficient will be

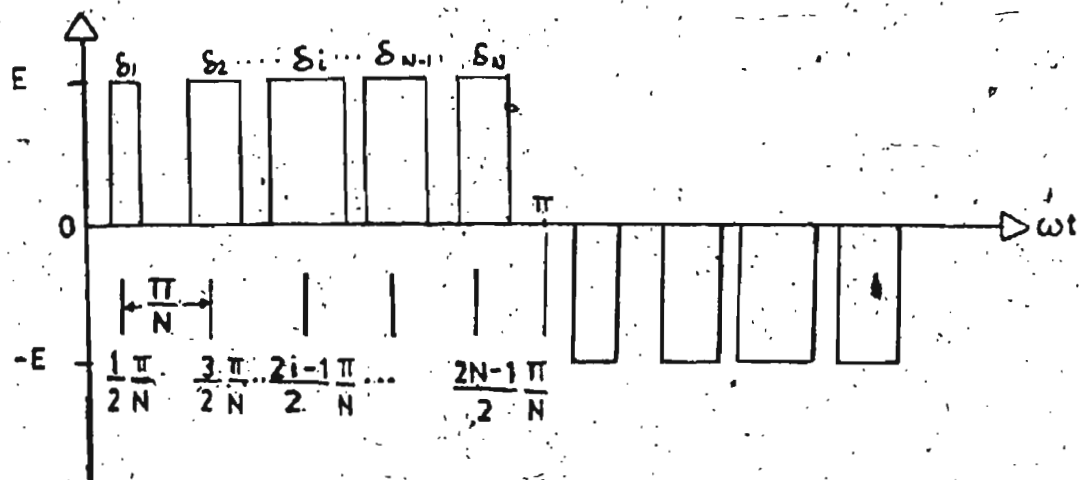
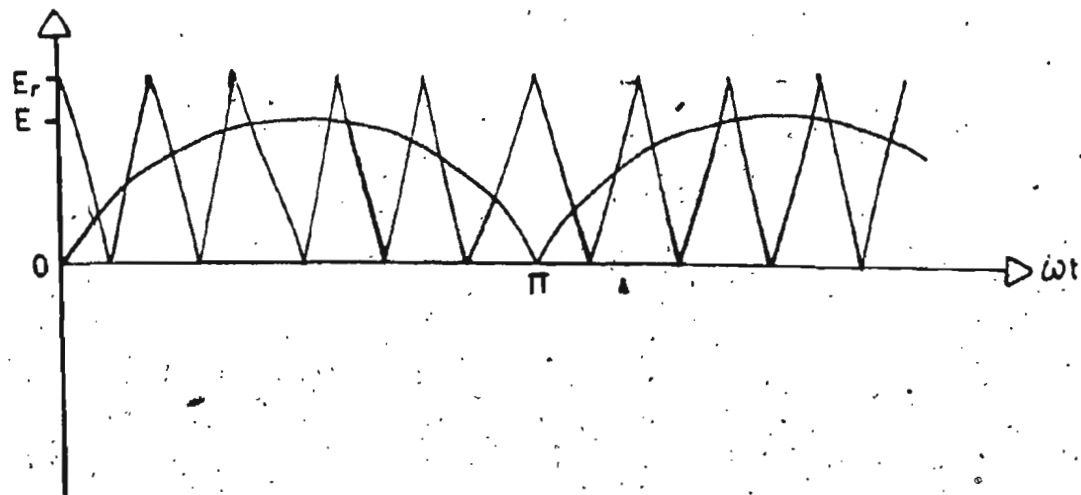


Fig. A.5

Illustration of theoretical pulse position  
determination of sine modulated wave

$$A_{nT} = \sum_{i=1}^N \frac{2}{\pi} E_{dc} \int_{\frac{2(i-1)}{2} \Delta - \frac{\delta_i}{2}}^{\frac{2(i-1)}{2} \Delta + \frac{\delta_i}{2}} \sin(n\omega t) d\omega t$$

$$= \frac{2E_{dc}}{n\pi} \sum_{i=1}^N [-\cos(n\omega t)]_{\frac{2(i-1)}{2} \Delta - \frac{\delta_i}{2}}^{\frac{2(i-1)}{2} \Delta + \frac{\delta_i}{2}}$$

$$= \frac{2E_{dc}}{n\pi} \sum_{i=1}^N \left\{ -\cos \cdot n \left[ \frac{2(i-1)}{2} \Delta + \frac{\delta_i}{2} \right] \right.$$

$$\left. + \cos n \left[ \frac{2(i-1)}{2} \Delta - \frac{\delta_i}{2} \right] \right\}$$

After simplification

$$A_{nt} = \frac{4E_{dc}}{n\pi} \sum_{i=1}^N \left\{ \sin \left[ n \left( i - \frac{1}{2} \right) \frac{\pi}{N} \right] \cdot \sin n \frac{\delta_i}{2} \right\}$$

So

$$V_{ab} = \sum_{n=1,3,\dots}^{\infty} A_{nt} \sin(n\omega t)$$

$$= \sum_{n=1,3,\dots}^{\infty} \sum_{i=1}^N \left\{ \left[ n \left( i - \frac{1}{2} \right) \frac{\pi}{N} \right] \cdot \sin \left( \frac{n\delta_i}{2} \right) \right\}$$

$$= \frac{4E_{dc}}{\pi} \sum_{n=1,3,\dots}^{\infty} \frac{1}{n} \sum_{i=1}^N \left\{ \left[ n \left( i - \frac{1}{2} \right) \frac{\pi}{N} \right] \cdot \sin \left( \frac{n\delta_i}{2} \right) \right\}$$

## APPENDIX E

## Three Phase Delta Modulation Circuit Implementation and Logic Circuits:

Three phase delta modulated inverter requires almost the same circuit implementation of single phase circuits. For the three phase implementation of delta modulated logic we need a three phase reference sine wave generator, three identical single phase delta modulated inverter circuits and three identical single phase logic circuits for three phases to produce the gating signals of thyristors (timing diagram of which is shown in the Fig. 5.4 of Chapter V)

## The 3-Phase Sine Reference Wave Generator:

As described in section 5.2 of Chapter 5, the three phase sine reference wave generated from a circuit which converts a square wave into 3-phase square wave, this three phase variable frequency square wave is converted to constant amplitude variable frequency triangular wave which in turn is converted to variable frequency, constant amplitude sine waves.

The practical circuit used for the three phase sine wave generator is illustrated in Fig. A.7 and circuit diagram.

## The Modulation Circuit:

The variable frequency 3-phase sine wave is fed to the modulation circuit (each for one phase) identical to the

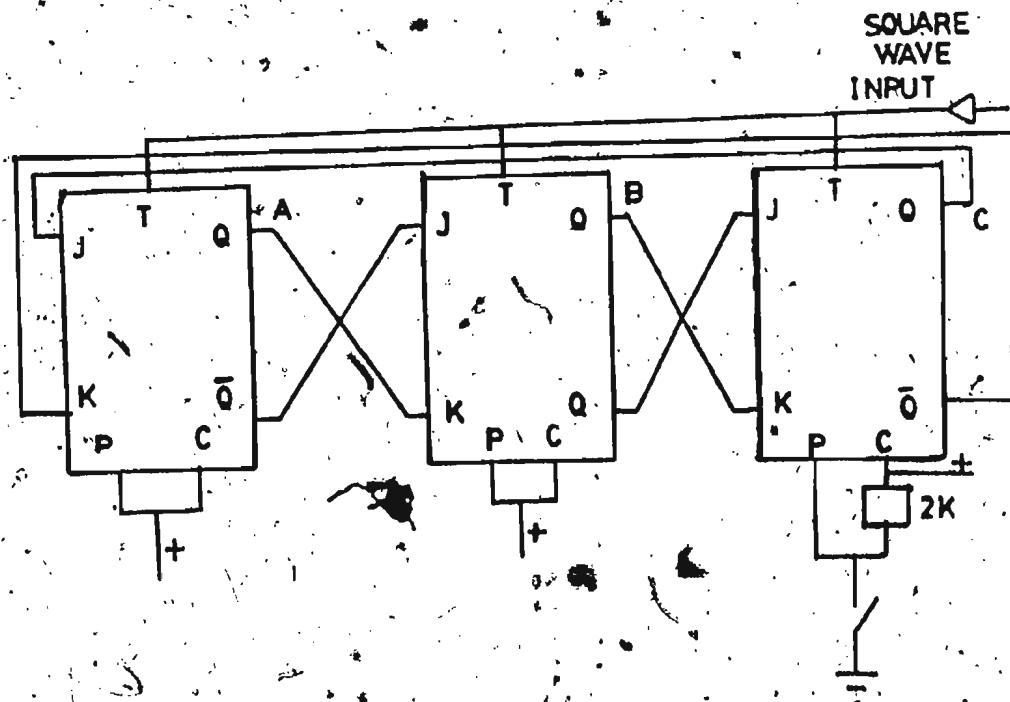
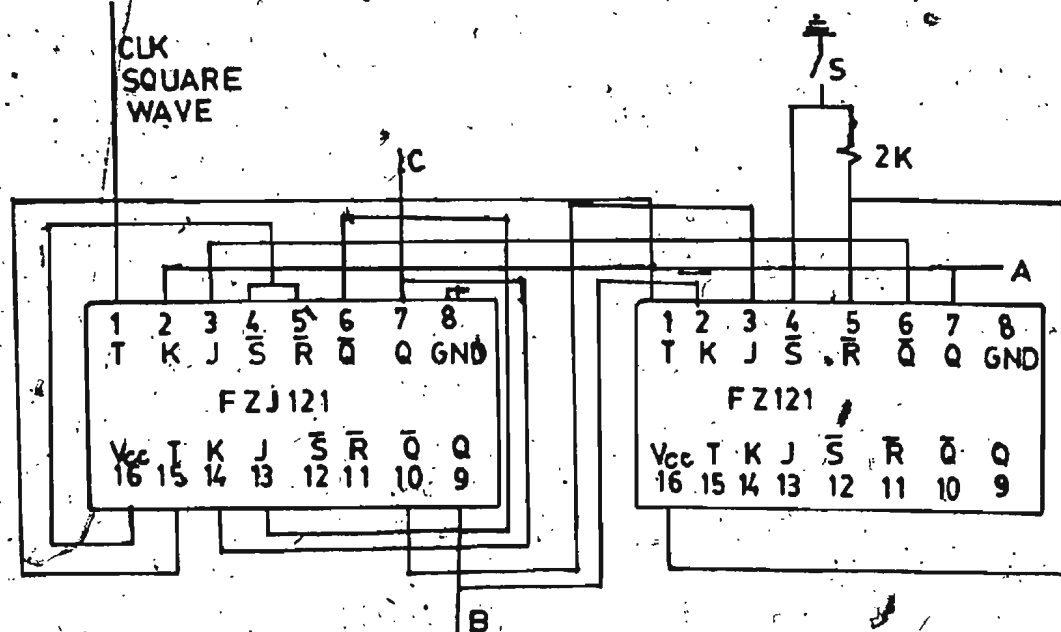


Fig. A.6

Schematic and actual circuit diagram of 3-phase square wave generator

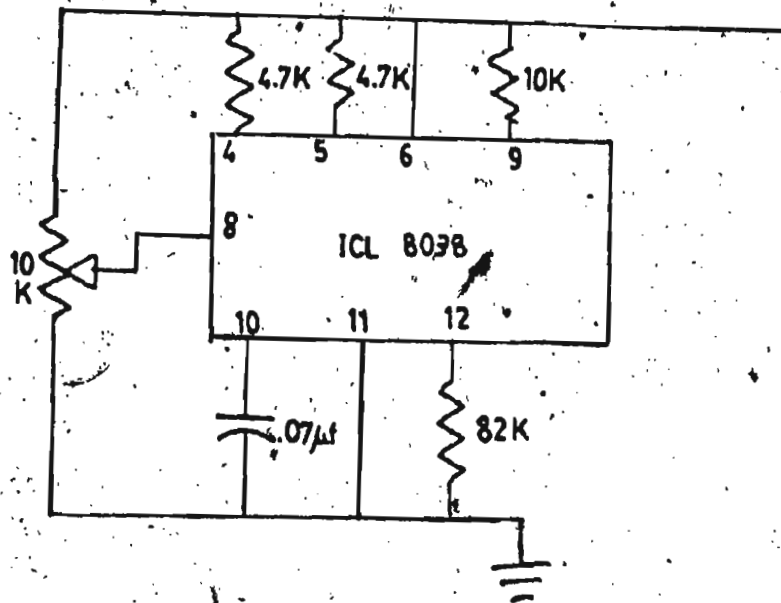


Fig. A.7(a) VCF converter used for 3 phase reference wave generator

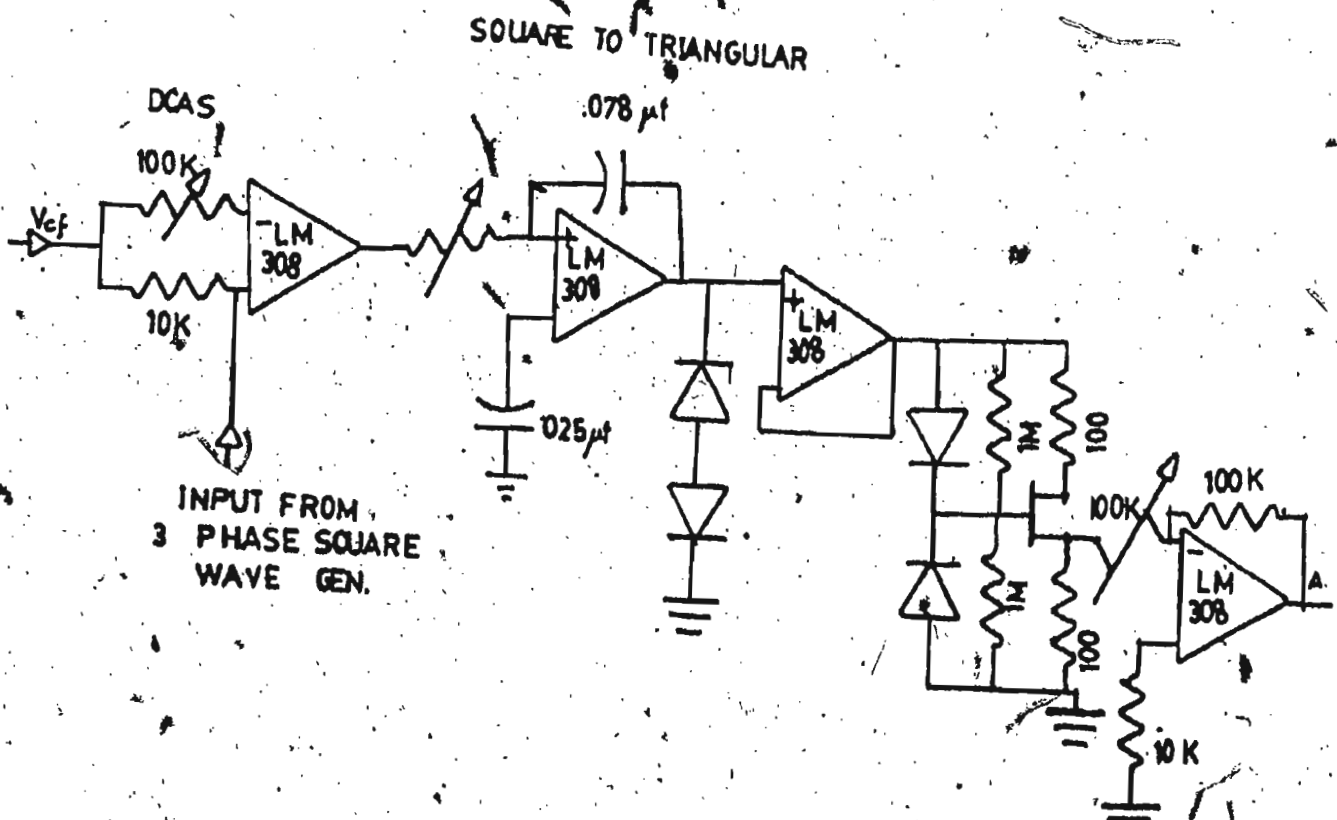


Fig. A.7(b) Square wave to sine wave inverter

circuit used for 1-phase modulation. However the circuit parameters are changed as shown to adjust the maximum commutation number desired. .

**The Logic Circuit:**

The logic circuits for the implementation of gating signals illustrated in the timing diagram of Fig. 5.4 of Chapter 5 is given in the Fig. A.9.



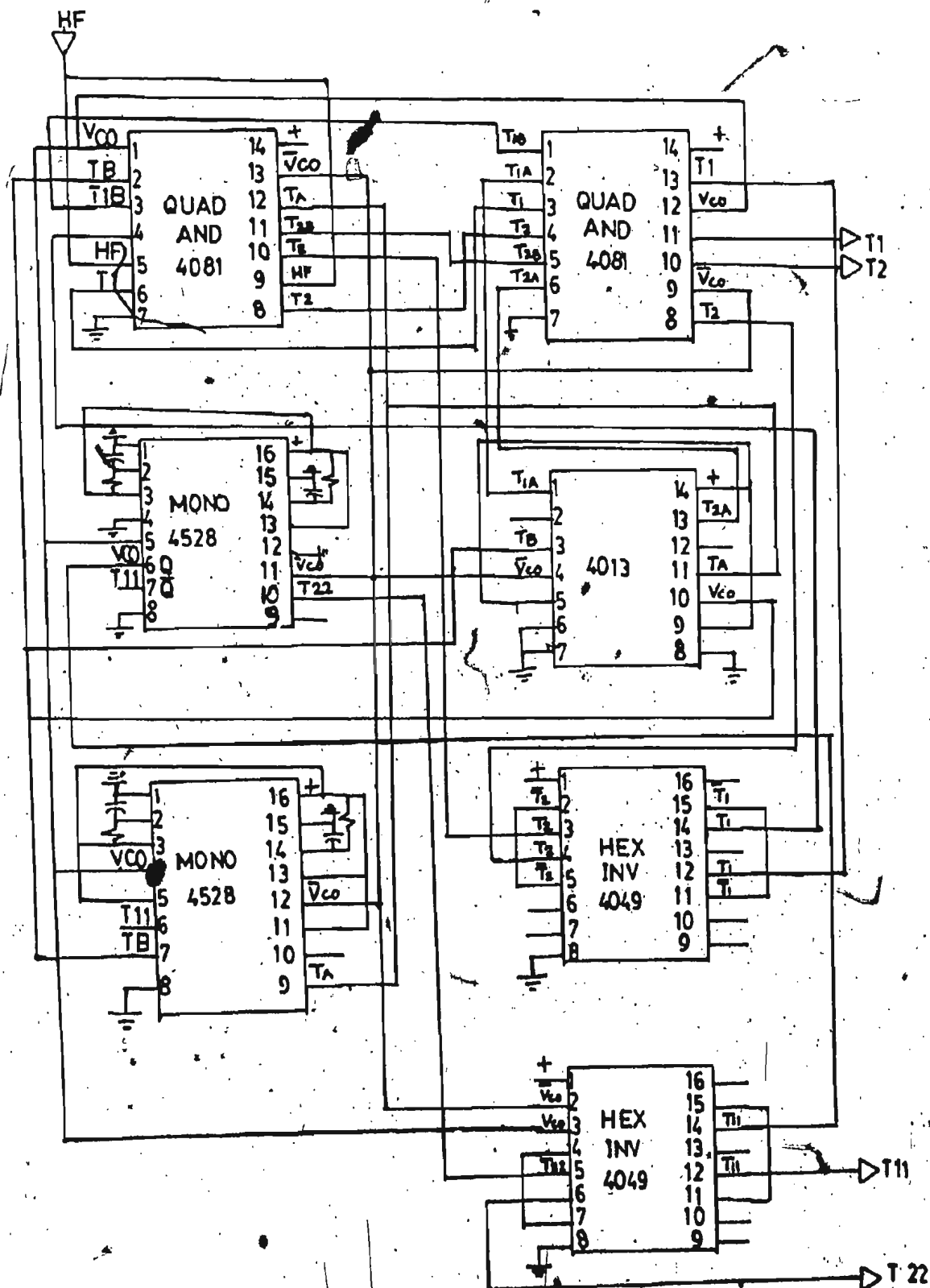
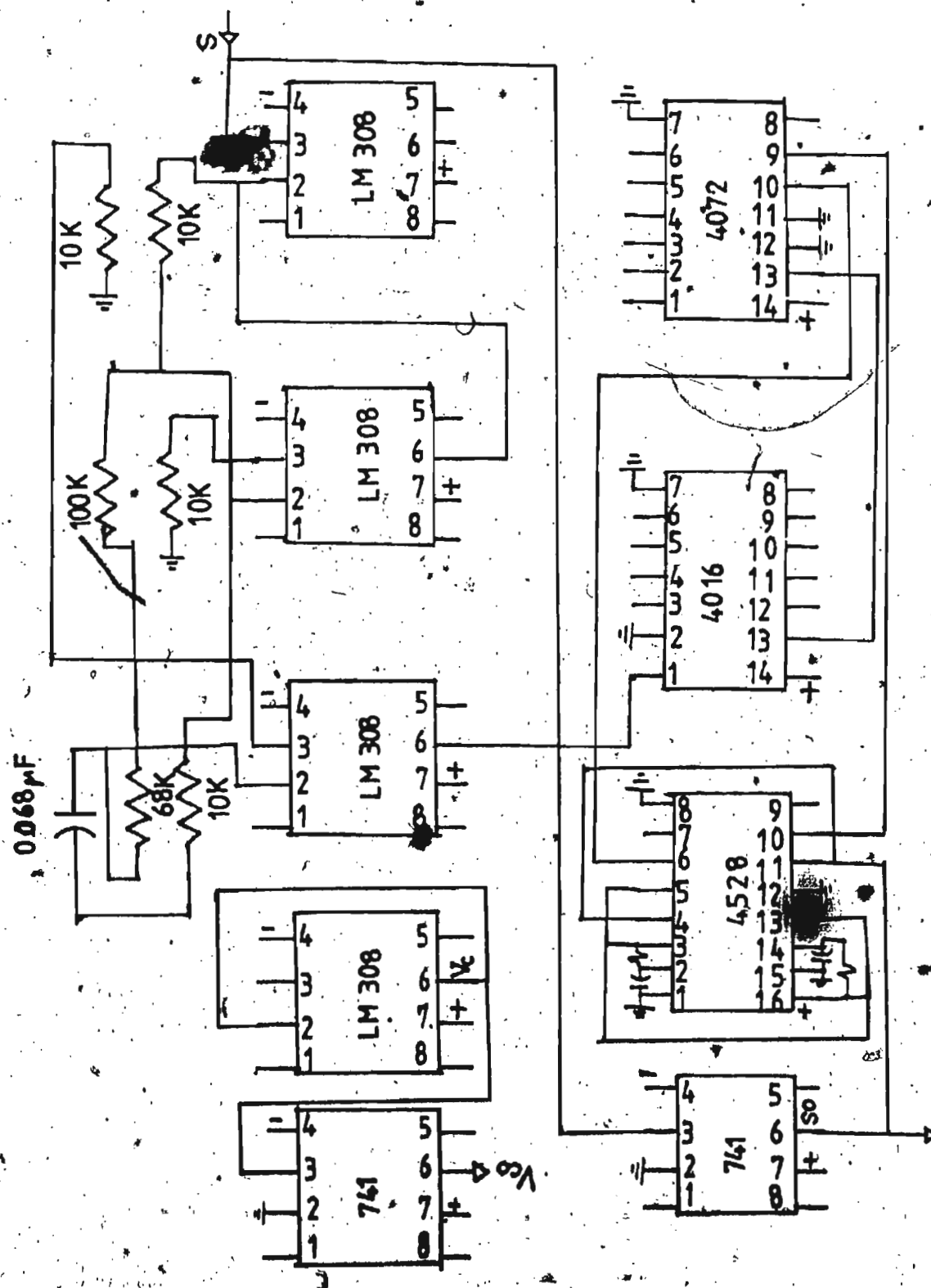


Fig. A.8

Actual circuit diagram of one phase of the 3-phase delta modulator

Fig. A.9

Actual circuit diagram of the logic circuits for producing gating signals of 3-phase inverter



# APPENDIX-F

## Table

Experimental Results for R-L load

$L = 45.7 \text{ mh}$

$R = 20\Omega$

$V_{DC} = 115V$

Freq. in Hz	$V_R = 5.5$				$V_R = 6.00$				$V_R = 6.75$			
	V (v)	I (k)	P (w)	$I_{dc}$ (k)	V (v)	I (A)	P (w)	$I_{dc}$ (A)	V (v)	I (A)	P (w)	$I_{dc}$ (A)
20	103.5	.82	18.3	.95	104	.87	20.3	.98	104.5	.98	24	.99
30	105	.98	25	.95	106	1.08	29.1	1.0	108	1.42	48	1.1
40	106	1.21	35	1.0	108	1.45	50.4	1.15	109	2.1	98	1.45
50	108	1.54	54	1.15	109.5	1.9	82.7	1.32	109.9	2.74	165	1.9
60	109	1.97	89	1.32	110	2.35	123	1.5	110.9	3.08	204	2.1
70	110	2.26	113	1.5	109.6	2.41	130	1.5	113	3.07	206	1.99
80	111	2.42	128	1.52	111.5	2.69	158	1.65	112	2.82	175	1.7
90	112	2.49	137	1.45	115	2.61	150	1.5	111	2.6	150	1.5
100	112	2.4	129	1.32	112.4	2.42	130	1.35	112	2.42	131	1.35
110	112	2.26	114	1.2	112.8	2.24	113	1.2	112.3	2.26	115.2	1.2

Table

Practical Results for R-Load

$R = 20 \Omega$   $V_{in}(D.C.) = 115V$

Freq. in Hz	$V_R = 5.5 V$				$V_R = 6.00$				$V_R = 6.75$			
	V (v)	I (A)	P (w)	$I_{dc}$ (A)	V (v)	I (A)	P (W)	$I_{dc}$ (A)	V (V)	I (A)	P (W)	$I_{dc}$ (A)
20	93.8	4.4	407	4.4	93.7	4.48	418	4.6	93.5	4.38	408	4.4
30	94.0	4.408	417	4.5	94.1	4.46	419	4.5	95.5	4.46	425	4.5
40	95.5	4.51	429	4.6	96.2	4.55	435	4.6	98.4	4.6	447	4.6
50	97.2	4.6	446	4.7	98.2	4.61	451	4.7	101	4.71	475	4.7
60	99.4	4.67	464	4.75	100.8	4.72	475	4.8	104.5	4.86	506	4.8
70	101.6	4.8	485	4.8	103	4.83	496	4.85	108.3	5.03	545	5.00
80	103.5	4.87	503	4.9	105.6	4.95	521	5.0	108.5	5.07	550	5.01
90	106.5	4.98	530	5.05	108	5.05	544	5.0	108	5.08	551	5.02
100	108	5.05	544	5.00	107.4	5.02	541	5.1	107.8	5.04	542	5.02
110	108	5.04	541	5.10	107.4	5.02	540	5.0	107.7	5.05	544	5.02
120	167.4	5.06	551	5.2	107.5	5.02	539	5.0	107.4	5.03	539	5.0

Table

Experimental Results for Induction Motor Load

1/2 hp  $V_m = 115V$  AC

Freq. in Hz	$V_R = 5.5V$				$V_R = 6.75V$				$V_R = 7.5V$			
	N (rpm)	$P_{dm}$ (W)	$T_{dm}$ (N-m)	$I_m$ (A)	N (rpm)	$P_{dm}$ (W)	$T_{dm}$ (N-m)	$I_m$ (A)	N (rpm)	$P_{dm}$ (W)	$T_{dm}$ (N-m)	$I_m$ (A)
40	1120	157	.625	5.26	1100	224	.891	7.05	-	-	-	-
45	-	-	-	-	-	-	-	-	1220	352	1.244	8.06
50	1400	209	.665	6.27	1380	309	.983	8.01	1380	380	1.209	8.09
60	-	-	-	-	1700	382	1.01	8.95	1685	426	1.13	8.25
65	1810	323	.79	7.18	-	-	-	-	-	-	-	-
70	1910	317	.72	8.04	1920	441	1.002	8.73	1880	459	1.05	9.75
80	2170	350	.69	8.57	2120	469	.933	9.44	2175	445	.885	8.46
90	2380	422	.746	9.39	2400	425	.751	8.75	2440	419	.7409	8.417
100	2810	358	.569	6.60	2700	382	.607	8.11	2735	383	.6098	7.8
110	3090	320	.462	6.37	3050	338	.489	6.87	2990	356	.515	7.75
120	3350	304.5	.403	6.56	3350	312	.413	6.42	3386	303	.401	6.35

Table

Experimental Results for Induction Motor Load

1/4 hp  $V_m = 115V$  AC

Freq. in Hz	$V_R = 5.5V$				$V_R = 6.75V$				$V_R = 7.5V$			
	N (rpm)	$P_{dm}$ (W)	$T_{dm}$ (N-m)	$I_m$ (A)	N (rpm)	$P_{dm}$ (W)	$T_{dm}$ (N-m)	$I_m$ (A)	N (rpm)	$P_{dm}$ (W)	$T_{dm}$ (N-m)	$I_m$ (A)
40	-	-	-	-	1040	95.6	.38	3.25	-	-	-	-
45	1225	90.34	.3195	3.42	-	-	-	-	1175	228.2	.807	5.85
50	1385	112.1	.356	3.70	1320	151.1	.48	5.15	1360	273	.869	5.7
60	1600	174.1	.4618	5.05	1660	200	.53	4.65	1590	312	.827	6.73
70	1890	226	.5136	4.81	1900	247	.56	5.02	1900	294	.668	5.48
80	2100	250	.497	5.75	2170	194	.55	5.47	2120	281	.559	5.79
90	2480	256	.452	4.74	2490	238	.42	4.14	2425	257	.4544	5.19
100	2750	249	.396	4.42	2770	240	.382	4.19	2685	244.6	.389	5.02
110	3010	232	.335	4.49	3040	232	.335	4.22	3015	228	.3298	4.46
120	3290	226	.2997	4.28	3245	226	.299	4.5	3300	219	.2904	4.02

Appendix GMotor Parameters (at 60 Hz)

115V, 1/4 hp Induction Motor:

$$r_1 = 2.84 \, \Omega$$

$$r_2 = 3.1042 \, \Omega$$

$$x_1 = 4.695 \, \Omega$$

$$x_2 = 4.695 \, \Omega$$

$$r_{aux} = 6.88 \, \Omega$$

$$x_\phi = 32 \, \Omega$$

$$w_{core} = 74 \text{ watts}$$

$$w_f = 8 \text{ watts}$$

$$L_1 = 0.0124 \text{ Henry}$$

$$L_2 = .0124 \text{ Henry}$$

$$L_\phi = .085 \text{ Henry}$$

115V, 1/2 hp Induction Motor:

$$r_1 = 1.375 \, \Omega$$

$$r_2 = 1.375 \, \Omega$$

$$x_1 = 1.92 \, \Omega$$

$$x_2 = 1.92 \, \Omega$$

$$x_\phi = 18.54 \, \Omega$$

$$w_{core} = 141 \text{ watts}$$

$$w_f = 49 \text{ watts}$$

$$L_1 = 0.00509 \text{ Henry}$$

$$L_2 = 0.00509 \text{ Henry}$$

$$L_\phi = 0.049 \text{ Henry}$$

## APPENDIX H

## Computer Programs:

1. Fourier Analysis of PWM Inverter  
(Number of pulse kept constant)
2. Fourier Analysis of PWM Inverter  
(Modulation index kept constant)
3. Fourier Analysis of Delta PWM
4. Performance of passive loads fed from DM inverter
5. Performance of 1-phase Induction Motor fed from DM inverter
6. Determination of load current waveshape for passive loads
7. Determination of number of commutation in DM inverter



```

C      FOURIER ANALYSIS OF PWM INVERTER
C      DL(I)= I TH PULSE LOCATION
C      THETA(I)= I TH LOCATION
C      DELT=DISTANCE BETWEEN SUCCESSIVE PULSES
C      N=NUMBER OF PULSES PER HALF CYCLE
C      W=MODULATION INDEX, ER/EC
C      A(NS)= NTH HARMONIC AMPLITUDE
C      ANC(N)=AN/A1=NTH HARMONIC / FUNDAMENTAL
C      DIMENSION A(200),THETA(200),AA(200),ANC(200)
      CALL ASSIGN(1,'HM1.DAT')
      CALL ASSIGN(2,'HM3.DAT')
      CALL ASSIGN(3,'HM5.DAT')
      CALL ASSIGN(4,'HM7.DAT')
      PI=3.1415926
      V=1.0
      N=11
      DELT=PI/N
      DO 80J=1,5
      W=.05+((J-1.)/4.)
      DO 40NS=1,15,2
      EDC=(4.*V)/(PI*NS)
      SUM1=0.0
      DO 50I=1,N
      THETA(I)=((2.*I-1.)/2.)*DELT
      DL=DELT*W*ABS(SIN(THETA(I)))
      AA(I)=SIN((NS*THETA(I)))*SIN((NS*DL)/2)
      SUM1=SUM1+AA(I)
50    CONTINUE
      A(NS)=EDC*SUM1
40    CONTINUE
      AIM=(4.*V)/PI
      DO 70NN=1,15,2
      ANC(NN)=ABS(A(NN))/AIM
70    CONTINUE
      WRITE(1,*) W,ANC(1)
      WRITE(2,*) W,ANC(3)
      WRITE(3,*) W,ANC(5)
      WRITE(4,*) W,ANC(7)
60    CONTINUE
      STOP
      END

```

```

C   FOURIER ANALYSIS OF PWM INVERTER
C   DL(I)= I TH PULSE LOCATION
C   THETA(I)= I TH PULSE LOCATION
C   DELT=DISTANCE BETWEEN SUCCESSIVE PULSES
C   N=NUMBER OF PULSES PER HALF CYCLE
C   W=MODULATION INDEX ER/EC TAKEN AS 1, .75, .5, .25
C   A(NS)= NTH HARMONIC AMPLITUDE
C   AN(NI)= NORMALISED HARMONIC AMPLITUDE AN/A1
C   DIMENSION A(200), THETA(200), AA(200), AN(200)
C   CALL ASSIGN(1, 'HM9.DAT')
C   CALL ASSIGN(2, 'HM11.DAT')
C   CALL ASSIGN(3, 'HM13.DAT')
C   CALL ASSIGN(4, 'HM15.DAT')
C   W=1.25
C   PI=3.1415926
C   V=1.0
C   DO 30N=3, 13, 2
C   DELT=PI/N
C   DO 40NS=1, 15, 2
C   EDC=(4.*V)/(PI*NS)
C   SUM1=0.0
C   DO 50I=1, N
C   THETA(I)=((2.*I-1.)/2.)*DELT
C   DL=DELT*W*ABS(SIN(THETA(I)))
C   AA(I)=SIN(NS*THETA(I))*SIN(NS*DL)/2)
C   SUM1=SUM1+AA(I)
50  CONTINUE
C   A(NS)=EDC*SUM1
40  CONTINUE
C   AIM=(4.*V)/PI
C   DO 70NN=1, 15, 2
C   AN(NN)=ABS(A(NN))/AIM
70  CONTINUE
C   WRITE(1,*) N, AN(9)
C   WRITE(2,*) N, AN(11)
C   WRITE(3,*) N, AN(13)
C   WRITE(4,*) N, AN(15)
30  CONTINUE
C   STOP
C   END

```

```

C      FOURIER ANALYSIS OF DELTA MODULATED WAVE
      DIMENSION DL(100),TC(100),AC(100),AAC(100),AK(100),BB(100)
      CALL ASSIGN(1,'HM9.DAT')
      CALL ASSIGN(2,'HM11.DAT')
      CALL ASSIGN(3,'HM13.DAT')
      CALL ASSIGN(4,'HM15.DAT')
C      PULSE WIDTH DETERMINATION
      VR=6.75
      DV=1.5
      DO 90JJ=1,11
      F=20.+(JJ*10.-10.)
      S=3200.
      PI=4.*ATAN(1.)
      W=2.*PI*F
      TC(1)=0.0
17      X=(DV+VR*SIN(W*TC(1)))/S
      B=X-TC(1)
      IF(B.LE..000005)GO TO 18
      TC(1)=TC(1)+.000001
      GO TO 17
18      TC(1)=X
      K=1
      DL(1)=TC(1)*W
      IF(DL(1)-1.5)16,200,200
16      K=1
      DO 21I=2,30
      TC(I)=0.0
      IK=I-1
19      Y1=(2.*DV+S*TC(IK))/S
      Y2=((VR*SIN(W*TC(IK))-VR*SIN(W*TC(I)))/(S*(-1.)**I))
      Y=Y1+Y2
      C=Y-TC(I)
      IF(C.LE..000005)GO TO 20
      TC(I)=TC(I)+.000001
      GO TO 19
20      TC(I)=Y
      DL(I)=TC(I)*W
      K=K+1
      Q=DL(I)-DL(1)
      IF(Q.GE.9.00)GO TO 22
21      CONTINUE
22      DL(K)=PI
      NP=K
C      FOURIER ANALYSIS
      VS=15.
      DO 40NS=1,40,2

```

```

EDC=(2.*VS)/(PI*NS)
SUM1=SINCNS*DL(1)
SUM2=1-COSCNS*DL(1)
DO 50M=2,NP
  MN=M+1
  MM=M-1
  Z=(-1.)**MN
  AA(M)=Z*((SINCNS*DL(M))-SINCNS*(DL(MM))))
  SUM1=SUM1+AA(M)
50  CONTINUE
  AK(NS)=EDC*(SUM1)
  A(NS)=PI*ABS(AK(NS))/(4.*VS)
40  CONTINUE
  WRITE(1,*)F,A(9)
  WRITE(2,*)F,A(11)
  WRITE(3,*)F,A(13)
  WRITE(4,*)F,A(15)
  GO TO 100
200 CC=1.
  VS=15.
  DO 300NK=1,21,2
    Y=NK
    AK(NK)=(4.*VS)/(3.1415*Y)
    A(NK)=ABS(AK(NK))/((4.*VS)/PI)
300  CONTINUE
    WRITE(1,*)F,A(9)
    WRITE(2,*)F,A(11)
    WRITE(3,*)F,A(13)
    WRITE(4,*)F,A(15)
100 KCL=0.0.
80  CONTINUE
  STOP
  END

```

```

C   ANALYSIS OF DELTA PWM INVERTER WITH PASSIVE LOAD
    DIMENSION T(200), DL(200), AAC(400), AVC(400), AI(400), BB(400)
    CALL ASSIGN(1, 'A1.DAT')
    CALL ASSIGN(2, 'A2.DAT')
    CALL ASSIGN(3, 'A3.DAT')
    CALL ASSIGN(4, 'A4.DAT')
    PB=661.25
    BI=5.7
    BV=115
    FB=60.00
C   PULSE WIDTH DETERMINATION
    VR=7.5
    DV=1.50
    DO 90JJ=1, 10
    F=30.+(JJ*10.-10.)
    S=3100
    PI=.7854
    W=2.*PI*F
    TC=.00045
    DT=W*TC
    T(1)=0.0
17  X=(DV+VR*SIN(W*TC(1)))/S
    B=X-T(1)
    IF(B.LE..000005)GO TO 18
    T(1)=T(1)+.000001
    GO TO 17
18  T(1)=X
    K=1
    DL(1)=T(1)*W
    IF(DL(1)-1.5)16, 200, 200
16  K=1
    DO 21I=2, 30
    T(I)=0.0
    IK=I-1
19  Y1=(2.*DV+S*T(IK))/S
    Y2=((VR*SIN(W*TC(IK))-VR*SIN(W*TC(I)))/(S*(-1.)**I))
    Y=Y1+Y2
    C=Y-T(I)
    IF(C.LE..000005)GO TO 20
    T(I)=T(I)+.000001
    GO TO 19
20  T(I)=Y
    DL(I)=T(I)*W
    K=K+1
    Q=DL(I)-DL(1)
    IF(Q.GE.2.9)GO TO 22

```

```

21      CONTINUE
22      DL(K)=PI
      NP=K
C      FOURIER ANALYSIS
      VS=110.5
      DO 40 NS=1,31,2
      EDC=(2.*VS)/(PI*NS)
      SUM1=SIN(NS*DL(1))
      SUM2=1-COS(NS*DL(1))
      DO 50M=2,NP
      MN=M+1
      MM=M-1
      Z=(-1.)**MN
      AA(M)=Z*((SIN(NS*DL(M))-SIN(NS*DL(MM)+DT)))
      BB(M)=Z*((COS(NS*DL(MM)+DT)-COS(NS*DL(M))))
      SUM2=SUM2+BB(M)
      SUM1=SUM1+AA(M)
50      CONTINUE
      SUM=SQRT(SUM1*SUM1+SUM2*SUM2)
      AV(NS)=EDC*SUM
40      CONTINUE
      GO TO 100
200     CC=1.0
      DO 300 NN=1,31,2
      Y=NN
      AV(NN)=(4.*VS)/(PI*Y)
300     CONTINUE
100     R=22.
      AL=.0452
      DO 500LN=1,31,2
      AX=2.*PI*F*AL*LN
      AZ=SQRT(R*R+AX*AX)
      AI(LN)=AV(LN)/(AZ*1.41421)
500     CONTINUE
      CI=0.0
      VI=0.0
      DO 700LI=1,31,2
      CI=CI+AI(LI)*AI(LI)
      VI=VI+(AV(LI)*AV(LI))/2.
700     CONTINUE
      CIR=SQRT(CI)
      VIR=SQRT(VI)
      PF=PT/(VIR*CIR)
      VL=VIR/BV
      PL=PT/PB

```

UI=CIR/BI  
FU=F/FB  
WRITE(1,\*) FU, PL  
WRITE(2,\*) FU, VL  
WRITE(3,\*) FU, PF  
WRITE(4,\*) FU, UI  
PT=(CIR\*CIR)\*R  
CONTINUE  
STOP  
END

C

```

STEADY STATE ANALYSIS OF 1-PHASE INDUCTION MOTOR WITH DELTA INVERTER
DIMENSION TC(300),DL(300),AA(400),AV(400),SC(400),R2(200),X2(200)
DIMENSION XMC(200),X1(200),WS(200),AZF(200),AZB(200),RF(200)
DIMENSION RB(200),XF(200),PCU(200),PIN(200),XB(200),RT(200),XT(200)
DIMENSION ZT(200),AI(200),PGF(200),PGB(200),TD(200),PD(200)
REAL NR,N1,L1,L2,LM,P
CALL ASSIGN(1,'A1.DAT')
CALL ASSIGN(2,'A2.DAT')
CALL ASSIGN(3,'A3.DAT')
CALL ASSIGN(4,'A4.DAT')
WC=37.
R1=2.02
L1=.0074
L2=.0056
LM=.1771
R2(1)=4.12
P=4.
VR=6.8
DV=1.5
DO 90JJ=1,11,1
F=20.+(JJ*10.-10.)
N1=(120.*F)/P
NR=0.95*N1
SS=3200
PI=4.*ATAN(1.)
W=2.*PI*F
TC(1)=0.0
17 X=(DV+VR*SIN(W*TC(1)))/SS
B=X-TC(1)
IF(B.LE..00005)GO TO 18
TC(1)=TC(1)+.00001
GO TO 17
18 TC(1)=X
K=1
DL(1)=TC(1)*W
IF(DL(1)-1.5)16,200,200
16 K=1
DO 21I=2,30
TC(I)=0.0
IK=I-1
19 Y1=(2.*DV+SS*TC(IK))/SS
Y2=((VR*SIN(W*TC(IK))-VR*SIN(W*TC(I)))/(SS*(2-1.)*W))
Y=Y1+Y2
C=Y-TC(I)
IF(C.LE..000005)GO TO 20
TC(I)=TC(I)+.000001

```



```

20      60 TO 10
      T(I)=Y
      DL(I)=T(I)*W
      K=K+1
      Q=DL(I)-DL(1)
      IF(Q.GE.3.00)60 TO 22
21      CONTINUE
22      DL(K)=PI
      NP=K
      VS=115.0
      DO 40NS=1,49,2
      EDC=(2.*VS)/(PI*NS)
      SUM1=SIN(NS*DL(1))
      DO 50M=2,NP
      MN=M+1
      MM=M-1
      Z=(-1.)**MN
      AACM=Z*((SIN(NS*DL(M)))-SIN(NS*(DL(MM))))
      SUM1=SUM1+AACM
50      CONTINUE
      AV(NS)=EDC*(SUM1)
40      CONTINUE
      60 TO 100
200     CC=1.0
      VS=115.0
      DO 300NK=1,49,2
      Y=NK
      AV(NK)=(4*VS)/(PI*Y)
300     CONTINUE
100     KCL=0.0
      DO 32KN=1,49,2
      IF(AV(KN).LE..00001)60 TO 23
      S(KN)=(KN*N1-NR)/(KN*N1)
      60 TO 14
23      S(KN)=(KN*N1+NR)/(KN*N1)
14      DUM=1.0
      R2(KN)=(KN/KN)*R2(1)

      TYPE*,R2(KN)
      X2(KN)=KN*2.*PI*L2*F
      X1(KN)=KN*2.*PI*L1*F
      XM(KN)=KN*2.*PI*LM*F
      TYPE*,XM(KN)
      WS(KN)=KN*2.*PI
      XCOM=(CX2(KN)*X2(KN))+XM(KN))+((XM(KN)*XM(KN))*X2(KN))
      AZF(KN)=(R2(KN)**2.)/(S(KN)**2.)+(CX2(KN)+XM(KN))**2.)

```

AZB(KN)=(R2(KN)\*\*2.)/(C2-S(KN)\*\*2.)+(CX2(KN)+XM(KN))\*\*2.)  
 RF(KN)=(R2(KN)\*XM(KN)\*XM(KN))/(S(KN)\*AZF(KN))  
 RB(KN)=(R2(KN)\*XM(KN)\*XM(KN))/(C2-S(KN))\*AZB(KN)  
 XF(KN)=(XCOM+(R2(KN)\*R2(KN)\*XM(KN))/S(KN))/AZF(KN)  
 XB(KN)=(XCOM+(R2(KN)\*R2(KN)\*XM(KN))/(C2-S(KN)))/AZB(KN)  
 RT(KN)=.5\*RF(KN)+.5\*CKN+R1  
 XT(KN)=.5\*XF(KN)+.5\*XB(KN)+X1(KN)  
 ZT(KN)=SQRT(RT(KN)\*RT(KN)+XT(KN)\*XT(KN))  
 AI(KN)=AV(KN)/ZT(KN)\*1.414  
 PGF(KN)=AI(KN)\*AI(KN)\*.5\*RF(KN)  
 PGB(KN)=AI(KN)\*AI(KN)\*.5\*RB(KN)  
 PCU(KN)=S(KN)\*PGF(KN)+(C2-S(KN))\*PGB(KN)  
 PD(KN)=PGF(KN)-PGB(KN)-S(KN)\*PGF(KN)+(C2-S(KN))\*PGB(KN)  
 PIN(KN)=PGF(KN)-PGB(KN)+(AI(KN)\*\*2.)\*R1  
 CONTINUE  
 V=0.0  
 APD=0.0  
 APCU=0.0  
 AI1=0.0  
 API=0.0  
 DO 132KK=1,49,2  
 APCU=APCU+PCU(KK)  
 V=V+(AV(KK)\*AV(KK))/2.  
 AI1=AI1+AI(KK)\*AI(KK)  
 API=API+PIN(KK)  
 APD=APD+PD(KK)  
 132 CONTINUE  
 VI=SQRT(V)  
 AIN=SQRT(AI1)  
 PO=APD-WC  
 TO=PO/((1-S(1))\*W)  
 EFF=PO/API  
 PF=API/(VI\*AIN)  
 WRITE(1,\*)F,PO  
 WRITE(2,\*)F,TO  
 WRITE(3,\*)F,EFF  
 WRITE(4,\*)F,PF  
 80 CONTINUE  
 STOP  
 END

```

C      INPUT CURRENT TO LOAD AND VOLTAGE WAVE DETERMINATION OF DELTA PWM
C      INVERTER WITH PASSIVE LOAD
      DIMENSION T(200),DL(200),AA(400),AV(400),AI(400),BB(400)
      CALL ASSIGN(2,'AI14.DAT')
C      PULSE WIDTH DETERMINATION
      VR=7.00
      DV=1.000
      F=50.
      S=3200
      PI=4*ATAN(1.)
      W=2*PI*F
      T(1)=0.0
17     X=(DV+VR*SIN(W*T(1)))/S
      B=X-T(1)
      IF(B.LE..000005)GO TO 18
      T(1)=T(1)+.000001
      GO TO 17
18     T(1)=X
      K=1
      DL(1)=T(1)*W
      IF(DL(1)-1.57)16,200,200
16     K=1
      DO 21 I=2,30
      T(I)=0.0
      IK=I-1
19     Y1=(2.*DV+S*T(IK))/S
      Y2=((VR*SIN(W*T(IK))-VR*SIN(W*T(I)))/(S*(-1.)*I))
      Y=Y1+Y2
      C=Y-T(I)
      IF(C.LE..000005)GO TO 20
      T(I)=T(I)+.000001
      GO TO 19
20     T(I)=Y
      DL(I)=T(I)*W
      K=K+1
      Q=DL(I)-DL(1)
      IF(Q.GE.3.14)GO TO 22
21     CONTINUE
22     DL(K)=PI
      NP=K
C      FOURIER ANALYSIS
      VS=110.5
      DO 40 NS=1,19,2
      EDC=(2.*VS)/(PI*NS)
      SUM1=SIN(NS*DL(1))
      SUM2=1-COS(NS*DL(1))

```

```

DO 50M=2,NP
MN=M+1
MM=M-1
Z=(-1.)**MN
AA(M)=Z*((SIN(NS*DL(M)))-SIN(NS*DL(MM))))
BB(M)=Z*((COS(NS*DL(MM)))-COS(NS*DL(M)))
SUM1=SUM1+AA(M)
SUM2=SUM2+BB(M)
50  CONTINUE
SUM=SQRT(SUM1*SUM1+SUM2*SUM2)
AV(NS)=EDC*(SUM)
40  CONTINUE
60 TO 100
200 CC=1.
DO 300NN=1,19,2
Y=NN
AV(NN)=(4.*VS)/(PI*Y)
300 CONTINUE
100 R=20.
AL=0.0
DO 500LN=1,19,2
AX=2.*PI*F*AL*LN
AZ=SQRT(R*R+AX*AX)
AI(LN)=AV(LN)/AZ
500 CONTINUE
DO 111=1,501
TT=.00006*(111-1)
V=0.0
CI=0.0
DO 211=1,19,2
V=V+AV(J)*SIN(W*J*TT)
CI=CI+AI(J)*SIN(W*J*TT)
WT=2*PI*F*TT
2  CONTINUE
WRITE(2,*)WT,CI
1  CONTINUE
STOP
END

```

```

C      DETERMINATION OF COMMUTATION PER SECOND
      DIMENSION DL(100),T(100),A(100),AA(100),AK(100),BB(100)
      CALL ASSIGN(2,'CN3.DAT')
C      PULSE WIDTH DETERMINATION
      VR=5.00
      DV=1.25
      DO 90JJ=1,13
      F=10.+(JJ*10.-10)
      S=3000
      PI=4.*ATAN(1.)
      W=2.*PI*F
      T(1)=0.0
17      X=(DV+VR*SIN(W*T(1)))/S
      B=X-T(1)
      IF(B.LE..000005)GO TO 18
      T(1)=T(1)+.000001
      GO TO 17
18      T(1)=X
      K=1
      DL(1)=T(1)*W
      IF(DL(1).GE.1.57)GO TO 200
      DO 21I=2,30
      T(I)=0.0
      IK=I-1
19      Y1=(2.*DV+S*T(IK))/S
      Y2=((VR*SIN(W*T(IK))-VR*SIN(W*T(I)))/(S*(-1.)*I))
      Y=Y1+Y2
      C=Y-T(I)
      IF(C.LE..000005)GO TO 20
      T(I)=T(I)+.000001
      GO TO 19
20      T(I)=Y
      DL(I)=T(I)*W
      K=K+1
      Q=DL(I)-DL(1)
      IF(Q.GE.3.14)GO TO 22
21      CONTINUE
22      DL(K)=PI
      NP=K
      NC=2*NP*F
      FCR=NC/2
      WRITE(2,*)F,NC
      GO TO 100
200     CC=1
      FCR=F
      NC=2*FCR

```

A-43

100  
90

WRITEC2, WDF, NC  
PL=0.0  
CONTINUE  
STOP  
END









